Enhancing Mechanical Strength of a Polymer-Based Noise-Reducing Road Surface System

Von der Fakultät für Bauingenieurwesen der Rheinisch-Westfälischen Technischen Hochschule Aachen zur Erlangung des akademischen Grades einer Doktorin der Ingenieurwissenschaften genehmigte Dissertation

vorgelegt von

Sabine Tekampe, geb. Faßbender

Berichter: Universitätsprofessor Dr.-Ing. habil. Markus Oeser
Universitätsprofessor Dr.-Ing. Christian K. V. Schulze
Universitätsprofessor Dr. Alvaro García-Hernandez

Tag der mündlichen Prüfung: 17. Januar 2024

Published Papers

1. Investigation on an Absorbing Layer Suitable for a Noise-Reducing Two-Layer Pavement, Materials, 13(5), 1235, https://doi.org/10.3390/ma13051235
2. Investigation of the Reusability of a Polyurethane-Bound Noise-Absorbing Pavement in Terms of Reclaimed Asphalt Pavement, Materials, 15(9), 3040, https://doi.org/10.3390/ma15093040
3. Development of a Novel Polymer-Based Road Surface Layer with Focus on Noise Reduction and Durability, Bauingenieur, 97(10), DOI: 10.37544/0005-6650-2022-10-61
4. Assessing the Durability and Acoustic Performance of a Novel Two-Layer Pavement System, Sustainability, 15(23), 16475, https://doi.org/10.3390/su152316475

Acknowledgement

This work was carried out during my time as a research associate at the Institute of Highway Engineering, RWTH Aachen University. My tenure as a research associate and a doctoral candidate significantly influenced me, teaching me how to organize myself, take a stance, and develop enormous perseverance, without which I would not have completed this work.

Therefore, I would like to express my deep gratitude to my advisors, Univ.-Prof. Dr.-Ing. habil. Markus Oeser and Univ.-Prof. Dr.-Ing. Christian Schulze, who afforded me the opportunity to join the position at ISAC and encouraged my growth there. I am grateful for the trust that Univ.-Prof. Dr.-Ing. habil. Markus Oeser placed in me over the past years and for his constant encouragement to successfully complete my projects and the doctoral thesis. Additionally, I extend my sincere thanks to Univ.-Prof. Dr.-Ing. Christian Schulze, from whom I learned a lot. I would also like to express my appreciation to Univ.-Prof. Dr. Alvaro García-Hernandez, who took over the institute's management at ISAC this summer and particularly supported me in the final stages of my doctoral thesis.

Moreover, I want to extend my heartfelt gratitude to my colleagues at ISAC and our student assistants, as they form a fantastic and supportive team that stands by each other and offers advice. Of course, my gratitude specifically goes to my department Construction Engineering: Julian, Frédéric, Paul, Nora, Pengfei, and former colleagues Nicolas and Milad, who are not just colleagues but friends as well.

However, the most crucial support in the journey towards my doctoral thesis came from my family and friends. Thank you for consistently supporting me in pursuing my doctoral studies and following my path. Therefore, I would like to express my special thanks to my parents, Claudia and Rolf, for enabling my studies in Aachen and always believing in me. Also, I want to thank my sister, Steffi, for always being there for me.

The greatest gratitude goes to my husband Falk and my son Fritz. The time of my doctoral thesis was a very challenging period, during which you both tremendously supported me in my endeavors and believed in me.

Abstract

Nowadays, there is a shift in the mobility needs of the population based on various societal and economic phenomena. This is due to factors such as urbanization driven by globalization and the ongoing scarcity of resources. Considering these challenges, the construction of sustainable and functionalized roads becomes essential. These roads are designed to notably reduce noise and pollutant emissions generated by road traffic. Additionally, to address resource scarcity, they are made from alternative construction materials.

Against this background, a noise-reducing surface layer system has been developed in the past, offering a fundamental approach to addressing the aforementioned issue. The system provides significant noise reduction concerning tire-road noises and is made from polymeric materials. However, it fails when exposed to traffic loads.

Given the escalating urgency for the development of innovative, sustainable, and functionalized transportation routes, this work chose the previously developed research project as a starting point for further advancement towards a resilient and noise-reducing pavement system.

The focus of this work is to optimize the existing surface system, comprising a drivable textured layer and an underlying absorption layer, to achieve a high strength and noise-reducing effect. Initially, the individual components of the pavement system were designed to be more robust. This was done through extensive laboratory studies to determine the performance properties of both layers, leading to the determination of optimal mixture compositions. Subsequently, the individual components, the absorption and texture layers, were first combined into an integrated system at a laboratory scale and then at a real-scale to experimentally verify the system's mechanical and acoustic effectiveness.

It was observed that the mechanical optimization of the system led to a reduced potential for noise reduction but, in return, exhibited high resistance against the loads from vehicular traffic.

The optimized noise-reducing pavement system from this study thus represents an opportunity to positively impact public health while also contributing to the development of a resilient and robust infrastructure for a sustainable future.

Kurzfassung

Heutzutage tritt auf Basis unterschiedlicher gesellschaftlicher und wirtschaftlicher Phänomene eine Änderung des Mobilitätsbedarfs der Bevölkerung auf. Grund dafür sind zum Beispiel die mit der Globalisierung einhergehende Urbanisierung und die fortschreitende Rohstoffverknappung. Unter Berücksichtigung dieser Herausforderungen, gilt es, nachhaltige und funktionalisierte Straßen zu bauen, die insbesondere die Lärm- und Schadstoffemissionen durch den Straßenverkehr reduzieren und zusätzlich, im Hinblick auf die Rohstoffverknappung, aus alternativen Baustoffe hergestellt werden.

Vor diesem Hintergrund wurde in der Vergangenheit ein lärmreduzierendes Deckschichtsystem entwickelt, das einen grundlegenden Ansatz zur Lösung der oben genannten Problematik bietet. Das System bewirkt eine hohe Lärmreduzierung gegenüber Reifen-Fahrbahn-Geräuschen und wird aus polymeren Baustoffen hergestellt. Allerdings versagt es bei Beanspruchung durch Verkehrslasten.

Mit dem Blick auf die sich verstärkende Dringlichkeit der Entwicklung innovativer, nachhaltiger und funktionalisierter Verkehrswege, wurde in dieser Arbeit das zuvor entwickelte Forschungsvorhaben als Ausgangspunkt für eine Weiterentwicklung hin zu einem widerstandsfähigen und lärmreduzierenden Deckschichtsystem gewählt.

Fokus dieser Arbeit ist, das vorhandene Deckschichtsystem, das aus einer befahrbaren Texturschicht und einer darunter befindlichen Absorptionsschicht besteht, mechanisch zu optimieren, um damit das Ziel, eine hohe Festigkeit und eine lärmreduzierende Wirkung zu erhalten, zu erreichen. Dazu wurden zunächst die einzelnen Bestandteile des Deckschichtsystems, robuster konzipiert. Dies erfolgte anhand umfassender Laborstudien zur Feststellung der Performance-Eigenschaften beider Schichten aus der die Festlegung der optimalen Mischgutzusammensetzungen erfolgte. Anschließend wurden die Einzelbestandteile, Absorptions- und Texturschicht, zuerst im Labormaßstab und anschließend im Realmaßstab zu einem Gesamtsystem zusammengeführt, um in einem Real-Versuch die Wirksamkeit des Systems mechanisch und akustisch zu überprüfen.

Es konnte festgestellt werden, dass die mechanische Optimierung des Systems zu einem reduzierten Lärmminderungspotenzial führt, aber im Gegenzug eine hohe Widerstandsfähigkeit gegenüber den Lasten aus dem Straßenverkehr aufweist.

Das optimierte lärmreduzierende Deckschichtsystem aus dieser Studie bildet daher eine Möglichkeit, die Gesundheit der Bevölkerung positiv zu beeinflussen und gleichzeitig zur Entwicklung einer resilienten und widerstandsfähigen Infrastruktur für eine nachhaltige Zukunft beizutragen.

Contents

List of Figures

List of Tables

1 Introduction

1.1 Motivation

In recent years, the impact of intensifying societal and economic factors such as globalization, coupled with increasing urbanization and progressing resource scarcity, has become more pronounced on the mobility needs of the population.

The majority of the German population currently resides in metropolitan regions (71 %) [13], leading to high population and housing density, which results in escalating living costs. Consequently, more individuals are being displaced from urban centers and are relocating to the surrounding area to live closer to potential job opportunities and leverage the advantages offered by metropolitan areas. This trend has led to an increase in commuter flows and high volumes of traffic [13]. As a consequence, roads originally designed for lower traffic volumes are now inadequate. Additionally, many of these roads, predominantly constructed during the building boom of the 1970s [12], have reached the end of their life cycle. The significant surge in traffic combined with failing roads has resulted in numerous construction sites, closures, and subsequent traffic jams. The amplified traffic density in densely populated areas also generates high levels of road traffic noise and escalating emissions, exposing residents to chronic conditions that not only diminish their quality of life but can also lead to long-term health issues [14, 4].

The existing transportation infrastructure is no longer capable of accommodating the increasing mobility demands, thus necessitating the design of new, sustainable, and efficient roads that not only address the traffic volume but also lead to a reduction in noise. Alternatively, the alteration of the population's mobility habits (increased use of public transportation, city tolls, etc.) would be a complementary solution, which is already promoted through the German government's mobility transition. However, this solution does not directly involve the road sector but requires impetus from other stakeholders.

The precarious situation of resource scarcity must also be considered. Currently, only 16 % of renewable resources are utilized in Germany for the production of goods [7]. Fossil fuels (25 %), such as petroleum, brown and hard coal, as well as mineral resources (45 %), including sand, gravel, crushed natural stones, limestone, and gypsum, collectively account for

70 % of the resource usage in the domestic consumption and investment sector (construction, equipment, machinery) [7].

Asphalt roads play a significant role in resource scarcity as they rely on fossil fuel, specifically crude oil from which bitumen is derived. Additionally, asphalt consists largely of mineral resources (approximately 90 %), forming the aggregate structure of the material. All components essential in asphalt production draw from non-renewable resources, hence working against ecological sustainability. Furthermore, the production of asphalt significantly contributes to a high CO_2 footprint due to its extensive energy requirements, which must be reduced for environmental conservation. Therefore, the development of alternative construction materials that diminish the CO_2 emissions and conserve our valuable finite resources and environment is of paramount importance.

The illustrated aspects significantly contribute to the potential failure in achieving the United Nations' 17 Sustainable Development Goals (SDG). The SDGs were adopted by heads of state and government at the summit meeting in New York on September 25, 2015, whose urgency for implementation was underscored once again in 2019 [2].

Particularly, Goals 3, 9, 11, 12, 13, and 15 can be supported by innovations in road infrastructure: Goal 3 aims to ensure healthy lives and promote well-being for all individuals; Goals 9, 11, and 12 focus, among other aspects, on establishing resilient infrastructure, protecting innovations, ensuring safe, resilient, and sustainable cities and settlements, and guaranteeing sustainable production; Goal 13 is highly relevant, emphasizing the urgent intensification of actions to combat climate change and its effects; and Goal 15 calls for the protection of land ecosystems and the promotion of their sustainable use.

It becomes evident that a highly complex challenge exists concerning infrastructure design, which must be addressed by stakeholders in politics, infrastructure planning, and the road construction industry, among others. Specifically, the participants in road construction (research and industry) can contribute to building innovative, functionalized, and long-lasting roads that promote the attainment of the UN's 17 Sustainable Development Goals (SDGs) and resolve the specific issues occurring in urban agglomerations.

Therefore, this study presents an approach that mitigates the issues of high road traffic noise through the functionalization of roads. Simultaneously, the polymer-based resources used therein present an alternative to the utilization of finite resources, representing a stride towards sustainability and the realization of reducing CO_2 emissions.

The subject of this study is the optimization of a two-layer noise-reducing surface system comprising a functionalized wearing course layer, which in combination with an underlying

open-porous and flexible layer, mitigates tire-road noise. Both developed layers are polymer-based materials that have the potential to be manufactured from renewable resources. Simultaneously, the system offers recycling for shredded used tires, which are utilized as filler material.

By implementing this noise-reducing system, an attempt is made to integrate new polymeric construction materials into the road sector to alleviate resource scarcity. Additionally, the system is intended to act as a high-performance material, exhibiting high durability and resistance to wear under consistently increasing traffic. This reduces the frequency of maintenance interventions and enables a decrease in traffic congestion. Ultimately, the surface layer system engenders a noise-reducing effect, shielding urban dwellers from being significantly disturbed or affected by road traffic noise.

Overall, the development of this system can contribute significantly to reducing major issues on the roads and in the affected areas, thereby enhancing the quality of life for individuals.

1.2 Introduction, Overview, and Methodology of the Study

Based on the outlined challenges, which had been foreseen several years ago but had not manifested as drastically, Schacht [10] devised a two-layer road surface system aiming for maximum noise reduction. The system comprises a wearing course directly used by traffic and an underlying absorption layer, as depicted in Figure 1.1 (a). Given the context of escalating resource scarcity, the objective was to design the system using alternative construction materials, intending to move away from bitumen-bound asphalt, known for its substantial CO_2 footprint.

Schacht's aim was to significantly reduce the noise generated by road traffic through the "Low-noise Innovative Plastic-based Surface Layer System" (LIDAK-system). To achieve this, he utilized insights from previous research that explain the origins of noise and applied them to his system.

Road traffic noise primarily originates from the passage of vehicles on roads, where vehicle-induced propulsion noises and aerodynamic noises occur. Additionally, tire-road noise is generated by the rolling of tires on the road surface.

Propulsion noises, for example, are generated by motor, cooling, or exhaust noises of vehicles, while aerodynamic noises are sounds produced by a moving vehicle in conjunction with wind [8]. Both of these mechanisms are contingent upon the design of automobiles and can be attributed to the domain of action within the automotive industry.

The third characteristic of noise generation is tire-road noise. Tire-road noise occurs when the tire rolls on the road surface, resulting in tire vibrations due to the rolling process (mechanical excitation), or these noises are caused by sound radiation (aerodynamic excitation). The former primarily emerges from the shape (texture) of the road surface, stimulating tire vibrations, supported by adhesion and friction processes ("stick-slip" and "stick-snap"). However, the aerodynamic noises arise due to the developing sound generated by the tire's bounce on the road and are further intensified by the "Horn Effect" (formation of a sound cone between the tire and the road). In this scenario, noise generation is attributed to the interaction between the tire and road, which can be mitigated through alterations in the tire itself [11] and by novel surface layer concepts.

The magnitude of noise generated by these mechanisms is highly contingent upon the driving speed of the vehicles. Literature indicates that at speeds exceeding 40 km/h for cars and 60 km/h for trucks, tire-road noises predominate over propulsion noises. Therefore, particularly when considering higher driving velocities, reducing tire-road noise becomes pertinent [1, 8].

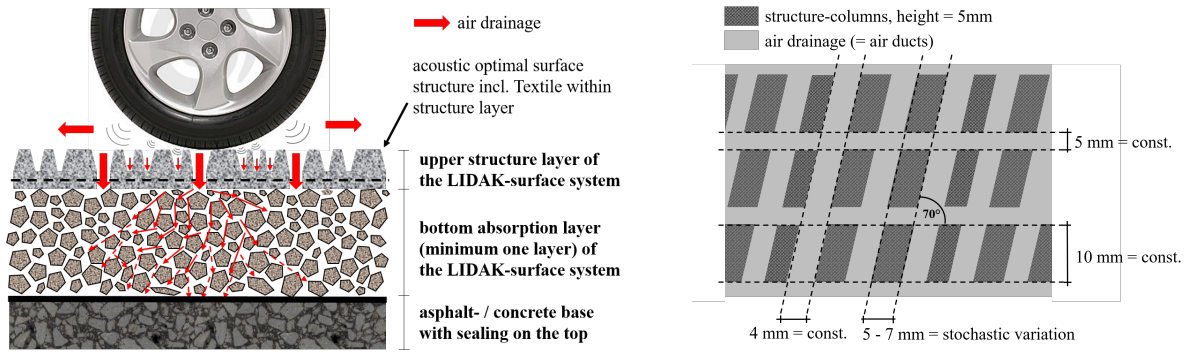

(a) (b)

Figure 1.1: (a) LIDAK schematic illustration and (b) top view of the preferred structure of the texture layer by [10].

Schacht thus focused on reducing tire-road noise, which can be influenced by engineering adjustments of road surface layers. His objective was to achieve maximal noise reduction of tire-road noise through the system, which led to the development and acoustic optimization of the drivable wearing course. It mainly comprises cold plastic resin, commonly used for road markings and exhibiting high resistance to tire abrasion. In its uncured state, the cold plastic resin can be molded into any desired shape. In Schacht's work [10], this material was used to form a geometrically unique texture that significantly reduces the generation of tire-road noise. Through a specific arrangement of driving columns and a large air drainage system, the texture layer results in the tire rolling over a flat surface, minimizing tire vibrations (Figure 1.1 (b)). Furthermore, the integrated air drainage system provides the opportunity to reduce aerodynamic noise typically generated by the compression and decompression processes of

tires as they roll on a road surface. Additionally, the layer was perforated to guide any remaining tire-road noise and surrounding propulsion noises to an underlying absorption layer.

Below the texture layer, he placed an absorption layer, its composition closely resembling a poro-elastic road surface (PERS). PERS comprises aggregates, rubber particles, and polyurethane as a binder, characterized by a substantial proportion of rubber particles of a minimum of 20 %, however, typically utilizing significantly higher rubber contents. Moreover, it is distinguished by a high void content of at least 20 % [9]. The rubber particles, derived from recycled materials, positively contribute to sustainability.

The LIDAK system [10] offers numerous advantages. Its primary advantage is delivering sustained noise reduction of up to 8 dB(A) in comparison to bitumen-bound conventional asphalt, which significantly contributes to mitigating traffic noise. The enduring acoustic efficiency can be attributed, among other factors, to the absence of the clogging phenomenon (pore clogging due to dirt). Moreover, known occurrences like aggregate breakouts due to ravelling on the surface of the absorption layer are excluded. Another advantage lies in the system's permeability, primarily designed to allow air passage, reducing air-induced noise; however, it also promotes water permeability, contributing to the de-sealing of roads.

However, the system's disadvantages are also notable, with its primary drawback being that it offers low mechanical strength. During tests for resistance against ravelling, substantial damages to the structural wear layer were evident. If such damages were to occur in real-world scenarios, further use of the system would no longer be viable. Additionally, the manufacturing and installation process of the LIDAK-system proves to be highly labor-intensive, prompting Schacht to recommend the industrial prefabrication of the texture layer.

Schacht designed the LIDAK surface layer system with a primary focus on sustainability and noise reduction, thereby laying the groundwork for the realization of some of the 17 Sustainable Development Goals (SDGs). In doing so, he set an initial milestone towards achieving the third SDG, ensuring the health and well-being of every individual.

The focus on noise reduction remains central in the continued advancement of research. The advantage offered by a system based on Schacht's work [10] lies in actively harnessing all available engineering acoustic properties to counteract the noise, that is generated when the tire rolls on the road surface. Existing noise-reducing road surfaces, such as the poor noise stone mastic asphalt (SMA LA) or noise improved mastic asphalt (LV MA), typically address only one or two noise generation mechanisms simultaneously and thus do not achieve maximum effectiveness [3]. In his study, Gogolin designed an overview of noise-reducing road surfaces, aligning them with their acoustically significant operational principles [3], which are depicted in Figure 1.2 and complemented by the newly developed surface layer systems.

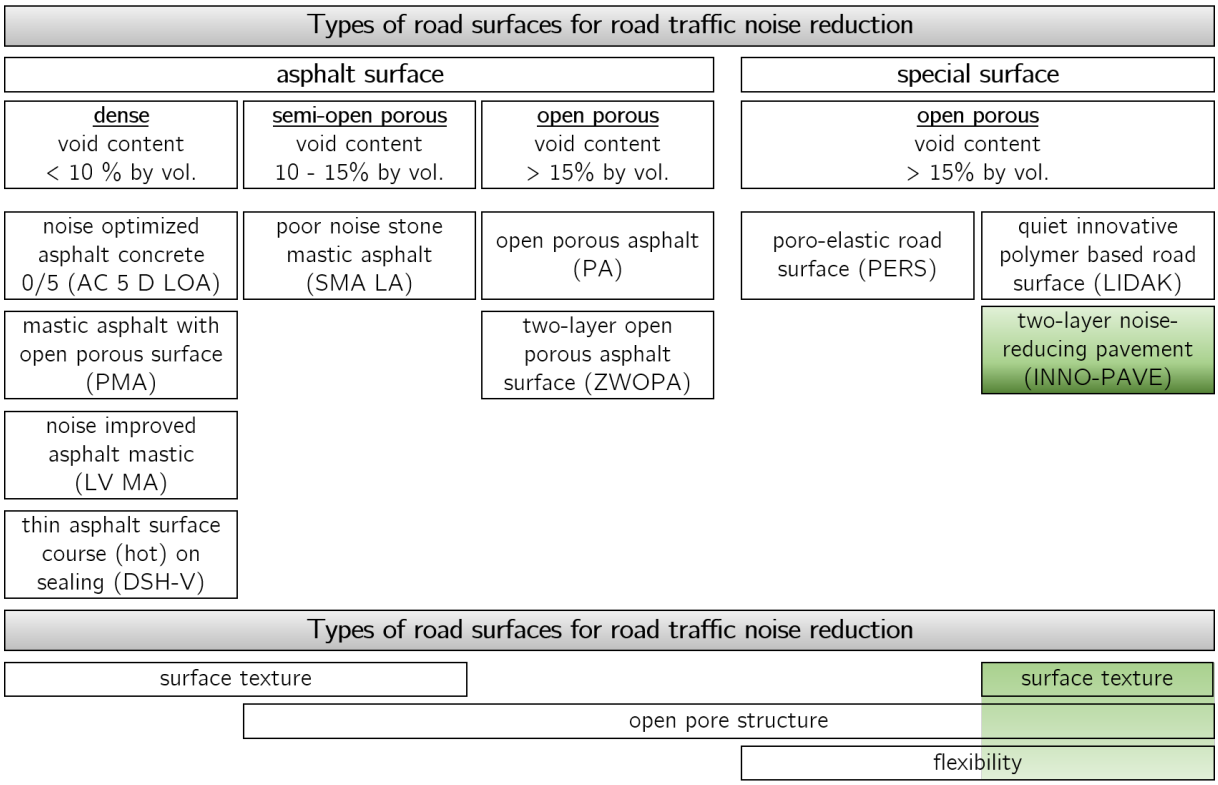

Figure 1.2: Illustration of noise-reducing road surfaces of Germany by [3] combined with the LIDAK surface and newly developed surface from this study (green).

From an engineering perspective, road surfaces can be equipped with noise-reducing potential in terms of texture, open porosity, and flexibility characteristics. The texture significantly influences tire vibration excitation. When the texture is formed with a concave shape (such as a "plateau with grooves"), it tends to produce lower tire-road noise. This shape is typically created in asphalt types exposed during installation to rolled compaction (SMA, AC, PA). However, this case is irrelevant in the two-layer surface layer system, as the drivable layer is industrially cast from polymers. Moreover, open porosity, i.e., the void content and its branching within the road layer, contributes to the sound absorption of noise, as the sound, in the form of waves, is absorbed, distributed, and thereby attenuated by the cavities. Concurrently, the open-porous layer leads to the reduction of noises generated by air-pumping (compression and decompression processes) or amplified by the Horn Effect, as the air, which would otherwise be trapped in dense road surfaces during the rolling process, can escape through the open-porous layer. Finally, the flexible design of the road can additionally induce noise reduction. When a tire encounters a flexible surface, vibrations can be absorbed and dampened by the flexible medium. In contrast, when a tire meets a rigid layer, the rigid surface does not absorb tire vibrations but causes strong rebounding, amplifying vibrations within the tire [1, 8].

Schacht takes into account all the presented engineering characteristics and integrates them into the artificially produced surface layer system LIDAK, making it a highly acoustically

effective tool, which is optimized in this study.

The focus of the optimization first lies on the absorption layer, aiming to ensure its strength (SDG 9). Alternative binders are utilized to counteract resource scarcity. These binders have the potential to be produced from renewable resources, as described by Renken in his work concerning the use of polyurethane [5], or to be newly manufactured with a high proportion of recycled content, as introduced by the manufacturer Röhm GmbH regarding recycled methyl methacrylate (RMMA) in the market [6]. Both the mechanical stabilization of the layer and the use of alternative binders address the issues and goals outlined in the motivation, reflecting a specific measure to combat climate change and implement the resilience of our infrastructure (SDG 9 and 13). The composition of the mixture continues to be designed as open-porous as possible, aligning with the goals of acoustic effectiveness. This design additionally results in the creation of an air- and water-permeable system, allowing water to infiltrate and thus de-seal the road surface. During rainfall events, surface water can then be directed over larger areas to the natural environment. This promotes groundwater replenishment and the associated terrestrial ecosystem (SDG 15) while safeguarding cities and their infrastructure from extensive water-related damages (SDG 11).

Alongside the pure mixture optimization of the absorption layer, in light of resource scarcity, an evaluation is conducted to assess whether the mixture of artificially produced materials in the form of reclaimed asphalt (PU-RAP) can be introduced to a new mixture. This study will ultimately determine the impact of adding PU-RAP on the performance properties of the resultant new mixture. The aim of this initiative is to directly demonstrate the potential for systems based on alternative materials to be reintegrated into the circular economy and whether they provide added value. This approach was chosen to underscore the sustainability of the system (SDG 12).

Further optimization is required for the wear layer developed by Schacht, which, following testing in the Aachen Ravelling Tester (ARTe), displayed significant damage, that renders it unsuitable for real-world load bearing. In this study, the wear layer of the LIDAK system is mechanically optimized. The focus lies on the optimization of the layer's geometry, fabric selection, and coating, as well as the material composition, all of which significantly influence the acoustic effectiveness of noise reduction. Through these adjustments, the layer is able to withstand higher stresses, enabling it to bear higher loads without sustaining damage.

Through this optimization step, another milestone towards achieving several of the United Nations' 17 Sustainable Development Goals (SDGs) can be reached. The stabilization of the texture layer supports the goal of establishing resilient infrastructure (SDG 9) and more resilient cities (SDG 11). Additionally, by employing highly robust and weather-resistant alternative binders such as the Polymethylmethacrylate (PMMA) used here, a step towards utilizing bitumen alternatives is taken, aligning with an important measure to combat climate

change (SDG 13). Furthermore, the texture layer is designed to consist of individual texture elements interconnected solely by an optimized textile. This optimization, as opposed to Schacht's LIDAK system, provides better flexibility and permeability of the layer, supporting surface desegregation and thus contributing to the goal of sustainable management of our land ecosystems (SDG 15). Fundamentally, it can be recognized that the optimizations made to the texture layer address the same goals covered by the absorption layer.

All optimizations must ultimately integrate into the implementation of the overall system so that the comprehensive system can be realized, encompassing the advantages of both layers and be translated into real-scale applications. In this regard, the combined interaction between the absorption layer and the texture layer is examined to demonstrate their stability in the combined system. Furthermore, the focus is also directed toward the acoustic effectiveness of the overall system, which can be demonstrated in real-scale applications. The composition of the layers necessitates several investigations, considering the interaction between the single layers and the application of the overall system on conventional bitumen-bound asphalt surfaces. The objective of this study is to demonstrate that the optimized system can be used as a replacement within the existing structure, serving as a means to enhance the existing infrastructure and contribute to the stabilization of infrastructure and cities (SDG 3, 9, 11, 15).

The presented advancement of the two-layered noise-reducing system predominantly aims to optimize the system to be robust while simultaneously reducing noise. Therefore, in this work, several aspects that could be considered in the development of a new system are explicitly excluded to maintain focus on the essentials. These include aspects such as the use of rock alternatives, performing a life cycle analysis, the clogging behavior, the connection to suitable drainage systems, tire wear resulting from the polymeric wearing course, consideration of potentially contaminated infiltrated water, and the health compatibility of alternative construction materials. These aspects are intended to be addressed by respective experts in their fields and further scrutinized in detail in the future.

However, the following aspect should be addressed to underline its importance: During the production of test specimens, test plates, and full-scale layers, a clean execution was always ensured while utilizing personal and laboratory protective equipment as stipulated in the safety data sheets of the materials (especially the polyurethane) to guarantee maximum protection for all involved. Nonetheless, it was observed in some instances that during the mixing process of the absorption layer, a few individuals experienced mild allergies to rubber or polyurethane, even with the reinforced safety measures in place. Consequently, safety precautions were enhanced, such as mandating the use of face masks during handling. Investigating the compatibility of these substances with human health is not within the scope of this study. However, this aspect was noticed negatively, urging the manufacturers

of the rubber particles and polyurethane to conduct further studies in this domain to prevent potential illnesses resulting from this manufacturing process. At present, it can be stated that the production of the absorption layer material should also take place outdoors under high safety measures, which implies greater effort and physical constraints for its implementation on a full scale. The production of the texture layer plates, on the other hand, was conducted under stringent safety measures in a laboratory setting (indoors) as the manufacture of this component required constant temperature and speed conditions.

Based on the content initiated so far, the question arises within the scope of this research whether it is feasible to further develop Schacht's two-layer pavement system [10] to meet the aforementioned requirements.

To address the question, a multi-scale research approach has been chosen, encompassing optimization from the material level (microscale) to the real-scale level (macroscale) concerning the research question. The schematic representation of the methodology is illustrated in Figure 1.3.

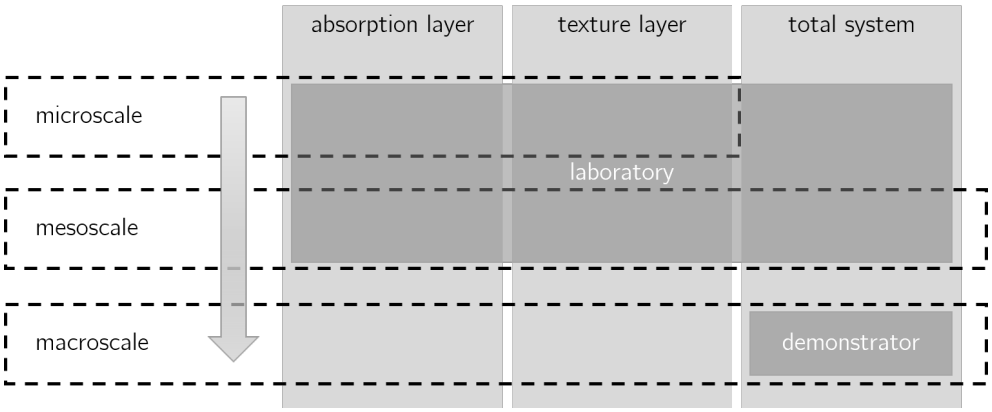

Figure 1.3: Methodology

Initially, the approach involved focusing on the development of single layers, which were individually optimized mechanically and acoustically (microscale). This developmental step was carried out in the laboratory by producing small test specimens (cylinders, prisms) and evaluating their functionality and performance. Parameter studies were conducted to explore various properties of potential mix variations, such as their absorption capacity, behavior under permanent and cyclic deformation, tensile and compressive behaviors, as well as their performance under cold conditions. This facilitated an overview of material properties, allowing a comparison with asphalt or other polymer-based asphalts, consequently determining an optimal variant that exhibits strength on one side and acoustic efficacy on the other.

In the next phase, the layers were produced in larger-scale dimensions (mesoscale) as panels (32x26x4 cm^2) in the laboratory, enabling a more comprehensive evaluation of their behavior under conditions mimicking real-world scenarios. For instance, it allowed the assessment of

the layers' cohesion, their resistance to wear, their susceptibility to rutting, as well as tests for resistance against ravelling. This step served as preparation for upscaling the layers to full-scale size.

As the behavior of the entire system cannot be entirely depicted on a laboratory scale, it was eventually implemented at the full-scale level. Only at the full-scale, actual vehicular traffic such as using a CPX-Trailer (Close-Proximity-Method) or heavy traffic (Mobile Load Simulator MLS 30) can be conducted. Additionally, the full scale allows for an assessment of real-world applicability.

1.3 Thesis Structure

This work deals with the development of a surface layer system that reduces noise generated by tire-road noise while being able to withstand high road traffic demands. It consists of four main chapters, each corresponding to a scientific article. Chapters Two to Four describe the optimization of individual components of the noise-reducing road surface, while Chapter Five presents the effectiveness analysis on a full-scale basis.

This means that Chapter Two deals with the optimization of the absorption layer. This chapter extensively examines stabilizing the absorption layer to define an optimal mix that can withstand road traffic loads while retaining noise reduction capabilities. A comprehensive performance analysis is conducted on the absorption layer in this chapter to determine material behavior concerning deformation, fatigue, low temperatures, and absorption properties.

Following is Chapter Three, which revisits the topic of the absorption layer. This chapter focuses on exploring the recyclability of the absorption layer developed in the first chapter. The goal is to produce the absorption layer, comprised of polymeric components, as reclaimed asphalt and then use this reclaimed asphalt to create a new absorption layer. Through a parametric study, the chapter demonstrates the effects of adding asphalt granulate in different proportions on the material properties: deformation, fatigue, low-temperature behavior, and absorption characteristics of the absorption layer.

Next in Chapter Four is the development of the texture layer, which is applied to the optimized layer from Chapters Two and Three. This chapter is a joint paper describing the advancement of the texture layer concerning its mechanical stability and wear resistance. The texture layer is composed of PMMA elements combined with a polyvinyl alcohol (PVA) textile to create a permeable and flexible layer. As detailed in this chapter, the surface geometry was optimized to reduce the generation of tire-road noises while enduring traffic stress. Simultaneously, the manufacturing process is analyzed at this stage and transitioned into an optimized prefabricated construction method.

Chapter Five is dedicated to evaluating the composition of the absorption layer (Chapter Two) and the texture layer (Chapter Four) on a real scale, conducting a comprehensive impact analysis of the pavement system on the demonstration area duraBast of the Federal Highway Research Institute (BASt). The chapter investigates the measures necessary to ensure an adequate connection between the layers and thus the stability of the entire system on a large scale, as well as how the integration of the entire system can be implemented into the existing bitumen-bound infrastructure. A substantial part of this chapter consists of the real-scale impact analysis of the overall system, demonstrating both mechanical stability and the noise-reducing effect.

1.4 Funding

The presented work is based on the research project INNO-PAVE: "Foundations of structural design, structure, and new polymeric materials for road surface systems" within the joint project "Fundamental exploration of polymeric materials and innovative manufacturing and installation technologies for road surface systems" (09/2015 - 04/2019). It was funded by the Federal Ministry of Education and Research (BMBF).

References

[1] T. Beckenbauer. “Physik der Reifen-Fahrbahn-Geräusche – Geräuschentstehung, Wirkmechanismen und akustische Wirkung unter dem Einfluss von Bautechnik und Straßenbetrieb.” In: *Geräuschmindernde Straßenbeläge in der Praxis – Lärmaktionsplanung* 4 (2008).

[2] Federal Government of Germany. *Deutsche Nachhaltigkeitsstrategie: Weiterentwicklung 2021*. Ed. by Federal Government of Germany. Berlin, 2020. URL: https://www.bundesregierung.de/resource/blob/975274/1873516/9d73d857a3f7f0f8df5ac1b4c349fa07/2021-03-10-dns-2021-finale-langfassung-barrierefrei-data.pdf?download=1 (visited on 11/05/2023).

[3] D. Gogolin. “Rheologische Kennwerte bitumenhaltiger Bindemittel zur Charakterisierung akustischer Eigenschaften von Asphaltdeckschichten.” PhD-Thesis. Bochum: Ruhr University Bochum, 2012.

[4] A. Peters et al. *Die Rolle der Luftschadstoffe für die Gesundheit: Eine Expertise im Namen der Internationalen Gesellschaft für Umweltepidemiologie (ISEE) und der European Respiratory Society (ERS)*. 2019. URL: https://www.swisstph.ch/fileadmin/user_upload/Die_Rolle_der_Luftschadstoffe_f%C3%BCr_die_Gesundheit_-_Expertise_der_ISEE____ERS_richtigesLogo.pdf (visited on 11/06/2023).

[5] L. Renken. “Development of PU-Asphalt - from the concept to the practical implementation.” PhD-Thesis. Aachen: RWTH Aachen University, 2019.

[6] Röhm GmbH. *DEGAROUTE proTerra: Designing safe Traffic and saving resources.* URL: https://www.degaroute.com/en/degaroute-r-proterra (visited on 11/05/2023).

[7] *Rohstofffußabdruck 2018: Anteil nachwachsender Rohstoffe bei 16%: Pressemitteilung Nr. 323 vom 7. Juli 2021.* 2021. URL: https://www.destatis.de/DE/Presse/Pressemitteilungen/2021/07/PD21_323_32.html (visited on 10/31/2023).

[8] U. Sandberg and J. A. Ejsmont. *Tyre/Road Noise Reference Book.* Harg, Kisa, Sweden: INFORMEX, 2002.

[9] U. Sandberg et al. *State-of-the-Art regarding poroelastic road surfaces (PERSUADE - PoroElastic Road SUrface: An Innovation to Avoid Damages to the Environment).* 2010. URL: https://persuade.fehrl.org/ (visited on 01/05/2020).

[10] A. Schacht. “Entwicklung künstlicher Straßendeckschichtsysteme auf Kunststoffbasis zur Geräuschreduzierung mit numerischen und empirischen Verfahren.” PhD-Thesis. Aachen: RWTH Aachen University, 2015.

[11] N. Sliwa and U. Weck. *Verbundprojekt "Leiser Straßenverkehr - Reduzierte Reifen-Fahrbahn-Geräusche".* Ed. by Bundesanstalt für Straßenwesen. Bergisch Gladbach, 2004.

[12] Statista. *Straßen in Deutschland.* 2023. URL: https://de.statista.com/statistik/studie/id/12547/dokument/strassen-in-deutschland-statista-dossier/ (visited on 10/31/2023).

[13] Statistisches Bundesamt. *Großstadtregionen im Wandel: Die Mehrheit der Bevölkerung lebte 2021 in Großstadtregionen.* URL: https://www.destatis.de/DE/Themen/Querschnitt/Demografischer-Wandel/Aspekte/demografie-grossstadtregionen.html (visited on 10/31/2023).

[14] J. Wothge. “Die körperlichen und psychischen Wirkungen von Lärm.” In: *UMID 01/2016 Umwelt und Mensch - Informationsdienst* (2016), pp. 38–43. URL: https://www.umweltbundesamt.de/sites/default/files/medien/2218/publikationen/umid_1_2016_uba_laerm.pdf (visited on 11/04/2023).

2 Investigation on an Absorbing Layer Suitable for a Noise-Reducing Two-Layer Pavement

This paper was published under:

Faßbender, Sabine and Oeser, Markus: "Investigation on an Absorbing Layer Suitable for a Noise-Reducing Two-Layer Pavement". In: Materials, 13(5), 1235, https://doi.org/10.3390/ma13051235, 2020.

2.1 Abstract

A polyurethane-based rubber-modified layer within a road superstructure leads to the absorption of traffic emissions. Noise emissions have quite a negative effect on society since they lead to high stress levels and health risks for people. Therefore, constructional methods of noise-reducing road layers have been developed before. This research paper focuses on the question of whether the existing noise-reducing road constructions, which have low durability, can be optimized in terms of a longer duration while simultaneously maintaining the noise-reducing effects. Within this research, a large parametric study contributed to an optimal solution of a noise-reducing and durable layer. We found that noise absorption is mainly dependent of the void content of the pavement and its flexibility. Also, a result is that the durability of a road layer is based on the properties of the binder as well as the composition of the mixture, i.e., the grading curve. As we used polyurethane binders within our mixtures, which have a low dependency on regular environmental temperatures after their complete chemical reaction, we can imply a low-temperature dependence of the entire polyurethane asphalt mixture. Based on these results, the construction of a noise-reducing and durable road layer is a great solution. The application of such road layers leads to lower traffic emissions at major hotspots. These might be urban highways, where the infrastructure is too tight to build noise barriers, enclosures or tunnels.

2.2 Introduction

Traffic noise is a negative side effect that is constantly growing due to the increasing volume of traffic. For this reason, the reduction of traffic noise is the subject of long-term research, which must always be further developed. Within the scope of this topic, [25] developed a two-layer road surface system for noise reduction. The aim of the surface course system was to reduce the noise caused by road traffic by developing new artificial materials. This was achieved by combining a two-layer surface course system. The surface course system consists of a drivable thin layer of polymethyl methacrylate and fillers, and has a special texturing that greatly reduces the development of tire/road noise (wearing course). The wearing course consists of a surface that represents a concave shape. A concave surface occurs in all roller-compacted surfaces and forms an even road surface with gaps. This shape of the surface reduces the excitation of the tires to vibrate and thus reduces the development of tire-road noise. Air compressions are also avoided, as the formed gaps allow great air drainage. Further, it is designed to be permeable, so that any noise that continues to be generated can pass through it to the bottom layer. The bottom layer is a polyurethane-bonded layer of rubber particles and aggregates designed to absorb further noise [25, 26]. In Germany, low-noise asphalt compositions that are bitumen-bound and do not have sufficient durability are common. This led to the idea of using new materials such as polyurethane, which were

known to be suitable for specific material behavior by adjusting their chemical composition. While [25] mainly focused on the absorption properties of the system, this study focuses on the development of durability while maintaining the noise-reducing effect [26].

2.2.1 Performance of Noise Absorption through Road Layers

For the acoustics of road top layers, the type of surface course, the construction method, the mix composition, and the surface design are of importance. As soon as a road surface layer is open-graded, i.e., a porous asphalt or a drain concrete, the porosity of the surface allows traffic noise to pass the complex cavity system of the layer. This cavity system leads to an absorption of incoming sound waves. The structure and the cavity size of the cavity system decisively influence the sound absorption capacity of the layer [3].

The particle size distribution and the selection of the binder type as well, as the thickness of the noise-absorbing asphalt layer, are designed in a way that the cavity system is as pronounced as possible. In principle, the fine fractions of a mix formulation are not used for this purpose. However, the aim is to create a load-bearing construct. A single-stage grain mixture, such as the pervious pavements (PA) according to the German guideline TL Asphalt 07/13, enables such a load transfer due to the tilted aggregates underneath [3].

With a high porosity, it is possible to obtain approximately 100 % absorption within a small frequency range [3, 2]. Ref. [2] describes that for conventional porous asphalt, in a narrow frequency range at 800 Hz almost 100 % of the incident sound energy is absorbed. The absorption capacity depends on the position of the frequency range of the incoming sound waves. Depending on the thickness of the layer, different frequency ranges and frequency bandwidths can be absorbed [2].

In order to achieve noise absorption of the roadway, it is necessary to obtain an exact knowledge of the type of vehicles driving over it. The traffic collective, consisting of cars and trucks, generates sound waves of different frequency ranges. These are due to different tires and driving speeds. In order to maximize the absorption capacity of an asphalt layer, the maximum of the absorption frequency response of the layer must be superimposed with the spectral maximum of the tire-road noise from the traffic collective [3].

From Beckenbauer [2] it is known that the highest frequency of the sound level from a traffic collective with low truck share and high speeds is about 1000 Hz. However, other traffic flows with a higher truck share and lower travel speeds generate a wider frequency spectrum with two peaks within the absorbing curve in the range of 500 Hz to 1000 Hz. Ref. [2] also refers to the sound power levels of tire road noise and drive noise separately for passenger cars, light trucks and heavy trucks as a function of frequency and speed in his study. This shows that tire-road noise (TRN) is mainly between 500 and 2000 Hz and has a maximum

in the range of 800 to 1250 Hz. With regard to the acoustic effectiveness of the absorption of a road surface, the structural parameters of the layer must be adapted to the existing traffic collective.

According to [2], the layer thickness of the asphalt layer determines the position of the frequency maximum in the frequency range between 0 Hz and 8000 Hz. Furthermore, the layer thickness is responsible for the number of absorbable frequency maxima. The height of the porosity, i.e., the cavity system accessible from the outside, determines the height of the amplitude of the frequency maximum, i.e., the maximum absorption capacity.

In addition, the flow resistance in the widely branched cavity system affects the width of the amplitude of an absorbable frequency maximum. It represents a delay of the sound waves when flowing through the pores of a body [1]. Flow resistance is the resistance against air flow through a body. It is significantly influenced by the course of the pore channels and therefore increases with the thickness of the body [16]. The main characteristic of absorbing materials is the friction in the pore channels, which reduces air resistance by converting the kinetic energy of the sound waves into heat, thereby depriving it of power [16].

According to [22] and [3], the stiffness of an absorber layer leads to a noise optimization. This is also known as the mechanical impedance effect. Comparative tests with the same texture of sandpaper and different layers below (concrete layer and elastic layer), Ref. [3] could determine differences in noise generation at traffic crossings. Ref. [22] confirms this phenomenon and justifies it with the fact that sound waves of two materials whose impedance values are in the same order of magnitude can be better transferred to the other medium compared to materials whose impedances distinguish large. In our context, this could clearly mean that the mechanical vibrations emanating from a tire tread block can be better transferred to a rubber-containing substrate or can be damped and absorbed by it. If, on the other hand, the excited tire tread blocks hit a hard asphalt layer, the sound excitation may be stopped abruptly and, in extreme cases, no transfer to the ground occurs [22].

2.2.2 Performance of Mechanical Behavior of Open-Pore Rubber Modified Asphalt

Besides of acoustic effectiveness, the road user expects road safety, driving comfort and absolute availability with regard to the infrastructure while driving his vehicle. This expectation requires the building load bearers to guarantee functional requirements such as grip, evenness and noise reduction as well as the construction requirements for roads such as load-bearing capacity and durability. In order to ensure these requirements, a comprehensive knowledge of the material properties of the road surface to be used is required. Road pavements must

therefore meet performance requirements and be tested in terms of fatigue, deformation, and low temperature behavior.

Open-pore asphalt cannot fully meet the demands placed on it. As a result, open-pore asphalt bound with bitumen often fails prematurely. Recent studies by [27, 11, 13, 4, 19, 15] prove that the addition of rubber particles and additives or even the complete substitution of bitumen by alternative binders such as epoxy resin has a positive effect on the durability of open-pore asphalt. Refs. [27, 11, 13, 4, 15] show in various applications that the durability of the modified pavements is increased and the noise-reducing properties can thus be guaranteed over a longer period of time.

In order to improve the high-temperature resistance of asphalt with rubber granules, Ref. [4] investigated and compared the effects of additives on rubber compound asphalt and found that additives, such as Granular Polymer Durable additive (GPDa), have higher fatigue life and sensitivity to fatigue cracking as well as a good rutting performance.

Since in reality it is not possible to adjust the road construction in such a way that it fulfils all properties to the maximum degree, the different characteristics with regard to the use of certain asphalt layers are weighed against each other during the asphalt design and adjusted and optimized to the local requirements. This adjustment of the overall construction and the individual layer is based on material laws that describe the material behaviour.

2.3 Materials and Methods

Main materials of this study are aggregates, polyurethane binders, and crumb rubber. The coarse aggregate consists of basalt and a common limestone is used as filler. In addition to the mentioned components, rubber particles from shredded scrap tires are included in the mix. All aggregates were dried to a constant mass before the mixing process. The rubber particles were visually checked for moisture. As they were delivered in dry condition, they were added directly to the mixture. Subsequently, all components were mixed with the binding agent. The aim is to achieve the highest possible void content in elastic specimens in order to obtain the basic conditions for absorbing asphalt layers explained in Section 2.2.1. Aggregates and rubber particles are bonded with the single component elastified polyurethane adhesive Elastan* 6568/103 from BASF Polyurethanes GmbH (Lemförde, Germany).

The grading curve on which this study was initially based was the grading curve of a study by [25]. An international short overview of his study is available in [26]. Ref. [25] developed a two-layer road surface system, which has a noise-reducing effect. The system consists of two layers, a wearing course and an absorption layer. The latter is based on previous studies concerning poro-elastic road surfaces (PERS) [24, 17, 22, 23] and shows deficits in its stability. Therefore, the layer is optimized in terms of durability using this study,

as the previous developments [24, 17, 22, 23, 25] only offer maximum noise absorption but a far from adequate suitability for use. The absorption layer developed by [25] ([26]) was therefore further developed. The further development of the absorption layer is the basis of this publication.

A major problem with the use of PERS layers is their high flexibility, which means that the layer will exhibit higher deformation when loaded. This elasticity leads to a good absorption capacity in terms of noise, as the transmission of the resulting structure-borne noise in the layer is reduced by the rubber particles. It may be possible to use such a system as a single layer, even if the high deflections result in increased rolling resistance. This is a significant proportion of tire resistance, along with frictional and aerodynamic resistance, and influences the energy consumption of the vehicle and the driving behavior of the user. Due to the constant deformation of the material, fatigue cracks can occur within the rubber particles or the binder matrix.

If the absorption layer is combined with a wearing course of very stiff material joined by a flexible reinforcement, the absorption layer must be protected from high stress through the edges of the texture layer elements. The stress input of an element that can be pressed into an elastic layer is highest when the absorption layer has maximum elasticity. If, on the other hand, the absorption layer is stiffer, the texture layer element cannot get into a high inclined position and presses itself less into the underlying layer, which leads to lower stress input (Figure 2.1).

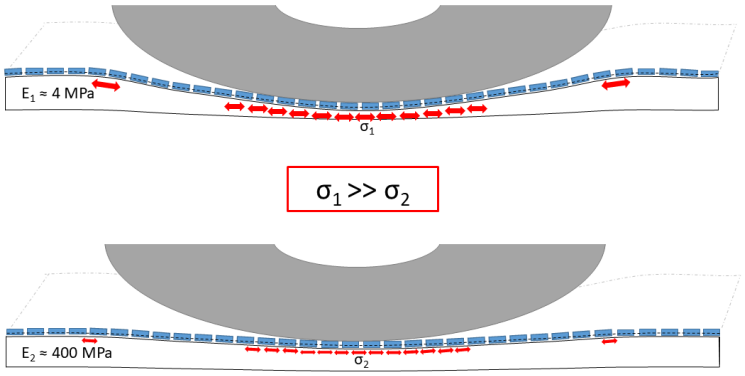

Figure 2.1: Exemplary representation of the stress input through the texture layer into the absorption layer at different stiffnesses of the substrate. (Top) high inclination of texture elements, (bottom) low inclination of the texture elements.

2.3.1 Determination of the Decisive Elastic Modulus Considering the Impact of the Stiff Top Layer

Based on simulations that have been conducted in the project called INNO-PAVE [18], an elastic modulus of E_{el} = 300 MPa allows deflections of the absorption layer of 0.5 mm. Although this deflection is high compared to conventional asphalts, it significantly reduces the stress peaks in the underlying absorption layer. This allows the system to be still elastic, but not subject to the enormous stresses that are likely to cause the material to fail quickly.

Hence, the aim was to increase the stiffness of the absorption layer to such an extent that no critical sinking depths occur and at the same time the acoustic effectiveness is maintained. However, two target values are formulated:

1. The elastic modulus of the layer must meet the stiffness requirements of at least 300 MPa: $E_{el} \geqslant 300$ MPa.
2. The sound absorption capacity in the frequency range of the tire-road-noise (TRN) (800 to 1250 Hz) should be as high as possible: $\alpha_{TRN} \rightarrow max$.

2.3.2 Approach and Test Matrix

Noise reduction through technical road surface construction measures refers to changes in the texture, porosity and flexibility of the road surface. Since in this case, it is not a directly trafficked layer, the optimization of the texture is not relevant. Rather, the focus should be on improving porosity and flexibility. The elasticity is significantly influenced by the proportion of crumb rubber in the polyurethane asphalt layer. The more coarse rubber particles are added to the grain structure, the higher becomes the flexibility of the grain structure. This is because the flexibility of individual grains allows them to be compressed more under load. However, since rubber is the determining factor for the poor stability of the system, the rubber content must be reduced. Hence, this study proceeds in such a way that the proportion of rubber is reduced iteratively. For each test specimen produced in the first part of this study, the acoustic effectiveness is examined on the basis of the acoustic tube and the elastic modulus on the basis of a uniaxial pressure swelling tests.

The porosity was tested in preliminary studies. These showed that test specimens with a void content of 35 % by volume deliver good results. [14] confirmed this in his studies. Various grading curves were tested for the work. In order to use a statement for the selection of the maximum grain size of the grading curve, several possible grading curves with the maximum grain sizes of 5 mm and 8 mm were tested. In the end, it was found that the grading curves in [6, 7] were suitable for the anticipated solution. The left grading curve [6] of Figure 2.2 is a grading curve from a German standard for an open-porous asphalt mix,

which is conventionally used for road paving. The right grading curve [7] of Figure 2.2 is a grain composition for an open-graded mixture used on agricultural roads in Germany. It is usually used unbound and therefore offers a high permeability for the infiltration of rainwater. As these grading curves deliver open-graded mixtures with small grain sizes, it was decided to use them with partial replacement of the aggregates by rubber particles and a binder content of 6 % by volume of the one component polyurethane.

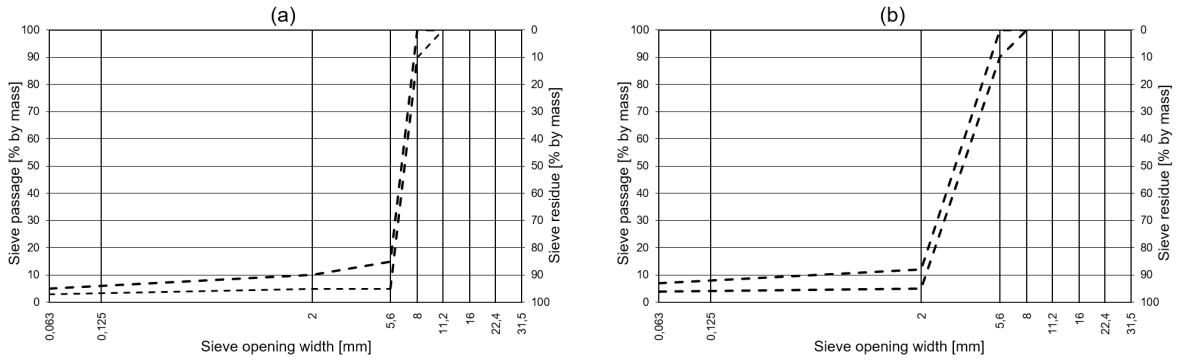

Figure 2.2: Grading curves according to the German guidelines of Porous Asphalt [6] (a) and [7] (b).

The tested variants are shown in Table 2.1. As can be seen, the variant matrix is incomplete. A few specimens were reproduced in order to assess further results on elastic behavior with Var 8 specimens. It should be noted that no acoustic tests have been carried out on the Variants Var 8-2.5, Var 8-7.5, and Var 8-12.5. An exact composition of the polyurethane-bound test specimens is shown in the Appendix in Table 2.5.

Table 2.1: Tested variants.

Crumb Rubber [% by Volume]	**Max. Grain Size 5 mm (Var 5)**	**Max. Grain Size 8 mm (Var 8)**
0	Var 5-0	Var 8-0
2.5	-	Var 8-2.5
5	Var 5-5	Var 8-5
7.5	Var 5-7.5	Var 8-7.5
10	Var 5-10	Var 8-10
12.5	-	Var 8-12.5
20	Var 5-20	Var 8-20

Impedance Measuring Tube

In this test method, the sound absorption coefficient of sound absorbers is determined using an impedance tube. The impedance measuring tube “AFD 1000 - AcoustiTube®” and the

associated analysis software “AFD 1001 - Determination of sound absorption coefficient according to DIN EN ISO 10534-2” [9] are used for this procedure.

The impedance tube (Figure 2.3) consists of a rigid and smooth cylindrical tube that is soundproof and airtight. At one end there is a loudspeaker (Figure 2.3, no. 4) and at the other end the specimen is positioned in a sample holder (no. 3). Two microphones are attached to the tube wall (no. 1 and 2). The diameter of the specimen is 100 mm, so that it fits exactly into the cross-section of the tube. The specimen height of 40 mm is determined in such a way that it corresponds to the layer thickness in practice. By measuring the incident and reflected sound energy, the sound absorption coefficient is calculated and given as a function of frequency. The impedance tube used here covers the frequency range from 250 to 2000 Hz, whereby the respective sound absorption coefficient is determined in 3.125 Hz steps. Since this is a test method in which the specimens are not altered or damaged, each specimen is examined three times, the degrees of absorption of the measurements are averaged and this average value is given as the test result.

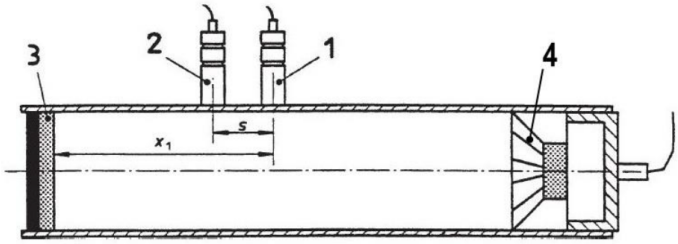

Figure 2.3: Impedance measuring tube according to [9].

With regard to the target of reducing tire-road noise, the sound pressure levels of the frequencies from 800 to 1250 Hz according to [2] are of particular importance. In the evaluation, the frequency-dependent absorption coefficients between these limits are considered (see Figure 2.4).

$$\begin{aligned} \alpha_{TRN} &= \frac{\sum_{F_u}^{F_o} \cdot \alpha_i}{F_o - F_u} \\ absorption\ value &: \alpha_{TRN} \\ lowest\ frequency = 800\ Hz &: F_u \\ highest\ frequency = 1250\ Hz &: F_o \\ absorption\ value\ at\ frequency\ i\ [-] &: \alpha_i \end{aligned} \tag{2.1}$$

To convert the relevant sound absorption coefficients to a measurement or variant-specific value, they are averaged within this range, so that for each measurement one absorption value of the tire-road noise can be given (α_{TRN}).

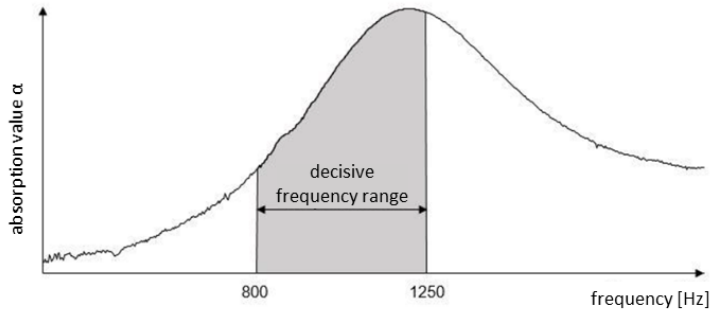

Figure 2.4: Decisive frequency range.

Uniaxial Loading Tests

The aim of this study is to create a flexible and durable absorption layer. As a binding agent, BASF's 1-component polyurethane Elastan* 6568/103 is used, since it was developed for flexible floors, such as sports fields and playgrounds. It is a very elastic binding agent with excellent adhesion to rubber particles.

In order to evaluate the elasticity of the mixture as a whole, the modulus of elasticity can be evaluated. This is the elastic component of the material. The viscous part of the material behavior is very low here and is therefore not used as a decisive factor for the evaluation.

For the experimental determination of the elastic modulus of asphalt, dynamic tests with uniaxial sinusoidal loading at a temperature of 20 °C are used. The sinusoidal load enables the e-modulus to be divided into its elastic and viscous components as Equation (2.2) shows. This can be carried out by using swelling tests [12].

$$\begin{aligned} |E^*| &= E'' + E' \\ storage\ modulus &: E' \\ loss\ modulus &: E'' \end{aligned} \tag{2.2}$$

Due to the elasticity of the specimens, the problem arose that the test stamp repeatedly lifted off the specimen during the test and the universal testing machine stopped frequently. By gradually increasing the contact stress from $\sigma_u = 0.025$ to 0.06 N/mm^2 it was possible to ensure that the stamp remains in contact with the test specimen. The upper contact stress was not changed ($\sigma_o = 0.35$ N/mm^2).

The absolute Young's modulus $|E^*|$ is determined by the continuous application of a dynamic sinusoidal voltage. Figure 2.5 shows a resulting strain reaction of a viscoelastic body. The strain is dependent on temperature, frequency and load.

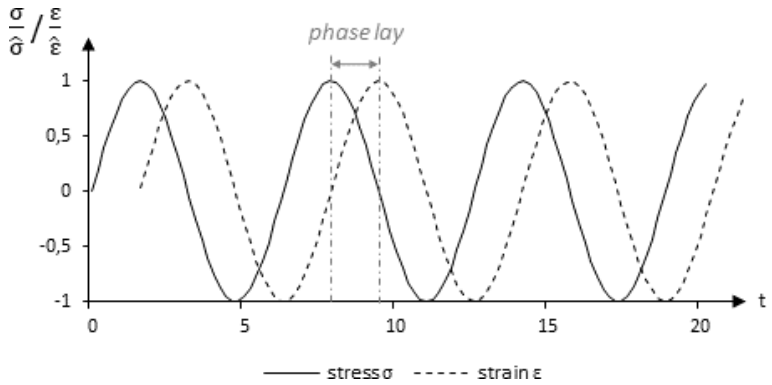

Figure 2.5: Sinusoidal loading according to [12].

The absolute Young's modulus is calculated from the amplitudes of the stress $\hat{\sigma}$ and strain $\hat{\varepsilon}$ using Equation (2.3). In addition, the phase angle is calculated, which can be determined from the phase lay $\triangle t$ between stress and strain amplitude or by the determination of the phase spectrum.

The result of the test is a creep curve with two phases, as Figure 2.5 is showing schematically. In detail, the force and displacement signals obtained from the uniaxial loading test were converted into stresses and strains and divided into their amplitude and phase spectra. This is possible through Fourier Transformation in Matlab®. The maximum amplitude of the stress $\hat{\sigma}$ and the strain $\hat{\varepsilon}$ and the corresponding phase angle ϕ can then be read off from the respective amplitude spectra and phase spectra at the load frequency. Hence, the absolute modulus $|E^*|$ is received from Equation (2.3).

$$|E^*| = \frac{\hat{\sigma}}{\hat{\varepsilon}} \tag{2.3}$$

According to Equation (2.2) the elastic an viscous components of $|E^*|$ are derived from Equations (2.4) and (2.5).

$$E'' = E_{el} = \frac{\hat{\sigma}}{\hat{\varepsilon}} \cdot cos\phi \tag{2.4}$$

$$E' = E_{vis} = \frac{\hat{\sigma}}{\hat{\varepsilon}} \cdot sin\phi \tag{2.5}$$

Testing of Fatigue Resistance

If a material is subjected to repeated loads, the resistance may be reduced by changing its internal stresses and its structure with each additional load. This results in a reduction in the strength of the material until failure occurs.

To determine the fatigue resistance, the method described in [10] is used throughout Germany. This method is intended for testing bituminous asphalt. Ref. [21] proposed a modified

procedure for testing polyurethane-bound asphalt. The test is carried out analogously to the DIN standard, but the strain paths of the dynamic fatigue test are adapted as a function of the material. First, the static flexural strength of the material is determined on the basis of [10]. Then the dynamic test is conducted on the basis of the path-controlled three-point bending test based on [10] in order to determine the stiffness. The tests to determine fatigue resistance are performed at a uniform test temperature of 20 °C.

To find out the static bending tensile strength, a prismatic specimen is integrated into the testing device. The load application device consists of two outer support rollers and an upper central roller for load transfer. The test specimen is mounted with its longitudinal axis perpendicular to the longitudinal axis of the rollers in the middle of the testing machine. After the specimen has been installed and tempered to 20 °C within the testing machine, the test begins with a load-controlled displacement by the upper support pressing on the specimen. The test is completed as soon as the test specimen fails. During deflection, the displacement and the applied force are measured to calculate the static flexural strength.

Following the static bending test, the dynamic three-point bending test according to [21] is performed to address the fatigue behavior. The method developed there is based on the procedure according to Annex C of [10]. In contrast to the original test, the strain amplitudes are determined as a function of the maximum deflection that was determined within the framework of the determination of the static flexural strength. The lower amplitude s_u remains the same as in the DIN standard. The upper amplitude, on the other hand, is set at 2/3 of the maximum deflection from the static flexural tensile test $s_o = \frac{2}{3} \cdot s_{max}$. This was found to be sufficient in the study conducted from [21]. The test setup, the specimens, and the test temperature of the three-point bending test are identical to the conditions of the static bending test. The roller of the upper support is sinusoidally shifted between the vertices s_u and s_o at a frequency of 10 Hz and the force applied is measured. The test is terminated after 20,000 load cycles [21, 10].

Testing of Low Temperature Behavior

When asphalt is exposed to low temperatures, internal stresses – so-called cryogenic stresses – occur. In addition, the road material is usually subjected to traffic, which also creates tensions – the mechanogenic stresses. To determine these stresses, uniaxial tension stress tests (UTST) and thermal stress restrained specimen tests (TSRST) are carried out on the material. The UTST causes the formation of mechanogenic stresses, whereas the TSRST causes cryogenic stresses. The aim is to determine the tensile strength reserve, which forms the stress reserve from cryogenic and mechanogenic stresses. Which allows the determination of possible additional stresses that can be absorbed. Both tests require prismatic specimens which are connected to the testing device at their end faces.

During the UTST, the specimen is brought to a defined temperature within the test chamber. The specimen is then subjected to tensile stress and the resulting stresses and strains are continuously recorded. The test is terminated as soon as the specimen fails. The tensile force at which the specimen failed is used for the evaluation. This is converted into a stress via the cross-section of the specimen. The test is carried out at a total of four temperature levels (+20 °C, +5 °C, −10 °C and −25 °C) so that a tensile strength is determined for the common service temperature range.

The TSRST causes the formation of cryogenic tensions. While the specimen is clamped in the test device and kept at a constant distance, the temperature is continuously lowered (10 K/h). The cooling causes temperature-related stresses which are recorded by the test device as a function of the temperature. They are called thermally induced stresses [5].

2.4 Results and Discussion

2.4.1 Evaluation of the Suitable Variant

The results of the tests mentioned above were evaluated in order to be able to make a decision for the preferred variant on the basis of this information. The pressure swelling test yielded the results shown in Figure 2.6. The evaluation of the layer performance is based on the elastic modulus of elasticity E_{el} in accordance with the best absorption properties. Three specimens of each variant have been tested. The final elastic modulus E_{el} used in the assessment is a mean value of the individual values.

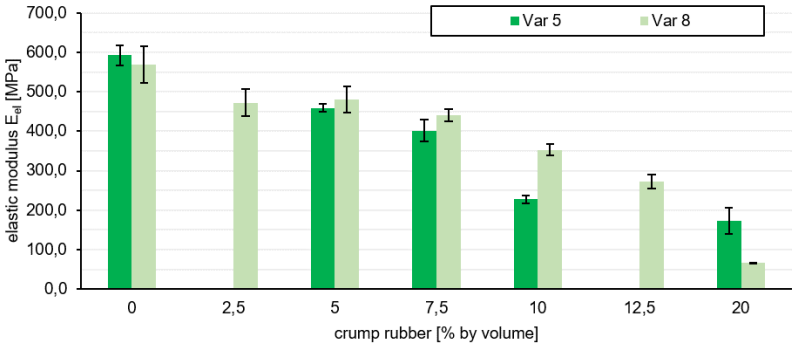

Figure 2.6: Evaluation of the elastic modulus of all tested variants.

The variants without crumb rubber have an elastic modulus E_{el} of 592.2 MPa (Var 5-0) and 568.8 MPa (Var 8-0). The more aggregates are substituted by rubber granulate, the smaller is the E_{el} of both grading curve variants, which is 172.7 MPa for Var 5-20 and 65.8 MPa for Var 8-20. It can be stated that the addition of rubber granulate leads to a reduction in stiffness. The force is transmitted within the polyurethane asphalt layer via a supporting skeleton formed by the aggregates. Due to the volume-accurate, proportional

substitution of the aggregates by crumb rubber, a part of the applied force is absorbed by the rubber granules.

Basically, it can be seen that the absorption curves of the variants tested in this study differ from those of a conventional porous asphalt PA 8. The PA 8-curve is integrated as a reference value in Figure 2.7 in order to compare it with the used mix variants from this study.

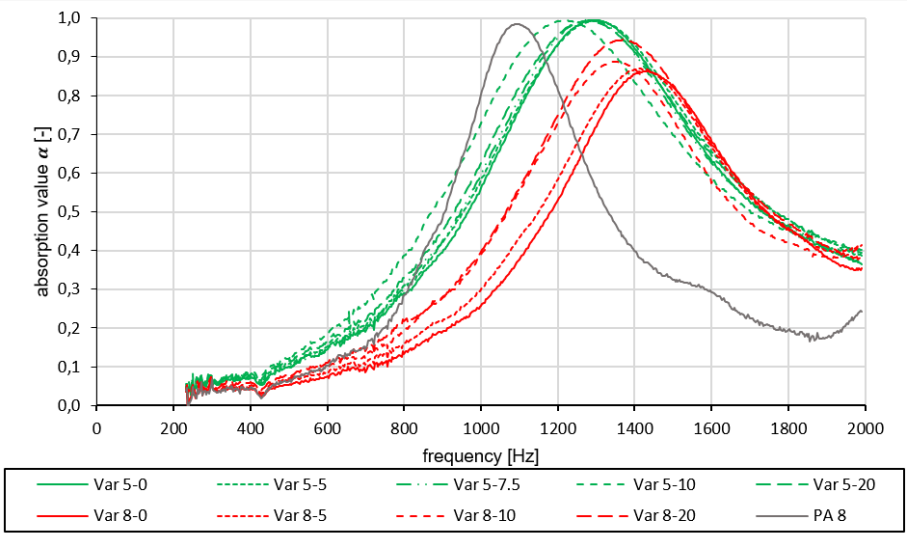

Figure 2.7: Absorption curves of all tested variants including a reference variant (PA 8).

Looking at the test results in Figure 2.7, it can first be seen that the frequency bands of the sound absorption coefficient of the tested variants have pronounced maxima in the range from 1200 to 1300 Hz (Var 5) and from 1350 to 1450 Hz (Var 8). The maximum values of the absorption coefficient of Var 5 with $\alpha = 0.99$ to 1.00 are significantly higher than those of Var 8 ($\alpha = 0.85$ to 0.95). In addition, the absorption maximum of Var 5 covers a wider frequency range ($\alpha \geqslant 0.5$ from approx. 900 to 1700 Hz) than the one of Var 8 ($\alpha \geqslant 0.5$ from approx. 1100 to 1700 Hz). Both variants Var 5 and Var 8 have slipped higher in the frequency range compared to the reference variant and their curves cover a wider frequency range. The wider shape of the absorption curves indicates that the new material guarantees higher degrees of absorption in a larger frequency range.

When comparing the absorption coefficients of Var 5, no clear influence of the rubber content can be discerned due to the very similar curves. However, it is noticeable that the maximum of Var 5-10 is shifted by approx. 100 Hz to a lower frequency range compared to the other four curves. In comparison to Var 5, clear differences can be observed in the curves of Var 8 depending on the rubber content. By increasing the rubber content, increased maximum degrees of absorption can be achieved with $\alpha = 0.925$ (Var 8-10) and $\alpha = 0.948$ (Var 8-20). In addition, a dependency of the associated frequency on the rubber content is discernible, as it moves into a lower frequency range. An explanation is that the cavities of Var 5

have smaller diameters or locally smaller volumes due to the reduced proportion of coarse aggregates. The cavity system in the test specimens, which is responsible for the absorption of the incident sound, becomes smaller and closer meshed as a result. The enlarged inner surface of the polyurethane asphalt skeleton absorbs the incident sound more effectively. Watching the absorption curves of the different variants Var 5 and Var 8, it can be seen that the amplitudes of the absorption curves differ. This is a consequence of higher flow resistance which is characterized through Var 5 which forms a narrow and branched cavity system resulting from a smaller grain size distribution.

In order to determine which variant is suitable both acoustically and in terms of durability, the proportion of space below the absorption curve in the range of 800–1250 Hz is used to evaluate all variants. The procedure was explained in Section 2.3.2. Finally, the normalization results in an absorption value for each tested variant α_{TRN}. Figure 2.8 shows that Var 5 has higher absorption values compared to Var 8. Figure 2.8 describes the absorption value of the respective variant in dependence of the rubber content. From this it can be clearly deduced that the grain size has a decisive influence on the absorption potential of a road layer, because all absorption values of Var 5 are significantly higher than those of Var 8. The PA 8 was also examined with regard to its absorption value. In Figure 2.8, the layer PA 8 is regarded as the comparative value, which shows that the variant Var 5 examined here has very similarly good noise-reducing properties. Since Var 5 contains additional rubber particles, we expect a further noise-reducing effect due to the mechanical impedance effect. This, however, is not examined in this study.

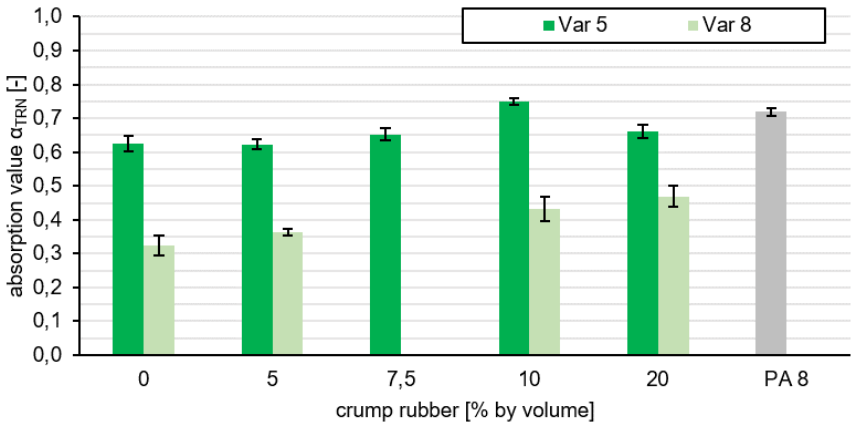

Figure 2.8: Representation of the absorption value via the proportion of crumb rubber.

In order to consider not only the acoustic effectiveness but also the durability, the calculated elastic moduli were plotted on the absorption values in Figure 2.9.

It can be seen that variants with a high absorption capacity have low elasticity values. There are also variants with a higher elastic modulus that have lower absorption values.

Nevertheless, on the basis of Figure 2.9, a statement can be made about the variant that has the best absorption coefficient at the minimum requirement of E-modulus $\geqslant$ 300 MPa.

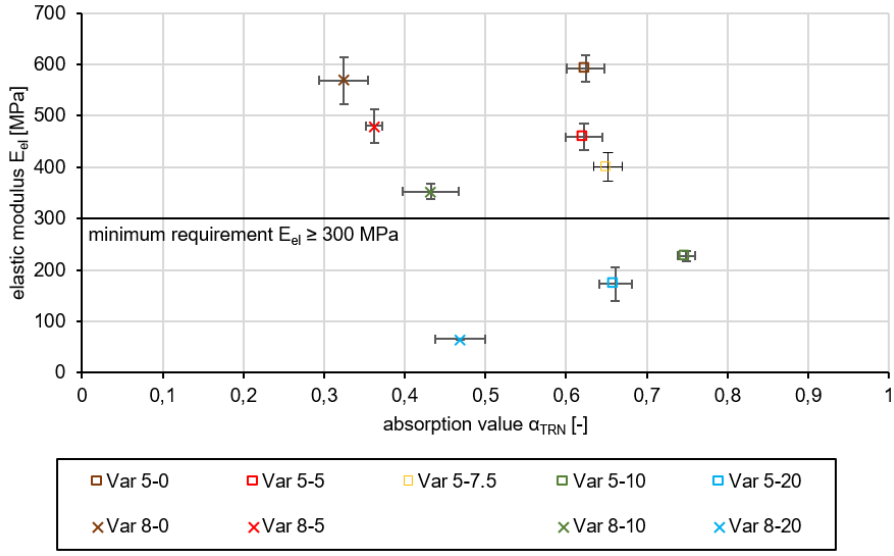

Figure 2.9: Representation of the elastic moduli across the absorption values of all tested variants.

Due to higher and wider acoustic absorption of sound, it can be concluded that Var 5 has better acoustic properties than Var 8. One possible cause is the finer pored and nested structure of the cavity network caused by the smaller aggregates, which leads to a shift of the absorption maximum to a lower frequency and a higher flow resistance. However, Var 5-7.5 forms the highest acoustic efficiency with a stable design. For this reason, it is examined and evaluated by asphalt performance tests in order to see whether it is suitable for use in road traffic.

2.4.2 Asphalt Performance of Var 5

To test the performance of the developed material, test specimens with the composition of the final variant Var 5 were prepared. This is followed by tests on deformation behavior using the pressure swelling test, tests on fatigue resistance using the three-point bending test, and tests on low-temperature behavior using the uniaxial tension stress test and the thermal stress restrained specimen tests. The specimens are produced in accordance with the dimensions required for testing and are shown in Table 2.2. In order to obtain the corresponding dimensions, plates were produced from which the test specimens were drilled or cut.

Table 2.2: Dimensions of tested specimens according to [10, 5, 8].

Performance Test	**Shape**	**Dimensions**	**Height**
pressure-swelling test	cylinder	100 ± 5 mm	60 ± 1 mm
three-point bending test	prism	40×40 mm^2	320 mm^2
uniaxial tension stress test and thermal stress restrained specimen test	prism	40×40 mm^2	160 mm^2

In order to evaluate the findings from this study, a comparison to values from the literature is conducted. The results of the variants tested by [20, 21] were used for this purpose. In his studies, Ref. [21] compared the polyurethane-bonded mixtures PU-Var. A and PU-Var. B with regard to performance characteristics, in which only the size of the maximum grain size of the aggregates used is differentiated. PU-Var. A consists of a grading curve with a maximum grain size of 8 mm whereas PU-Var. B contains a maximum grain size of 5 mm.

Pressure Swelling Test

The compression-swelling test according to TP Asphalt-StB [8] is carried out to test the deformation resistance of the material. The test specimen is loaded by a load stamp with a defined force over 10,000 cycles. The load is applied by a load pulse which applies a maximum stress of $\sigma_o = 0.35$ MPa in a haversine-shaped course. During the loading pause the specimen is exposed to an undervoltage of $\sigma_u = 0.025$. Since an unpublished preliminary study has shown that reacted polyurethane is nearly temperature-independent, the test temperature is reduced from 50 °C to 20 °C.

Deformation Resistance

Strain and strain rate of Var 5-7.5 are shown in Figure 2.10 as a function of the load cycle. The strain of the variant has the typical course of a pulse creep curve without a turning point. There is no failure of the test specimens according to the recorded data. This was confirmed in the visual evaluation of the test specimen after loading since no external damage was visible. After a stronger deformation at the beginning of the test, the strain rate decreases regressively ($\varepsilon^* = 0.142$ ‰$\cdot 10^{-4/n}$ after load cycle 1000) and approaches asymptotically zero within the 10,000 load cycles ($\varepsilon^* = 0.017$ ‰$\cdot 10^{-4/n}$ at the end of the test).

In comparison to reference variants PA 8 and PU-Var. B taken from [21], Var 5-7.5 has an extremely high resistance to deformation. While the PA 8 with a deformation of 90.42 ‰reaches the turning point at 263 load cycles and fails after about 750 load cycles, the strain rate of the Var 5-7.5 at the same time is only 2.28 ‰. Also, the associated strain rate (PA 8:

approx. 2.2 ‰·$10^{-4/n}$) is clearly lower with 0.569 ‰ ·$10^{-4/n}$. The tested PU-Var. B from [21] seems to have a similar course as the Var. 5-7.5 tested in this study. There is no turning point during the 10,000 load cycles and a deformation of approximately 10 ‰ is achieved. It fails after about 40,000 load cycles.

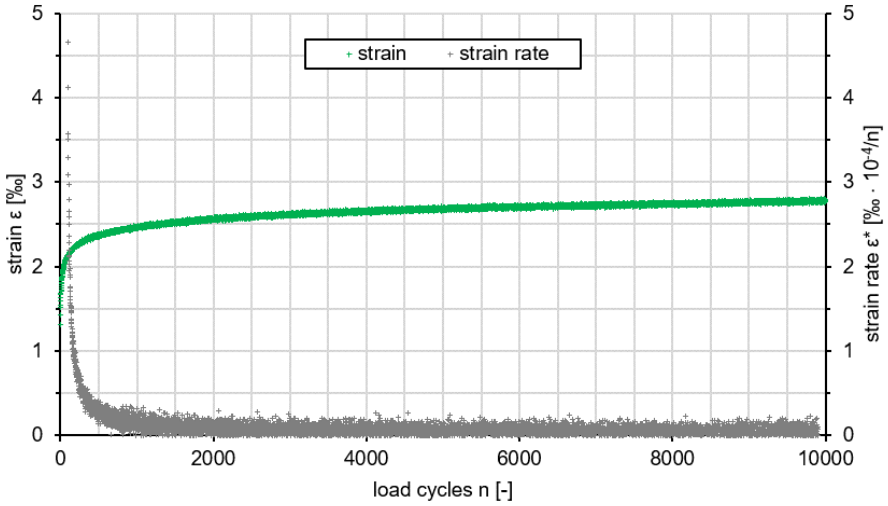

Figure 2.10: Results of the pressure swelling test and impulse creep curve (green) and strain rate (grey) of Var 5.

The resistant material behavior of Var 5-7.5 is mainly based on the use of the polyurethane binder. This will possibly be supported by the highly regenerative rubber granulate. The complete coating of the aggregates with polyurethane results in a monolithic structure despite the open-graded structure of the polyurethane asphalt mix. The reduction of the strain rate over the increasing number of load cycles can be attributed to the fact that no binder-induced creep occurs with polyurethane-bound aggregates and that the test specimen can only be damaged due to higher loads. A modification (increased loads) has been made by [21] for this case to cause the material to fail. This has not been applied to the present material, yet.

In conclusion, it can be stated that the deformation properties of the investigated Var 5-7.5 proved to be very good. Compared to a porous asphalt PA 8, there is very little deformation.

Results of the Three Point Bending Test

Following, the results of the three-point bending test are shown in Figure 2.11. Three tests on the same polyurethane asphalt mix have been conducted. Looking at them, it is visible that two of the three (A and B) have almost same course, while Var 5-7.5-C differs slightly. First, the absolute elastic modulus of the test specimens drops sharply to a relatively constant

level and shows hardly any fatigue in the course of time. At Var 5-7.5-C, the elastic modulus sinks slightly longer until it also stabilizes at a certain level.

The fatigue test results are also shown in Table 2.3. A specimen is considered fatigued when the stiffness $|E|$, which decreases over the period of loading, drops to half the initial stiffness. The initial stiffness is the stiffness recorded at the 100th load cycle. The load cycle at which fatigue occurs is important for evaluation in order to draw a comparison of fatigue times between different mixes. For the evaluation a mean value of all tested variants (A, B, and C) was taken as a basis. Compared to the initial stiffness after 100 load cycles, which at 537 MPa is significantly lower than that of the PU-Var. B ($|E|_{100}$ = 3322 MPa) of [21], there is only a slight decrease in stiffness over the further load cycles. After 20,000 load cycles, the mean stiffness of all tested variants is 386.1 MPa and thus still corresponds to 72 % of the initial stiffness $|E|_{100}$. No external damage or cracking could be observed on the test specimens after the end of the test.

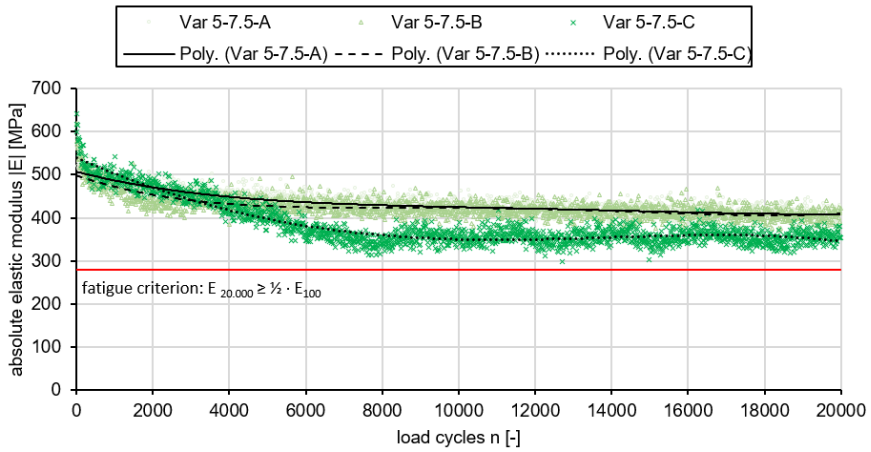

Figure 2.11: Results of the fatigue test; Stiffness decrease of three specimens of Var 5.

The number of load cycles at which the value of the elastic modulus assumes half of its initial value cannot be determined, since the tests were terminated after the 20,000 load cycles, in accordance with the test procedure of the DIN standard.

Table 2.3: Results of fatigue testing. PU-Var. A and B taken from [21].

Variant	$\mathbf{\lvert E\rvert_{100}}$ [MPa]	$\mathbf{n(1/2 \cdot \lvert E\rvert_{100})}$ [-]	$\mathbf{\lvert E\rvert_{20{,}000}}$ [MPa]
Var 5-7.5	537	not reached	386
PU-Var. A	2277	831	577
PU-Var. B	3322	4201	727

In summary, it can be said that the newly developed material Var 5-7.5 has a fundamentally

lower elastic modulus compared to other mix variants [20, 21]. However, the variant is characterized by its partial elasticity, which has decreased only slightly over the course of the tests carried out. Fatigue that occurred with other polyurethane-bound variants of [21] was not achieved by the variants tested in this study, although the test conditions adapted to the material were applied. Accordingly, the material has good fatigue resistance and is suitable for use in transport infrastructure.

Results of the Uniaxial Tensions Stress Test and the Thermal Stress Restrained Specimen Test

To evaluate the low-temperature behavior of asphalts, a combined evaluation of UTST and TSRST is performed. The maximum tensile stresses $\beta_{t,max}$ are plotted on a cubic spline curve in a diagram as a function of temperature. The curve of thermal stresses σ_{cry} of the material is integrated in the same diagram in order to determine the tensile strength reserve $\triangle\beta_t$ from the difference between the two curves.

The cryogenic behavior of Var 5-7.5 is shown in Figure 2.12. It can be seen that the cryogenic tensile stress has its maximum of 0.62 MPa ($\sigma_{cry(T)}$) at 20 °C, reaches a minimum at lower temperatures ($\sigma_{cry(T)}(5\ °C) = 0.06$ MPa) and rises again to $\sigma_{cry(T)}(-17.7\ °C) = 0.48$ MPa. The tensile strength reserve $\triangle\beta_t(T)$ resulting from the difference between the two input variables increases to 0.52 MPa at 5 °C and doubles to −20 °C (0.99 MPa).

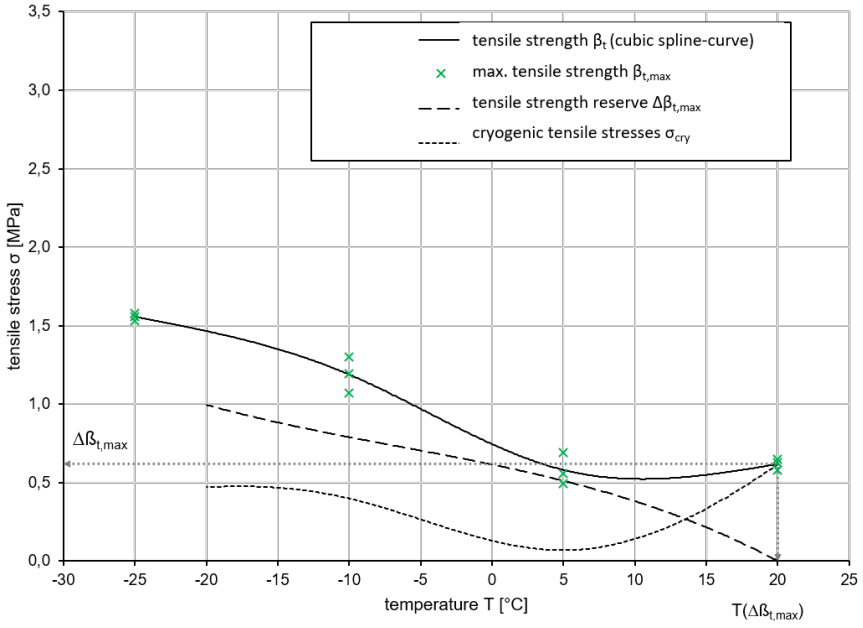

Figure 2.12: Results of the low temperature behavior of Var 5-7.5.

It can be seen that the cryogenic tensile stress increases to 0.52 MPa at 5 °C and doubles to −20 °C (0.99 MPa). Its function $\sigma_{cry(T)}$ has an initially degressive and then linear course.

The tensile strength reserve $\triangle\beta_t(T)$ resulting from the difference between the two input variables has its maximum of 0.62 MPa ($\triangle\beta_{t,max}$) at 20 °C, reaches a minimum at lower temperatures ($\triangle\beta_t(5\ °C) = 0.06$ MPa) and rises again to $\triangle\beta_t(-17.7\ °C) = 0.48$ MPa.

On the basis of the measurement results, the low temperature behavior of Var 5-7.5 can be assessed as inadequate. Even at a temperature drop to 5 °C, the tensile strength reserve for absorbing mechanogenic, i.e., traffic load-related tensile stresses drops to a critical level of 0.06 MPa. The tensile strength, which remains unchanged at this temperature, contrasts with increasing cryogenic stresses.

Therefore, the material has been modified in terms of its binder content. The polyurethane content would be increased from 6 % by volume (2.2 % by weight) to 13 % per volume (5 % by weight). This binder content was determined to be optimal in studies that tested several amounts of binder at low temperatures and it was determined in the study of [21] as well. An increase in the binder content considerably increases the material's tensile strength, but prospectively does not limit its deformation and durability behavior, as the polyurethane-film merely wraps around the aggregate to form a monolithic system. Excess material concentrates at the bottom of the specimen.

Probably the monolithic structure at Var 5-7.5 was not completely formed, so there were unglued areas in the aggregate structure. This circumstance could now be counteracted. Performance in terms of deformation and durability on the adjusted mixture should continue to be consistent if not better.

The low-temperature behavior of Var 5-7.5-T is shown in Figure 2.13. In contrast to Var 5-7.5, Var 5-7.5-T has a significantly higher tensile reserve, which is due to the high tensile strength of the material. By increasing the binding agent, the material can be compared with conventional asphalts and classified in an appropriate range.

A comparison of the variants from [21] with the characteristic values for low-temperature behavior is made using the Table 2.4. The maximum tensile strength reserve and the corresponding temperature were used for the evaluation.

Var 5-7.5-T does not achieve higher tensile forces in the low-temperature range than the polyurethane variant of [21] or the SMA 11 S [21]. However, the maximum tensile strength reserve values of the materials tested in this study occur at completely different temperatures. Especially cryogenic stresses decrease with increasing temperature. A difference to the PU-Var. A of [21] is the used crumb rubber and the elastified polyurethane in Var 5-7.5 and Var 5-7.5-T, which leads to a more elastified construction and thus, to lower tensile strength. A course that is common in conventional asphalt cannot be determined in the presented results. It should be noted that the low-temperature behavior of the comparative

values was investigated by different testing institutes (University of Siegen and asphalt-labor, Arno J. Hinrichsen GmbH & Co.) and that therefore identical test conditions cannot be guaranteed.

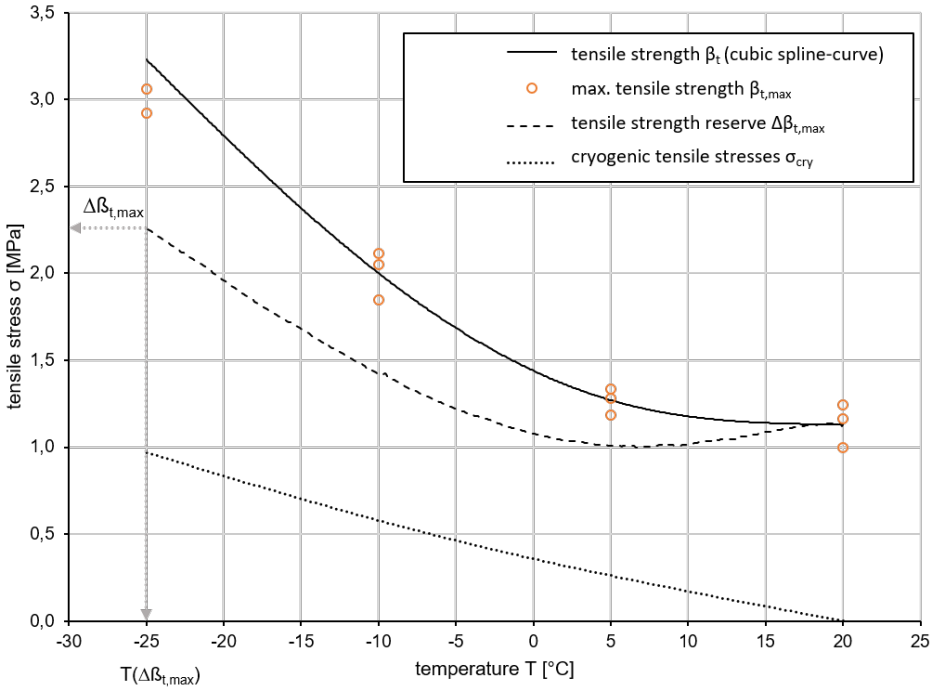

Figure 2.13: Results of the low-temperature behavior of Var-5-7.5-T.

Table 2.4: Results of low temperature behavior of Var 5-7.5, Var 5-7.5-T from this study and PU-Var. A and SMA 11 S from [21].

Variant		**Var 5-7.5**	**Var 5-7.5-T**	**PU-Var. A**	**SMA 11 S**
T	[°C]	20	−25	−9.9	−6.5
$\triangle\beta_{t,max}$	[MPa]	0.618	2.261	3.248	3.397

2.5 Conclusions

In this study, an innovative noise-reducing pavement layer was developed that can be placed under a special surface layer. A material has been developed that reduces noise and is durable, which was problematic with comparable materials from previous studies [3, 2, 17, 25, 24, 22, 23]. In order to achieve this goal, an iterative parameter study was carried out in which a potential material mixture was investigated by determining the elastic modulus and the absorption values. The best material composition was then subjected to tests to determine the performance characteristics in order to evaluate whether the polyurethane asphalt could be used for traffic infrastructure applications.

It could be proven that the developed material enables a 100 % absorption of the incoming

traffic noise in a defined frequency range. This absorption is made possible by a wide-branched cavity system in the layer. Compared to other tested variants, the optimal variant is characterized by a wider amplitude of the absorption curve. This means that the optimal variant can absorb more noise over a wider frequency spectrum than other variants. Hence, not only can noise of certain traffic collectives efficiently be absorbed, since it occurs in a defined frequency range, but the noise absorption can also work for changing traffic collectives. This is the result of a high flow resistance caused by narrow and rough pore spaces in the material, which are mainly due to the choice of the maximum grain size of 5 mm.

By testing the performance in terms of deformation resistance, fatigue resistance and low-temperature behavior, it can be shown that the material is suitable for use in road traffic. High deformation and fatigue resistances can be detected, which are given by the strong resilience of the tested specimens. The low-temperature behavior provides acceptable values.

In principle, it can be said that this material is qualified for use in road traffic with regard to noise reduction. The use of sustainable components and the integration of recycled rubber promotes the efficiency of building materials. This is because materials are recycled, which means conserving non-renewable resources. This is followed by a strengthening of the materials, which results in greater durability and saves the transport network many interventions due to repairs.

2.6 Appendix

Table 2.5: Mixture composition of tested 5 mm variants in % by volume.

Aggregate [-]	**Fraction** [mm]	**Density** [g/cm³]	**Var 5-0** [%]	**Var 5-5** [%]	**Var 5-7.5** [%]	**Var 5-10** [%]	**Var 5-20** [%]	**Var 5-7.5-T** [%]
limestone	filler	2.73	4	4	4	4	4	4
basalt	0–2	3.05	3	3	3	3	3	3
basalt	2–5	3.09	93	88	85.5	83	73	85.5
crumb rubber	super grob	1.1	0.0	5	7.5	10	20	7.5
polyurethane	Elastan	1.1	6	6	6	6	6	13

References

[1] S. Alber. "Veränderung des Schallabsorptionsverhaltens von offenporigen Asphalten durch Verschmutzung." PhD-Thesis. Stuttgart: University of Stuttgart, 2013.

[2] T. Beckenbauer. "Physik der Reifen-Fahrbahn-Geräusche – Geräuschentstehung, Wirkmechanismen und akustische Wirkung unter dem Einfluss von Bautechnik und Straßenbetrieb." In: *Geräuschmindernde Straßenbeläge in der Praxis – Lärmaktionsplanung* 4 (2008).

[3] T. Beckenbauer. "Reifen-Fahrbahngeräusche - Minderungspotenziale der Straßenoberfläche." In: *Fortschritte der Akustik, DAGA, Jahrestagung für Akustik* 29 (2003), pp. 20–29.

[4] X. Cheng et al. "Performance Evaluation of Asphalt Rubber Mixture with Additives." In: *Materials* 12(8) (2019).

[5] Forschungsgesellschaft für Straßen- und Verkehrswesen. *Arbeitspapier Tieftemperaturverhalten von Asphalt - Teil 1: Zug- und Abkühlversuche (FGSV 725)*. Köln, 2012.

[6] Forschungsgesellschaft für Straßen- und Verkehrswesen. *Merkblatt für Asphaltdeckschichten aus Offenporigem Asphalt (OPA) (FGSV 750)*. Köln, 2013.

[7] Forschungsgesellschaft für Straßen- und Verkehrswesen. *Merkblatt für Versickerungsfähige Verkehrsflächen (MVV) (FGSV 947)*. Köln, 2013.

[8] Forschungsgesellschaft für Straßen- und Verkehrswesen. *Technische Prüfvorschriften für Asphalt (TP Asphalt-StB) - Teil 25 B 1: Einaxialer Druck-Schwellversuch - Bestimmung des Verformungsverhaltens von Walzasphalt bei Wärme (FGSV 756 / 25 B1)*. Köln, 2018.

[9] German Institute for Standardisation. *DIN EN 10534-2:2001: Determination of Sound Absorption Coefficient and Impedance in Impedance Tubes - Part 2: Transfer-Function Method; Correction 11-2007*. Berlin, 2007.

[10] German Institute for Standardisation. *DIN EN 12697-24:2018-11: Bituminous Mixtures - Test Methods - Part 24: Resistance to Fatigue*. Berlin, 2018.

[11] A. Gupta, J. Rodriguez-Hernandez, and D. Castro-Fresno. "Incorporation of Additives and Fibres in Porous Asphalt Mixtures: A Review." In: *Materials* 12 (19) (2019).

[12] T. Huschek. "Zum Verformungsverhalten von Asphaltbeton unter Druck." PhD-Thesis. Zürich: ETH Zürich, 1983.

[13] S. Luo, Q. Lu, and Z. Qian. "Performance evaluation of epoxy modified open-graded porous asphalt concrete." In: *Construction and Building Materials* 76 (2015), pp. 97–102.

[14] S. Meiarashi. “Porous Elastic Road Surface as Urban Highway Noise Measure.” In: *Journal of the Transportation Research Board* 1880 (2004), pp. 151–157.

[15] M. A. Morcillo et al. “Life SOUNDLESS: New Generation of Eco-Friendly Asphalt with Recycled Materials.” In: *Environments* 6(4) (2019), p. 48.

[16] M. Möser. *Technische Akustik*. 9th ed. Berlin: Springer-Vieweg, 2012.

[17] N.-A. Nillson, N. Ulmgren, and A. Sandin. “A quiet poroelastic road surface manufactured in a normal asphalt mixing plant.” In: *The Journal of the Acoustical Society of America* 123 (2008).

[18] M. Oeser et al. *INNO-PAVE : Final report: "Grundlagen der konstruktiven Gestaltung, Struktur sowie neuer polymerer Werkstoffe für:Straßendeckschichtsysteme" im Verbundprojekt: "Grundlegende Erforschung polymerer Werkstoffe sowie innovativer Herstellungs- und Einbautechnologien für Straßendeckschichtsysteme" : Duration of research project: 09/2015-04/2019*. Aachen, 2019.

[19] L. Renken. “Development of PU-Asphalt - from the concept to the practical implementation.” PhD-Thesis. Aachen: RWTH Aachen University, 2019.

[20] L. Renken, S. Kreischer, and M. Oeser. “Entwicklung von Deckschichtmaterialien für versickerungsfähige Verkehrsflächenbefestigungen auf Basis alternativer Bindemittel - Teil I: Festigkeit, Permeabilität, Kornverlust.” In: *Straße und Autobahn* 9 (2015), pp. 601–608.

[21] L. Renken, S. Kreischer, and M. Oeser. “Entwicklung von Deckschichtmaterialien für versickerungsfähige Verkehrsflächenbefestigungen auf Basis alternativer Bindemittel - Teil II: Ansprache der Performance.” In: *Straße und Autobahn* 9 (2015), pp. 776–784.

[22] U. Sandberg and J. A. Ejsmont. *Tyre/Road Noise Reference Book*. Harg, Kisa, Sweden: INFORMEX, 2002.

[23] U. Sandberg and B. Kalman. “The Poroelastic Road Surface - Results of an Experiment in Stockholm.” In: *Proceedings of the Forum Acusticum, 4th European Congress on Acoustics, Budapest, Hungary* (2005).

[24] U. Sandberg et al. *State-of-the-Art regarding poroelastic road surfaces (PERSUADE - PoroElastic Road SUrface: An Innovation to Avoid Damages to the Environment)*. 2010. URL: https://persuade.fehrl.org/ (visited on 01/05/2020).

[25] A. Schacht. “Entwicklung künstlicher Straßendeckschichtsysteme auf Kunststoffbasis zur Geräuschreduzierung mit numerischen und empirischen Verfahren.” PhD-Thesis. Aachen: RWTH Aachen University, 2015.

[26] A. Schacht, S. Faßbender, and M. Oeser. “Development of an acoustically optimized multi-layer surface-system based on synthetics.” In: *International Journal of Transport Science and Technologie (IJTST)* 7 (2018), pp. 217–227.

[27] J. P. Wu, P. R. Herrington, and D. Alabaster. “Long-term durability of epoxy modified open-graded porous asphalt wearing course.” In: *International Journal of Pavement Engineering* 20 (2017), pp. 920–927.

3 Investigation of the Reusability of a Polyurethane-Bound Noise-Absorbing Pavement in Terms of Reclaimed Asphalt Pavement

This paper was published under:

Faßbender, Sabine and Oeser, Markus: "Investigation of the Reusability of a Polyurethane-Bound Noise-Absorbing Pavement in Terms of Reclaimed Asphalt Pavement". In: Materials, 15(9), 3040, https://doi.org/10.3390/ma15093040, 2022.

3.1 Abstract

A key aspect of sustainable pavement construction is the use of environmentally friendly designed pavement materials. These materials are characterized by the fact that they are renewable raw materials, require a low amount of energy during production, and in the best case, are made from a high proportion of recyclable materials in order to reduce waste. A number of recent studies have demonstrated the recyclability of waste materials that can be very well utilized in road construction. This study describes the recycling of a new and innovative topcoat system that already contains recycled materials. However, the focus is on guaranteeing the mechanical performance of the innovative absorption layer where different portions of used material are added. Therefore, low-temperature behavior, durability, fatigue, and noise absorption were investigated in detail and concluded that its function is preserved. In order to investigate these characteristics, the impedance measuring tube, the uniaxial cyclic compression test (UCCT), the three-point bending test (3PB), the uniaxial tension stress test (UTST), and the thermal stress restrained specimen test (TSRST) are used. However, the examined absorption material can be reused to build innovative roads.

3.2 Introduction

Sustainability is one of the most important issues to protect the planet Earth and to provide a good life for future generations. In the wake of this realization, action plans have been developed worldwide to protect and regenerate our planet.

On this occasion, the new Circular Economy Action Plan of the European Commission was adopted in 2020 [3]. This calls on the population to implement the European Green Deal, which requires the EU to promote regenerative growth by giving more back to the planet than is taken from it. In addition, resource consumption should be within the planet's carrying capacity, leading everyone to reduce their ecological footprint. Finally, another key goal is to double the circular use of materials in the coming years [3]. It was not only the European Commission that developed an action plan. The United Nations also has a sustainable development agenda for the world. This provides 17 goals to be implemented to achieve a sustainable planet. In addition to social and health goals, the focus is also on infrastructure and consumption goals. Goals 9 and 12, for example, aim to develop a resilient infrastructure and promote sustainable consumption and products. Here, the efficient use of natural resources and waste reduction are of great importance [27].

One approach to this process is the use of sustainable materials in the construction industry. Sustainable materials are characterized by the fact that they are renewable raw materials,

require a low amount of energy during production, and in the best case, are additionally made from a high proportion of recyclable materials.

In the course of developing an innovative pavement, a noise-reducing two-layer surface was developed by Faßbender and Oeser [4] first. Here, a bottom layer, which enables the absorption of noise, is made of rock, crumb rubber, and polyurethane. A void-rich pore structure of the material from [4] results in a high absorption capacity, which leads to a great noise reduction. Additionally, the material delivers high mechanical strength and durability.

The study by Faßbender and Oeser is based on the international findings of Sandberg, Ejsmont, Goubert, and Schacht ([14, 15, 25, 26]) which dealt with the investigation of poro-elastic pavements (PERS). PERS is a road surface with a high void content (30 - 40 vol.-%) made of aggregates, rubber particles (up to 90 wt.-%), and polyurethane binder.

The binder polyurethane replaces bitumen in the invented mixes. Polyurethane exists as a one- or two-component system composed of a polyol and an isocyanate. During production, a polyaddition reaction of polyols and isocyanates takes place, resulting in the formation of a urethane group [16]. Polyurethane can be manufactured from a variety of available raw materials and offers a wide range of applications with high stability [22, 1].

The development of high-performance road materials helps to ensure long-term durability and the relevant function of roads. To this end, many experiments on high-performance construction materials such as polyurethane-bonded asphalts have been done in the past. In particular, the research reports from the research projects LIDAK [19], INNO-BOND [24], INNO-PAVE [20] and the works from Renken [23, 22], Schacht [26], Lu [17] and Faßbender and Oeser [4] provide sufficient evidence of the sustainability of polyurethane-bound and permeable asphalt pavements. They are characterized as follows:

- They use polyurethane binder (i.e. Elastopave®), of which 83 % of the polyol component can be produced from renewable raw materials (e.g. ricinus oil) and thus, distance themselves from the conventional binder bitumen, which is not a renewable raw material [22].
- They provide infiltration capacity of surface water and thus prevent flooding [22, 17].
- They can reduce the heat island effect in cities, because of their density and low heat storage capacity [22].
- They offer a high noise reduction potential due to their cavity-rich structure with simultaneous long-term durability [22, 17, 4].

In addition to the development of the innovative an sustainable pavement materials, the potential of the recyclability of these materials is also of great importance. In Germany,

conventional asphalt recycling is generally carried out by adding reclaimed asphalt pavement material (RAP) to new Hot Mix Asphalt. Only RAP that is suitable according to the *Technical Terms of Delivery for Asphalt Granulate TL AG-STB 2009* [6] may be used. In order to keep the quality of the milled material high, layer-by-layer milling is recommended [5].

A distinction is made in the use of asphalt granulate between recycling and reuse. Recycling describes the process in which the added asphalt is processed into a new material and is then used, for example, in construction material mixtures for base layers with hydraulic binders. Reuse is the repeated use of a material, in which RAP is added to Hot Mix Asphalt [5]. If RAP is to be used in asphalt layers, the maximum amount to be added is calculated depending on the properties of the RAP. The addition of the RAP influences the quality of the fresh Hot Mix Asphalt, which must meet the requirements of the *Technical Terms of Delivery for Asphalt TL Asphalt-StB*. Once all quality requirements have been fulfilled, the mix is paved.

Against this background, the question arises whether innovative mixed pavement mixtures such as those of [22], [17], and [4] can also certainly be reused proportionately and whether this affects the mechanical properties of the finished material.

Building on the previous study by Faßbender and Oeser [4], the current study aims to find out whether the absorbing layer can be reused and shows similar material performance. This leads to the intent of this study, which is to investigate the extent to which polyurethane-based reclaimed asphalt pavement material (PU-RAP) can be used as an additive material for new polyurethane-bound asphalt mixes and whether the use of PU-RAP imposes any limitations on the functionality of the pavement. At the same time, the comparison is drawn with the variant from [4] without recycled components.

3.3 Methodology and Materials

3.3.1 Methodology

To answer the question as to whether the substitution of aggregates by PU-RAP degrades the material properties, a clear methodology is applied. The developed material from [4] is used as the basis for this study in order to enable a concrete comparison of the material properties of the freshly composed mix and the mix produced with PU-RAP.

For this purpose, in the first step, the mix from [4] is produced and processed into PU-RAP (see chapter 3.3.2). Then the material is manufactured again, but PU-RAP is substituted in different proportions. The material properties are then determined for the different variants. This is followed by the investigation of the material performance on the specimens, which

consists of the investigation of the absorption behavior, the deformation behavior, the fatigue behavior, and the low-temperature behavior.

3.3.2 Material

The grading curve developed by Faßbender and Oeser [4] is used as the starting point. The grading curve distribution was developed to provide optimal mechanical and acoustic properties of the poro-elastic absorption layer. The developed grading curve distribution forms an aggregate structure with a high void content. The base aggregate material consists of 4 vol.-% limestone filler, 3 vol.-% basalt sand, 85.5 vol.-% basalt crushed stone, and 7.5 vol.-% rubber granules from Genan GmbH (Dorsten, Germany) (also see Table 3.4). To this mix, polyurethane from BASF Polyurethanes GmbH (Lemförde, Germany) was added as a binder to ensure the functionality (see Table 3.1) and replace the conventionally used bitumen binder. The rubber granulate consists of recycled car tires and has grain sizes from 2 to 6 mm. In this work, the one-component binder used in the previous study [4] is replaced by a two-component polyurethane binder which is assumed to increase the final stiffness. The two-component binder is composed of a polyol (Elastopave 6551/102) and an isocyanate (IsoPMDI 92140), which are mixed before applying to the aggregates. The mixing ratio indicated by the manufacturer is 100:68. The polyol is based on vegetable oils 45 % of which are made from renewable raw materials (see product information form from BASF Polyurethanes GmbH in [22]). Table 3.5 in the appendix shows typical physical properties of the used polyurethane Elastopave® 6551/102.

Table 3.1: Mix design.

Mixture Components	**Amount**	**Unit**
aggregates	80.5	vol.-%
rubber granules	6.5	vol.-%
two-component polyurethane	13	vol.-%

Preparation of the PU-RAP

In order to produce the PU-based reclaimed asphalt pavement (PU-RAP), approximately 280 kg of the base material was prepared in a batch mixer and backfilled in the paving section of the Institute of Highway Engineering. For this purpose, a hole with a depth of 30 cm was excavated and filled with the polyurethane mixture. After curing of the mix, the layer was broken up. This process was done after 48h with the help of a conventional asphalt milling machine (Figure 3.1(b)). The layer was milled only in the center to avoid contamination of the milled material by the surrounding soil. After this, a roller compactor broke the material once again due to rolling over it on the ground in order to receive finer

material (Figure 3.1(e)). The milled and crushed material was collected and stored dry in containers. During the production of the PU-RAP, no separation of polyurethane and aggregates was carried out, which means that the old polyurethane is present in the PU-RAP as a solid component that adheres to the aggregate. Figure 3.1 provides an insight into the preparation process.

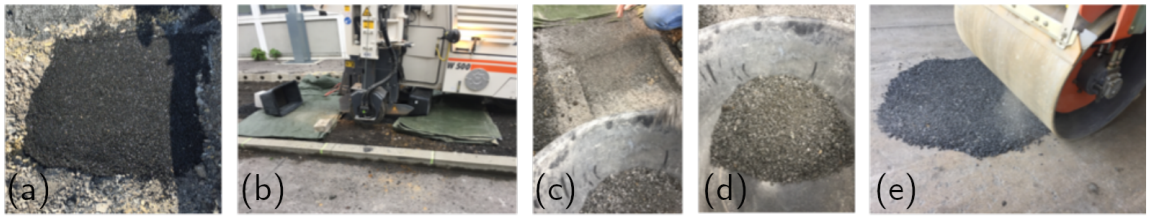

Figure 3.1: Preparation of the PU-RAP: (a) PU-asphalt pavement section on construction site. (b) Milling of the PU pavement. (c) View on the milled fractions after milling. (d) PU-RAP placed in bucket (e) Crushing of the PU-RAP by a roller compactor.

Furthermore, the PU-RAP was split into its individual fractions. After initial screening, it was found that the milled material had a too high oversize content to produce a grading curve according to [4] (high proportion of grain fractions larger than 8.0 mm in diameter). In order to have sufficient PU-RAP available for the production of the test variants, the oversize fraction was reduced once again by passing a compaction roller on a rigid base. The subsequent screening of the PU-RAP yielded a total mass of 80 kg in three different grain fractions. These three-grain fractions occupy the range of 0-8 mm grain diameter (Figure 3.1 (e)). Since the grading curve of the base material contains a defined filler fraction, the PU-RAP filler was also substituted proportionally.

Design of the Test Variants

Within the scope of this work, three variants were worked out in addition to a reference variant, which is produced based on the initial material taken from [4]. The initial material is volumetrically substituted by the PU-RAP material in the individual grain fractions. To each variant, a different proportion of PU-RAP material was added. This approach ensures that the same proportion of PU-RAP material is present in each grain fraction and that the grading curves defined in the previous study [4] can be realized. Table 3.2 shows the material composition.

Table 3.2: Substituted PU-RAP proportion of the fraction of the aggregate.

Variant		**RAP0**	**RAP25**	**RAP50**	**RAP75**
PU-RAP	[vol.-%]	0	25	50	75

The different variants are always made using the same procedure to ensure the greatest possible comparability. To produce the specimens for the investigation of the low-temperature behavior and the fatigue testing, specimen plates measuring 32 x 26 x 4 cm^3 were manufactured, from which the prismatic specimens were cut out. In order to avoid negative influence, the edge areas of the plates are removed.

The cylindrical specimens for the deformation resistance tests and the absorption capacity tests are prepared in single molds with a diameter of 100 mm and a height of 60 mm.

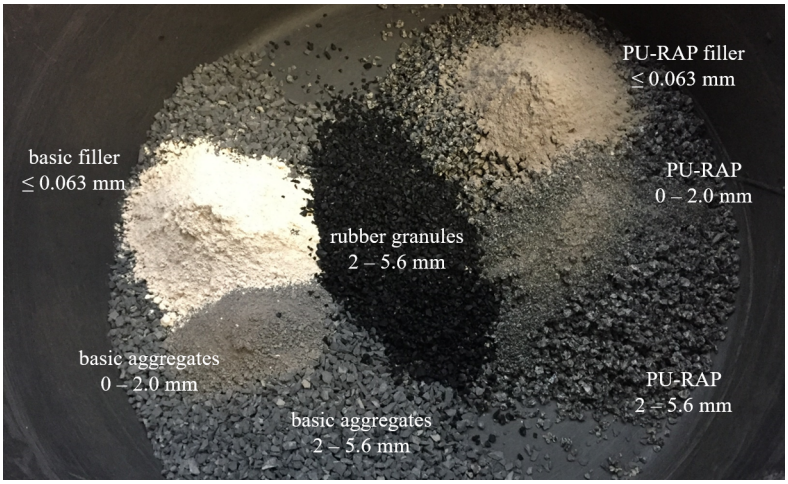

Figure 3.2: PU-RAP and basic material in visual comparison.

Looking visually at the PU-RAP compared to the original material, one difference, in particular, can be seen between the base filler and the recycled filler (see Figure 3.2). The lighter components are the basic materials, and the more gray ones are the recycled ones.

All variants are made with 13 vol.-% polyurethane and 7.5 vol.-% rubber and the aggregates are partially substituted with PU-RAP at 25 %, 50 %, and 75 %.

Due to low laboratory capacities, only three variants (RAP0, RAP25, RAP50) were investigated in the low temperature and fatigue tests. Deformation resistance and absorption capacity were tested on all four variants (RAP0, RAP25, RAP50, RAP75).

When the mixture is fully coated by the binder during mixing, it is filled into the mold. Finally, the material is compacted by a hand roller. The mold filled with the PU-RAP mixture must rest and cure for at least 24 hours. The asphalt plate can then be demolded and sawed to the required specimen dimensions.

Densities and Void Contents of Tested Specimens

The pycnometer method according to TP Asphalt-StB Part 5 [10] was used to obtain the maximum material densities for all materials as well as for the mixtures of the test variants. The asphalt mix is placed in a pycnometer and weighed. A defined amount of water is then

added and the sample is vacuumed. In the process, all accessible air voids are eliminated. By determining the masses of the sample with and without water and taking into account the existing material densities, the material density of the pure asphalt mix can be determined. Subsequently, the bulk density of the finished specimens was determined according to TP Asphalt-StB Part 6 [7] due to immersion weighing. The void contents of the individual specimens can then be determined from the maximum densities and the bulk densities.

3.3.3 Selection of Suitable Test Methods

Test methods for bitumen-bound asphalt are used to investigate the material behavior of the polyurethane-bonded asphalt, as these are used to evaluate its suitability for road use. These may not address the full material behavior of the new material yet, but they provide an initial opportunity to address the material and receive a comparison to conventional asphalt.

In order to determine the overall material performance of the specimens with the added PU-RAP, the tests that were carried out in the previous study [4] are applied. Thus, a comparability of the results can be generated.

Absorption Behavior

As in [4], the measurement of the acoustic efficiency by the impedance measuring tube (AFD 1000 - AcoustiTube ® according to *DIN EN ISO 10534-2*) [11] is used in this study. The impedance measuring tube allows a simple and fast measurement of the absorption coefficient of materials. In this test, a long tube with a sonic rim contains a loudspeaker that acoustically excites the air enclosed in the tube. At the end of the tube, a cylindrical specimen is installed. The sound excitation causes the sound to propagate in the longitudinal direction of the tube and hits the specimen, which reflects and/or absorbs the sound waves. A measuring device located behind the specimen measures the absorbed or reflected components of the sound waves. The method used in this study is called the wave separation method, which provides the absorption value α across a frequency range from 250 Hz to 2000 Hz [18].

Deformation Resistance with Uniaxial Cyclic Compression Test (UCCT)

In the context of this work, the UCCT was chosen to test the deformation behavior. Due to its haversine-impulse loading, it is suitable to represent the axle-load-simulating dynamic loading exerted on the pavement by passenger cars and heavy-load traffic. The test is carried out in accordance with *TP Asphalt-StB, Part 25 B 1* [8]. The UCCT is used to determine the strain rate.

According to *TP Asphalt-StB, Part 25 B 1* [8], a cylindrical plane-parallel specimen is uniformly subjected to a haversine pulse-shaped pressure swell load. The test sequence is characterized by load cycles that cause axial deformation on the specimen. The deformation parameter of this test is the strain rate, which is used to determine the resistance to deformation. The specimen has to be prepared as a cylinder with a diameter of 100 ± 5 mm and a height of h = 60 ± 1 mm using drilled cores from laboratory plates. Contrary to the instructions in the regulations, the specimens in this study were manufactured using molds with a diameter of 100 mm. During testing, the specimen is loaded by the haversine-pulse loading at an under stress of 0.025 MPa and a top stress of 0.35 MPa.

The deformation under the top load plate is recorded as a function of the loading cycle. The test is complete when either 10,000 load cycles are performed or a permanent deformation of more than 40 ‰ is reached.

Fatigue Behavior with Three-Point Bending Test (3PB)

Pavement fatigue is generated by the application of repetitive loads. In general, the loads are significantly lower than the maximum bending tensile strength of the material and, due to their constant repetition, cause damage accumulation that ultimately results in the failure of the material. The failure then manifests itself in cracks, which typically start from the bottom of the layer and propagate up to the top [28].

In order to investigate the fatigue behavior, the three-point bending test was used in this study. It is performed as a displacement-controlled test that describes the behavior of a beam-shaped prismatic asphalt specimen. The test setup imitates the practical case in which a moving load axis passes over the asphalt pavement.

The decision to use the three-point bending test is due to the comparability of the test results, as it has been used to analyze the previous material compositions of Faßbender and Oeser [4] as well as the material of Renken [23].

The fatigue resistance of conventional asphalt is described by *DIN EN 12697-24 Asphalt - Test methods - Part 24: Resistance to fatigue* [13]. The specimens are subjected to a flexural load, which imitates rolling wheel loads. In detail, the prismatic specimens are tested at a temperature of 20°C ± 1°C. The test specimens, with a maximum grain size of 22 mm, can either be cut out of specially manufactured slabs or cut out of an existing pavement with a minimum thickness of 50 mm. Deviating from the specifications described in [13], the dimensions specified for PU asphalt test specimens in this study are 40 x 40 x 320 mm^3 according to [23] and [4].

The specimen is installed in the test fixture for the three-point bending test and subjected to a sinusoidal load with constant amplitude by a centrally applied load application device

until the stiffness drops to half its initial value. Since *DIN EN 12697-24* [13] only applies to the testing of conventional asphalt, the procedure according to [23] is used in this study, as in the investigation of the basic material [4]. In the first step, a static flexural strength test is carried out to determine the flexural strength of the material. The maximum deflection s_{max} received from this is the basis for the subsequent displacement-controlled cyclic loads, whose displacement amplitude results from 2/3 of the maximum deformation s_{max}. The cyclically loaded specimens are then subjected to another static flexural tensile test to determine the residual flexural tensile strengths after dynamic loading.

Low Temperature Behavior

The service temperatures of pavements cover a wide temperature range which can significantly influence the material behavior. Bitumen-bound asphalts, for example, are highly temperature-dependent and change their elastoplastic properties considerably with increasing or decreasing temperature. The temperature behavior of polyurethane-bound pavements has not been researched as much. In particular, the influence of the addition of PU-RAP has not been the subject of research so far. Therefore, in the following, the low-temperature behavior is investigated with respect to the present variants of this study.

In addition to stresses due to traffic loads, cryogenic stresses in the pavement occur under the influence of cold temperatures. The superposition of these stresses can lead to damage if the tensile strength reserve of the pavement is not sufficient. For this reason, the study of the low-temperature behavior of asphalt is of great importance. The low-temperature behavior of asphalt can be described by means of direct tensile tests, cooling tests, relaxation tests, and retardation tests. In this study, the focus is on the Uniaxial Tension Stress Test and the Thermal Stress Restrained Specimen Test, because they describe the low-temperature behavior in a practical manner. The framework for this is *DIN EN 12697-46 Asphalt - Test methods for hot mix asphalt - Part 46: Resistance to cold cracking and low-temperature behavior in uniaxial tensile tests* [9]. The test procedure is analogous to the investigation of the low-temperature behavior in [4]. The tested prismatic specimens with the dimensions 40 x 40 x 160 mm^3 originate from specimen plates manufactured in the laboratory.

Uniaxial Tension Stress Test (UTST) The aim of the UTST is to stretch the clamped specimen at a constant temperature until it fails. For this purpose, the prismatic specimen is firmly bonded with its two end faces in the test fixture and then subjected to a tensile load at a constant strain rate at a defined temperature level. In total, four temperature levels must be covered (+20°C, +5°C, -10°C, and -25°C).

Thermal Stress Restrained Specimen Test (TSRST) The TSRST differs from the direct tensile test only in the type of loading. In this test, the specimen is fixed again, the specimen

length is kept constant and a temperature induction follows, which causes temperature-induced stresses (cryogenic stresses) in the specimen. The test temperature is decreased from +20°C by 10 K/h until the specimen fails or a minimum temperature of -40°C is reached.

The difference between the tensile strength $\beta_t(T)$ and the cryogenic stress $\sigma_{cry}(T)$ is the tensile strength reserve.

3.4 Experimental Results and Discussion

3.4.1 Densities and Void Contents

Figure 3.3 shows the maximum densities, the calculated bulk densities, and the experimentally determined bulk densities, as well as the void contents as averages for the variants.

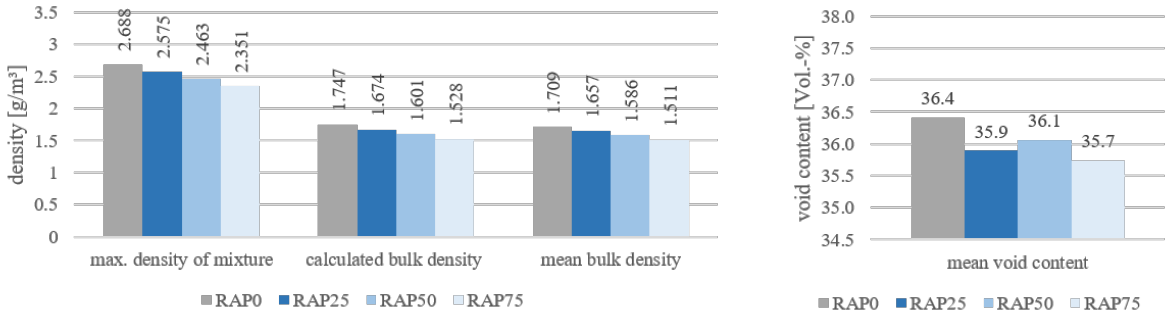

Figure 3.3: Mean maximum, calculated and experimentally determined bulk densities and void contents of all specimens.

First, it can be stated that the bulk densities of the variants which were previously determined by calculation, are confirmed by experimental testing according to TP Asphalt Part 6 [7].

When considering the material properties in relation to the variants, a clear decreasing trend can be seen with regard to the densities. With increasing substituted PU-RAP, both the maximum material densities and the bulk densities decrease. This is due to the fact that by adding the PU-RAP, additional old binder as well as old rubber particles are present in the mixture, which lowers the total bulk density. The individual densities can be taken from the Appendix, Table 3.4.

The void content shows a decreasing trend. This reduction is not decisive, because the bulk density was measured by dimensions according to [7], which is highly user-dependent. Other methods have not yet been effective for open-pore materials.

3.4.2 Absorption Potential

The sound absorption coefficient is determined in accordance with *DIN EN ISO 10534-2* [11] in the impedance measuring tube. The absorption coefficient can range from 0 to 1. The value 0 means that the surface reflects the sound completely. A value of 1, however, means that the sound is completely absorbed.

Figure 3.4 shows the results of the measurements with the impedance measuring tube. The absorption coefficients α over the frequency are shown. The absorption curve of the previous study [4] is depicted with a red dotted line. All other curves are results of the current study. Shown here are all individual measurements of the different variants (RAP0 (cyan), RAP25 (green), RAP50 (blue) and RAP75 (magenta)).

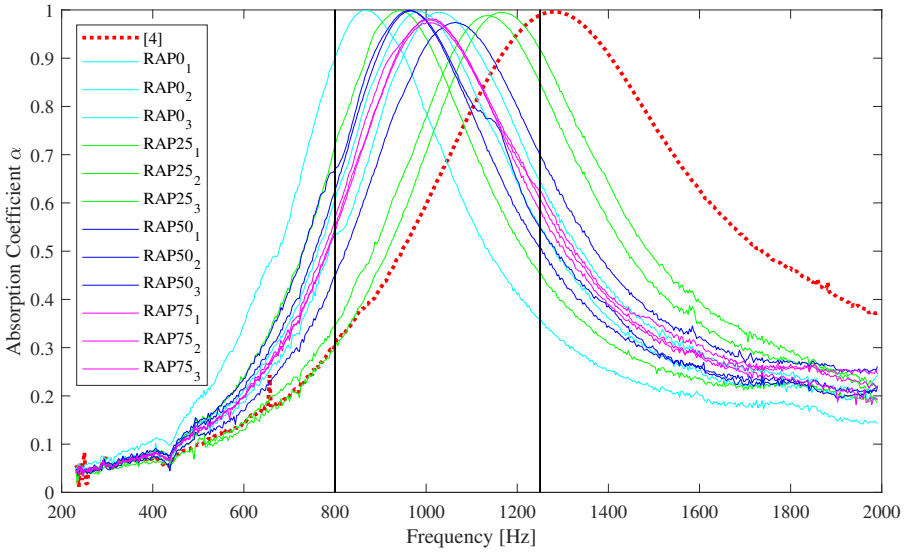

Figure 3.4: Absorption coefficient curves of the Variants RAP0, RAP25, RAP50, RAP75 and from Chapter Two [4].

Through analysis of the results, it becomes apparent that all variants that were acoustically investigated exhibit distinctive absorption amplitudes with a maximum of almost $\alpha = 1$. This means that all samples have a significant absorption capacity in certain frequency ranges. From literature [2, 21, 4], it is known that the degree of porosity influences the maximum absorption capacity. The higher the porosity, the higher the absorption coefficient. Considering these findings, it can be seen that the porosity of the variants presented here is generally very high, which is why a high absorption level is achieved in all tested variants.

In addition, the thickness of the layer as well as the resistivity are responsible for the frequency range in which the absorption curve is located. The thicker the layer, the lower the frequency range of the absorption amplitude. Furthermore, tortuosity affects the frequency range of the amplitude [2, 21]. It can be seen that all variants, including the newly manufactured base variant RAP0 (cyan), exhibit an absorption curve in the lower frequency range

than the variant from [4] (dotted red). This suggests that either the layer thickness or the tortuosity of the variants differ. Because the experimenters tried to make the layer thickness the same for all variants, the reason for the change of the frequency range is probably the tortuosity. This is presumably due to the fact that a two-component polyurethane was used here to produce the specimens instead of the one-component polyurethane used in [4]. If we omit the comparison with the variant from Oeser and Faßbender [4], variants RAP25, RAP50, and RAP75 show an increase in the frequency range compared with the reference variant, which may be due to an increase in tortuosity. The polyurethane wraps around the aggregates and does not collect in the gaps. Therefore, the channels in the layer could become narrower with a high void content present at the same time.

Looking at the samples tested in this study in Figure 3.4, it can be recognized that there is a scatter along the frequency range in the variants RAP0 (cyan), RAP25 (green) and RAP50 (magenta). Only the three test results of RAP75 (magenta) are stringent. In RAP25 and RAP75, in each case, one measurement deviates slightly. It is found, however, that the curves move within the frequency range of 800 to 1250 Hz, which is an important frequency range for traffic noise according to [2], and can thus efficiently absorb and reduce traffic noise for the human hearing [4].

Compared to the previous study [4], the results show that the proportion of addition of the PU-RAP does not reveal any apparent tendency for improvement or deterioration of the absorption properties. Moreover, it seems that the addition of a two-component polyurethane binder has a positive effect on the frequency range by moving the curves into the lower frequency range.

In [4], an effective normalized absorption value was introduced for evaluation, which reflects the absorption power in the decisive frequency range between 800 and 1250 Hz. This value is the area under the curve in the interval between 800 and 1250 Hz related to the difference between 800 and 1250 Hz. It takes into account not only the height of the absorption curve - i.e. the maximum absorption capacity - but also the width of the amplitude.

The absorption values are shown in Figure 3.5 as mean values in the form of bars. The markers show the individual results. As already indicated in Figure 3.4, it can be seen that the absorption capacity has increased, which could be due to the new composition with PU-RAP compared to the variant from [4]. Furthermore, it is noticed that the addition of the PU-RAP shows a slight positive trend, indicating that a higher absorption level is achieved with more PU-RAP added. However, this is a vague statement when considering the individual values.

In principle, it can be concluded that the absorption capacity of the variants made of recycled material is better compared to the original as their absorption level is higher. An increased

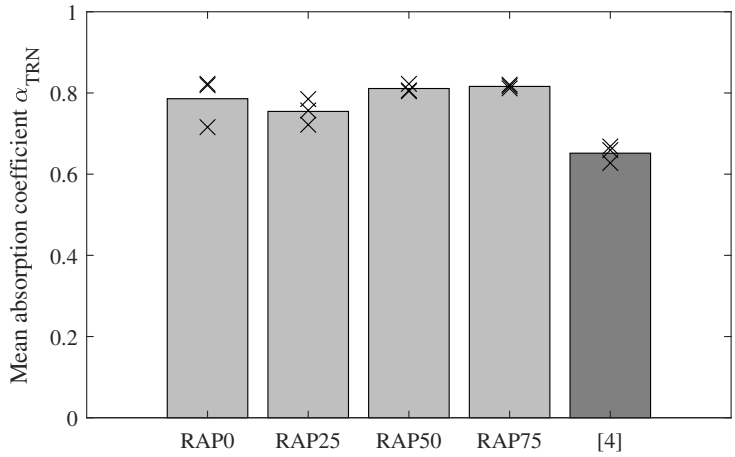

Figure 3.5: Mean absorption coefficient values of the variants RAP0, RAP25, RAP50, RAP75 and Chapter Two [4].

percentage of polyurethane (old and fresh polyurethane) may support the efficiency of the absorption. As a result, the material can be used with confidence and will continue to perform effectively in terms of acoustic efficiency.

3.4.3 Uniaxial Cyclic Compression Test

During the cyclic compression test according to [8], a cylindrical specimen is subjected to repetitive compressive loading with load pauses. The cyclic loading is used to investigate the resistance to deformation of the tested material.

As a result, the strain of the specimen is obtained which makes it possible to predict the extent to which the material will deform in the long term. The strain is determined according to [8].

The deformation curves in Figure 3.6 describe the accumulated strains due to load application. As can be seen in Figure 3.6, the deformation curves of the investigated specimens lie in a strain range between 0 and about 6 ‰. It can be seen that variant RAP75 (75 % PU-RAP) exhibits a more pronounced deformation behavior, which is visible due to a stronger scatter of the individual results. All deformation curves follow an asymptotic trend along the entire testing period of 10,000 load cycles. No inflection point is visible in the deformation curve, which is usual for conventional asphalt. This fact indicates that no sudden failure of the specimens occurs during the loading process.

In principle, it can be concluded that the specimens undergo an irreversible change in shape as a result of the input energy, although this change is quite small during long-term loading. This indicates that there is a high deformation resistance of the material. Nevertheless,

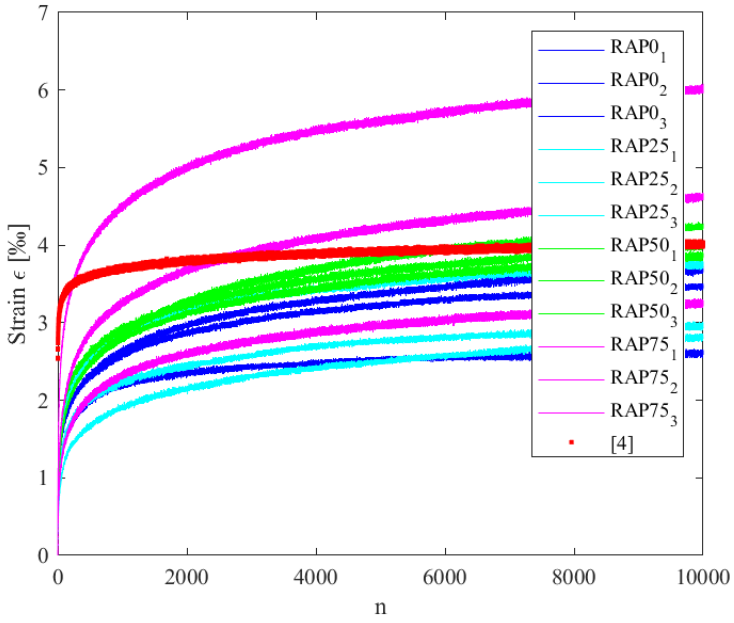

Figure 3.6: Strain of variants RAP0, RAP25, RAP50, RAP75 and mean strain of Chapter Two [4] due to the uniaxial cyclic compression test.

variant RAP75 yields larger deviations. The deviations could possibly be due to the rubber content contained in the PU-RAP as well as in the base compound.

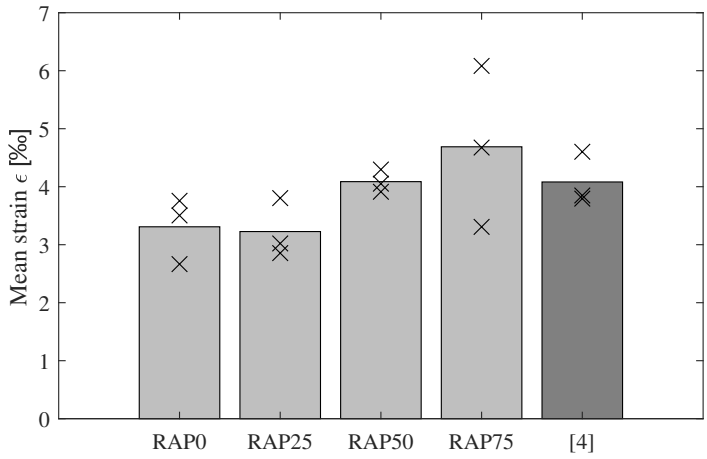

Figure 3.7: Mean maximum strain of variants RAP0, RAP25, RAP50, RAP75 and variant of Chapter Two [4] at 10,000 load cycles.

An illustration of the mean maximum strains at a load cycle number of n=10,000 is shown in Figure 3.7. Looking at the bar chart in detail, it can be seen that no clear trend of the PU-RAP addition is visible. Initially, it seems as if there would be a deterioration of the deformation resistance with increasing PU-RAP, because the bars of the variants RAP25, RAP50 and RAP75 show a positive trend. When considering the individual values, that are shown here as crosses, a scattering of the results is noticeable, which cannot surely confirm

the trend. However, no exact statement about a clear trend of the PU-RAP addition is possible.

A comparison with the variant from [4] (red line in Figure 3.7), in which the one-component polyurethane binder Elastan 6568/103 was used, shows that the variants from this study present ultimate strains of the same order of magnitude and thus have an equivalent high potential of deformation resistance. Obviously, the deformation resistance curve differs from the RAP variants, because it shows a rapid and short-term increase in strain, which is much steadier over the duration of the test.

3.4.4 Three Point Bending Test

The three-point bending test (3PB) with the modifications according to [23] is carried out to assess the fatigue behavior of the specimens produced with PU-RAP. The procedure is such that first a static flexural tensile test is carried out to determine the static flexural tensile strength, followed by a cyclic sinusoidal fatigue load with 20,000 load cycles. Finally, the residual bending tensile strength is determined by means of another static bending tensile test in accordance with *DIN EN 12390-5* [12] and [23] in order to assess the remaining material resistance.

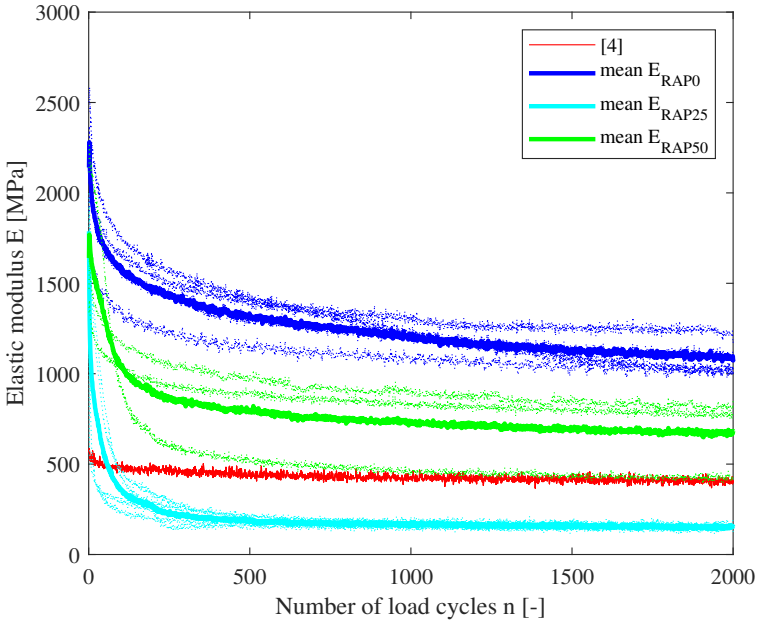

Figure 3.8: Course of the diminishing e-modulus of variants RAP0, RAP25, RAP50 and [4].

Figure 3.8 presents the course of the diminishing e-modulus for the tested specimens during loading. Outliers were eliminated beforehand. All curves are assigned to the respective variant by color. It can be seen that the curves of variant RAP50 lie in a narrow corridor. The curves of the variants RAP0 and RAP25 each have a curve that deviates slightly more

in its course. The highlighted curves indicate the average curve of the e-modulus of the respective variants RAP0, RAP25, and RAP50. Although constant test conditions were maintained both in the manufacturing process and in the testing process, there is a large spread within the course of the e-modulus curves. A correlation between the proportional addition of the PU-RAP and the present Young's-modulus curves is not evident here.

A comparison of the fatigue curves of this study with the previous study according to [4] clearly shows that the material behavior has changed considerably. The curves of the variants RAP0, RAP25, and RAP50 start at a high Young's modulus and decrease exponentially compared to the curves of [4], which are rather constant and almost identical in comparison. In Figure 3.8 it is not possible to see that three variants are shown, because they run superimposed.

The variants of this study were produced with two-component polyurethane, contrary to the variant from [4]. Because even the reference variant RAP0, which only has a different binder, shows such a strong development here, it becomes clear that the used binder has an enormous influence on fatigue resistance.

According to *DIN EN 12697-24* [13], the conventional failure criterion is used to evaluate the fatigue behavior. After the test is done, the stiffness is calculated across the number of load cycles with equation 3.1.

$$|E| = \frac{K_a \cdot l^3}{4 \cdot w_a \cdot b \cdot h^3}$$

$$\begin{aligned} absolute\ elastic\ modulus\ [MPa] &= |E| \\ force\ amplitude\ [N] &= K_a \\ support\ span\ [mm] &= l \\ maximum\ deflection\ of\ the\ center\ of\ the\ beam\ [mm] &= w_a \\ width\ of\ the\ specimen\ [mm] &= b \\ height\ of\ the\ specimen\ [mm] &= h \end{aligned} \tag{3.1}$$

A specimen is considered fatigued after the number of load cycles at which the initial stiffness (E_{100}) has decreased by half. The initial stiffness is defined as the stiffness of the specimen that exists after the 100th load change. The test is completed after 20,000 load cycles.

Table 3.3 shows the fatigue test results with respect to the fatigue criterion. For this purpose, the initial stiffnesses E_{100}, the load cycles when the fatigue criterion n is reached, and the stiffness at the end of the test $E_{20,000}$ are listed for all tested specimens.

Table 3.3: Results of fatigue testing.

Variant	**specimen no.**	$\mathbf{E_{100}}$ [MPa]	$\mathbf{n(0.5 \cdot E_{100})}$ [-]	$\mathbf{E_{20.000}}$ [MPa]
[4]	-	537	not reached	386
RAP0	5	1671	not reached	1013
	7	1998	not reached	1212
	8	1903	not reached	1101
	9	2232	1262	1042
RAP25	7	467	202	152
	8	1431	62	173
	9	1393	50	137
	10	558	53	133
RAP50	5	2091	82	430
	7	1460	not reached	831
	10	1266	not reached	779

Based on the values from Table 3.3, it can be confirmed that the reference variant RAP0 has good fatigue resistance. This, similar to the variant of [4] , does not reach the failure criterion, except in one sample. Compared to the variant from [4], the elasticity curves in this study are at a much higher level. The fact that in this study the two-component binder was used instead of the one-component one could be a reason. In previous investigations, it was found that the one-component polyurethane is more elastic and thus has lower elastic moduli. The fatigue criterion shows that the RAP0 and RAP50 variants have high fatigue resistance except for one specimen each. Apart from the exceptions, they do not reach the fatigue criterion. The fatigue curves from Figure 3.8 also show that the RAP0 and RAP50 variants have a higher initial stiffness, which can be seen in the position of the curves. Variant RAP25, on the other hand, reaches the failure criterion after a very short number of load cycles under 202 load cycles for every sample tested, which is about 1 % of the total number of load cycles. The lower level of Young's moduli is also reflected in the fatigue curves of variant RAP25.

A direct influence of the addition of PU-RAP cannot be detected in this case. The positioning of the RAP0 and RAP50 variants could indicate that the PU-RAP possibly lowers the Young's modulus, although no clear trend can be defined here. However, this could be explained by the fact that the higher the PU-RAP, the higher the rubber and polyurethane content in the compound, which is why the e-modulus is lower. However, variant RAP25 unfortunately does not support this statement. Nevertheless, both variants RAP0 and RAP50 show that they have a high fatigue resistance, because they do not reach the fatigue criterion. As a conclusion, variant RAP25 must be retested. The trend of the RAP0 and RAP50 variants makes sense in principle. Maybe an unfavorable PU-RAP charge was selected during

specimen fabrication, resulting in a useless plate from which the specimens were cut out.

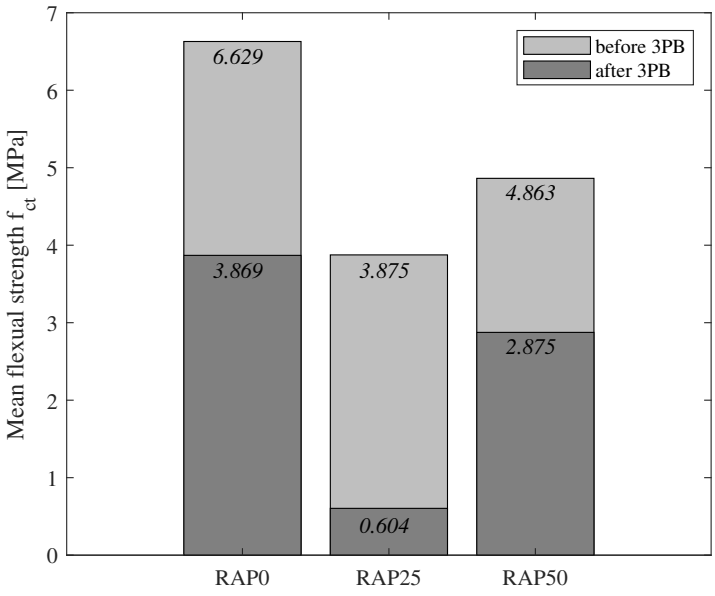

Figure 3.9: Flexural strength comparison before and after 3-point bending test.

Looking at the results of the flexural strength tests before and after the fatigue test, it can be seen that flexural loading caused extensive damage to the microstructure. The values before and after fatigue show this effect very clearly (Figure 3.9). Thus, the flexural strength of variant RAP0 has decreased by 42 %, the flexural strength of RAP25 has decreased by 84 %, and the flexural strength of variant RAP50 has decreased by 41 %. Here, too, variants RAP0 and RAP50 exhibit higher flexural tensile strengths than variant RAP25, where the flexural tensile strength is already strikingly low at the beginning. The high damage potential of 84 % again indicates that there is a structural problem with variant RAP25 that needs to be investigated again. However, variants RAP0 and RAP50, with about 40 % reduction in flexural tensile strength, also clearly indicate the damaging effect of fatigue testing. An influence of the PU-RAP on fatigue resistance cannot be detected here.

3.4.5 Results of Low-Temperature Behavior

To analyze the low-temperature behavior of polyurethane-bound pavements with substituted PU-RAP the procedure according to [9] is applied.

Both the Tension Stress Test (UTST) and the Thermal Stress Restrained Specimen Test (TSRST) are used to test the low-temperature behavior. The UTST gives tensile strengths at the temperature levels 20°C, 5°C, -10°C, and -25°C, which are represented by a cubic spline function. The TSRST indicates the stresses that develop in an expansion-restrained specimen when it is cooled down. From the two test results, it can be determined how high

the stress-bearing capacity of the pavement is and how much of this is available as a reserve for further loads, e.g. from traffic. This reserve is called the tensile strength reserve.

Figure 3.10 shows the results of the UTST and TSRST and the resulting tensile strength reserves of the variants RAP0, RAP25, and RAP50.

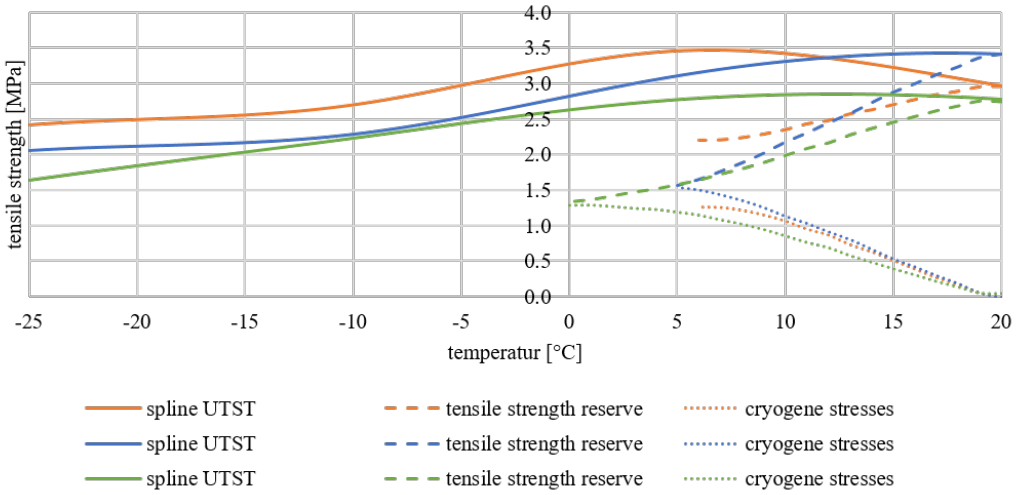

Figure 3.10: Results of the UTST and TSRST: RAP0 (orange), RAP25 (blue), RAP50 (green).

In Figure 3.10, it was recognized that in all TSRST of the variants RAP0 (orange), RAP25 (blue), and RAP50 (green), the resulting cryogenic stresses lead to early material failure. The samples were already damaged at temperatures starting at about 5°C (RAP0 and RAP25). Variant RAP50 broke at a temperature of 0°C. Thus, a tensile strength reserve is found here for all variants only in the temperature range between 5°C or 0°C to 20°C.

Considering the tensile strength reserves of the different variants, no clear influence of the different additions of the PU-RAP can be determined. Variant RAP0 starts at 20°C at a tensile stress of 2,9 MPa and decreases to about 2.2 MPa at 6°C. Variant RAP25 starts at 3.4 at 20°C and runs towards 1.6 MPa at 5°C, and variant RAP50 starts at 2.7 (20°C) and continues to 1.3 (0°C). It is true that the RAP0 and RAP25 variants, which contain a lower PU-RAP content, have a higher tensile strength reserve. However, variant RAP50 covers a broader temperature range and contains the highest proportion of PU-RAP. Thus, it is assumed that the addition and the proportion of PU-RAP do not have a significant effect on the low-temperature behavior.

If this is compared with the low-temperature behavior from [4] (black curves), it can be seen directly in Figure 3.11 that the materials differ greatly in their low-temperature behavior. The big difference between the two mixtures from [4] and from this study can be found in the different binders that are used. The two-component polyurethane used here is very sensitive to low temperatures. This trend was already observed in the research project INNO-PAVE

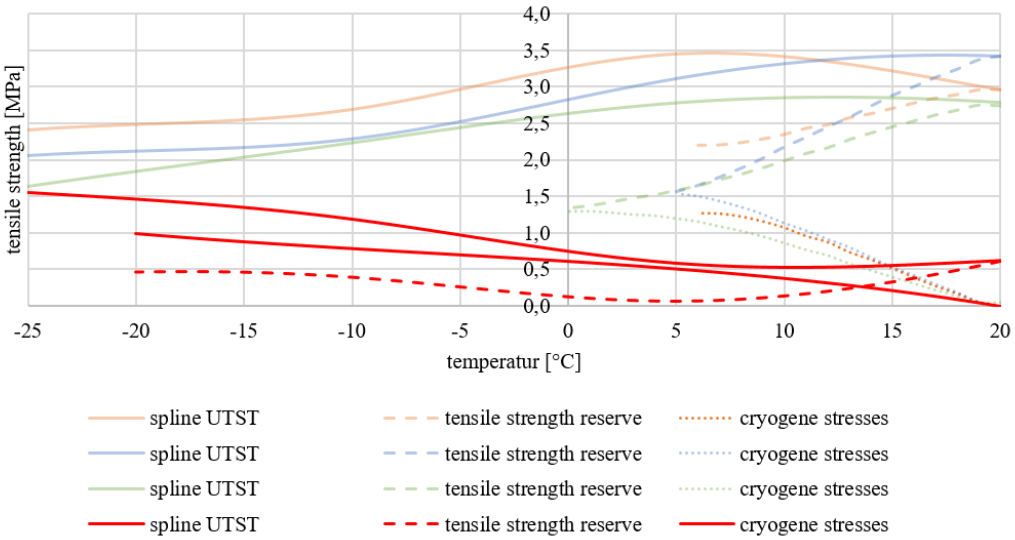

Figure 3.11: Results of the UTST and TSRST compared to [4]: RAP0 (orange), RAP25 (blue), RAP50 (green), and [4] (red).

[20] when it came to selecting the optimum binder. However, such a huge difference in the context of this study was not expected.

Figure 3.11 shows that the cryogenic stresses in the TSRST do not damage the specimens of [4] until a temperature of -20°C is reached. Previously, they rose steadily with decreasing temperatures but withstood the low temperatures. The tensile strength in [4] is quite low. This is due to the low quantity of binder used there. In the final mixture, the binder content was therefore adjusted.

Finally, the influence of the added PU-RAP does not seem evident in terms of the low-temperature behavior.

3.5 Conclusions

For the reuse of reclaimed asphalt, it is standard practice in Germany to add RAP to the new asphalt mixture in order to reduce waste and to conserve and reuse energy-intensive resources. This approach is not only important in bitumen-bound asphalts. This strategy should also be continued with regard to innovative and sustainable pavements as the action plans from the EU and UN demand. Therefore, this study investigated whether the addition of PU-RAP has an effect on the material performance of the polyurethane-bound rubber-modified pavement. Test methods for bituminous asphalt were used for this purpose and modified where necessary. In general, this study has shown that the addition of PU-RAP has an influence on the material behavior, which, however, does not show a clear trend. But in detail, this study has shown, that:

- The addition of PU-RAP has a positive influence on the absorption capacity of the polyurethane-bound rubber-modified pavement, as the frequency range can be adjusted.
- The addition of PU-RAP has no significant effect on the deformation behavior of polyurethane-bound rubber-modified pavement.
- The addition of PU-RAP does not affect the resistance to fatigue of the polyurethane-bound rubber-modified pavement.
- The addition of PU-RAP has no effect on the low-temperature behavior of the polyurethane-bound rubber-modified pavement.

It can therefore be stated very clearly that no damaging effect has been caused by the addition of PU-RAP. And it can therefore be assumed with certainty that PU-RAP can be added to fresh mixtures free of any problems and without affecting the material performance. In addition, due to the deviation to an alternative binder, a statement could be made about the effect of the two-component binder, which greatly affects the performance of the material and worsens the performance compared to the variant from Faßbender and Oeser [4].

In order to be able to evaluate the study holistically and conclusively, the following points must be considered in further studies in detail:

- The RAP was freshly made and unstressed as well as unaged when it was reconditioned. The study was in the first step intended to show the feasibility of reusing the PU-RAP. In the next step, it makes sense to take the RAP material from already stressed pavements and investigate the functionality.
- All tests should be prepared and tested again with the one-component binder from [4] to generate comparability. The influence of the PU-RAP can likely be worked out even better in this case.
- Additional specimens should be tested to support the conclusions made in this study.

3.6 Acknowledgements

We would like to thank our students Anna-Lena Krumpen and Lisa Münker, who supported us in the realization of the experiments.

3.7 Appendix

The following Table 3.4 shows the basic aggregate sizes and the related maximum densities of the additives of the designed mix.

Table 3.4: Aggregate sizes and maximum densities of the designed mix.

	aggregate size [mm]	**maximum density** [g/cm³]
lime sandstone filler	$\leqslant 0.063$	2.730
PU-RAP filler	$\leqslant 0.063$	2.582
basalt stone	0.063 - 2.0	3.050
PU-RAP	0.063 - 2.0	2.588
basalt stone	2.0 - 5.6	3.050
PU-RAP	2.0 - 5.6	2.605
rubber super-grob	2.0 - 5.6	1.100
polyurethane	-	1.100

The following Table 3.5 shows the typical physical properties of the polyurethane Elastopave® 6551/102 from BASF Polyurethanes GmbH [22].

Table 3.5: Typical physical properties.

Characteristics	**Unit**	**Measured value**	**Method**
Hardness	Shore ID	72	DIN 53505
Tensile strenth	N/mm²	32	DIN EN ISO 527
Elongation	%	40	DIN EN ISO 527
Tear strength	N/mm	40	DIN 53515
Density	g/cm³	1,1	DIN 53420

References

[1] BASF Polyurethanes GmbH. *Build a Brighter Future with Sustainable Construction.* URL: https://plastics-rubber.basf.com/global/de/performance_polymers/industries/pp_construction/sustainability.html (visited on 04/10/2022).

[2] T. Beckenbauer. "Physik der Reifen-Fahrbahn-Geräusche – Geräuschentstehung, Wirkmechanismen und akustische Wirkung unter dem Einfluss von Bautechnik und Straßenbetrieb." In: *Geräuschmindernde Straßenbeläge in der Praxis – Lärmaktionsplanung* 4 (2008).

[3] European Commission. *A New Circular Economy Action Plan – For a Cleaner and More Competitive Europe*. Brussels, 2020. URL: https://eur-lex.europa.eu/legal-content/EN/TXT/?uri=COM:2020:98:FIN (visited on 11/05/2023).

[4] S. Faßbender and M. Oeser. "Investigation on an Absorbing Layer Suitable for a Noise-Reducing Two-Layer Pavement." In: *Materials* 13.5 (2020).

[5] Forschungsgesellschaft für Straßen- und Verkehrswesen. *Merkblatt für die Wiederverwendung von Asphalt (M WA) (FGSV 754)*. Köln, 2013.

[6] Forschungsgesellschaft für Straßen- und Verkehrswesen. *Technische Lieferbedingungen für Asphaltgranulat (TL AG-StB) (FGSV 749)*. Köln, 2009.

[7] Forschungsgesellschaft für Straßen- und Verkehrswesen. *Technische Prüfvorschrift für Asphalt (TP Asphalt-StB) - Teil 6: Raumdichte von Asphalt-Probekörpern (FGSV 756/6)*. Köln, 2012.

[8] Forschungsgesellschaft für Straßen- und Verkehrswesen. *Technische Prüfvorschriften für Asphalt (TP Asphalt-StB) - Teil 25 B 1: Einaxialer Druck-Schwellversuch - Bestimmung des Verformungsverhaltens von Walzasphalt bei Wärme (FGSV 756 / 25 B1)*. Köln, 2018.

[9] Forschungsgesellschaft für Straßen- und Verkehrswesen. *Technische Prüfvorschriften für Asphalt (TP Asphalt-StB) - Teil 46A: Kälteeigenschaften – Einaxialer Zugversuch und Abkühlversuch (756/46A)*. Köln, 2013.

[10] Forschungsgesellschaft für Straßen- und Verkehrswesen. *Technische Prüfvorschriften für Asphalt (TP Asphalt-StB) - Teil 5: Rohdichte von Asphalt (FGSV 756/6)*. Köln, 2021.

[11] German Institute for Standardisation. *DIN EN 10534-2:2001: Determination of Sound Absorption Coefficient and Impedance in Impedance Tubes - Part 2: Transfer-Function Method; Correction 11-2007*. Berlin, 2007.

[12] German Institute for Standardisation. *DIN EN 12390-5:2019-10: Testing Hardened Concrete - Part 5: Flexual Strength of Test Specimens*. 2019.

[13] German Institute for Standardisation. *DIN EN 12697-24:2018-11: Bituminous Mixtures - Test Methods - Part 24: Resistance to Fatigue*. Berlin, 2018.

[14] L. Goubert. *Above the development and use of the poro-elastic road surface*. Brussels, 2011.

[15] L. Goubert and U. Sandberg. "The PERSUADE project: Developing the concept of poroelastic road surface into a powerful tool for abating traffic noise." In: *Proceedings of the INTER-NOISE 2010 – 39th International Congress on Noise Control Engineering 2010, Lisbon, Portugal, 15-16 June 2010* (2010).

[16] W. Kaiser. *Kunststoffchemie für Ingenieure: Von der Synthese bis zur Anwendung*. 2nd. München: Hanser, 2007.

[17] G. Lu. "Permeable Pavements – Hydraulic and Mechanical Investigations." PhD-Thesis. Aachen: RWTH Aachen University, 2019.

[18] M. Möser. *Technische Akustik*. 9th ed. Berlin: Springer-Vieweg, 2012.

[19] M. Oeser and A. Schacht. *Abschlussbericht Leise innovative Deckschicht auf Kunststoffbasis (LIDAK), FE 88.0108/2011*. 2014.

[20] M. Oeser et al. *INNO-PAVE : Final report: "Grundlagen der konstruktiven Gestaltung, Struktur sowie neuer polymerer Werkstoffe für:Straßendeckschichtsysteme" im Verbundprojekt: "Grundlegende Erforschung polymerer Werkstoffe sowie innovativer Herstellungs- und Einbautechnologien für Straßendeckschichtsysteme" : Duration of research project: 09/2015-04/2019*. Aachen, 2019.

[21] F. G. Praticó, D. Vizzari, and R. Fedele. "Estimating the resistivity and tortuosity of a road pavement using an inverse problem approach." In: *Proceedings of the 24th International Congress on Sound and Vibration, London, 23-27 July 2017* (2017).

[22] L. Renken. "Development of PU-Asphalt - from the concept to the practical implementation." PhD-Thesis. Aachen: RWTH Aachen University, 2019.

[23] L. Renken, S. Kreischer, and M. Oeser. "Entwicklung von Deckschichtmaterialien für versickerungsfähige Verkehrsflächenbefestigungen auf Basis alternativer Bindemittel - Teil II: Ansprache der Performance." In: *Straße und Autobahn* 9 (2015), pp. 776–784.

[24] L. Renken et al. *Schlussbericht INNO-BOND – Simulationsgestützte Entwicklung neuer Straßenbaustoffe und innovativer Herstellungs- und Einbautechnologien, FE 07.0264/2012/ARB*. 2016.

[25] U. Sandberg and J. A. Ejsmont. *Tyre/Road Noise Reference Book*. Harg, Kisa, Sweden: INFORMEX, 2002.

[26] A. Schacht. "Entwicklung künstlicher Straßendeckschichtsysteme auf Kunststoffbasis zur Geräuschreduzierung mit numerischen und empirischen Verfahren." PhD-Thesis. Aachen: RWTH Aachen University, 2015.

[27] United Nations. *Transforming Our World: The 2030 Agenda for Sustainable Development (A/RES/70/1)*. New York, America, 2015. URL: https://www.un.org/en/development/desa/population/migration/generalassembly/docs/globalcompact/A_RES_70_1_E.pdf (visited on 02/05/2022).

[28] Z. Zhang et al. "Concept and Development of an Accelerated Reapeated Rolling Wheel Load Simulator (ARROWS) for Fatigue Performance Characterization of Asphalt Mixture." In: *Materials* 14(24) (2021).

4 Development of a Novel Polymer-Based Road Surface Layer with Focus on Noise Reduction and Durability

This paper was published under:

Faßbender, S.; Oeser, M.; Eggersmann, R; Reese, S.; Koch, A.; Gries, T.; Pieroth, M.; Klein, A.; Elsing, A.: "Development of a Novel Polymer-Based Road Surface Layer with Focus on Noise Reduction and Durability". In: Bauingenieur, 97(10), pp: 323-330, DOI: 10.37544/0005-6650-2022-10-61, 2022.

4.1 Abstract

The object of the development is a textured and high-strength road surface layer, which can be applied to an existing road base. The noise generated by the interaction of tyres and road surface can be reduced by the layer with the main ingredient methyl-methacrylate, as it has a special shape that minimises the generation of noise in the interaction field between road surface and tyres. Due to its composition of methyl-methacrylate and a special filler, it has a high strength. As a result, noise reduction is realized by the simple application of the texture layer compared to conventional asphalt pavements. This noise reduction is comparable to the noise reduction achieved by currently used noise-reducing asphalt pavements, whose disadvantage is a low durability. Thus, a long-term and permanent noise reduction can be achieved by a fast construction progress due to the use of prefabricated elements. This leads to a minimisation of the duration and frequency of work sites and promotes a steady flow of traffic.

4.2 Current State of Technology

Road surfaces can reduce the generation of tire-road noise through deliberate composition adjustments. Yet, asphalt top layers have been modified in their composition to aim for a reduction in noise generation. In Germany, noise-reducing techniques include low-noise mastic asphalt (LV MA), noise-optimized stone mastic asphalt (SMA LA), noise-optimized asphalt top layer (LOA 5 D), porous mastic asphalt (PMA), and porous asphalt (PA), among others. The use of these road surfaces can achieve a noise reduction of up to 5 dB(A) [15]. The mentioned asphalt road surfaces consist of aggregates, bitumen, and optionally asphalt additives, and they influence the generation of tire-road noise through three mechanisms - either through the effect of surface texture, the effect of layer porosity, or the effect of layer flexibility. Asphalt surfaces installed until now have been designed to implement only one mechanism or, at most, two mechanisms simultaneously, and therefore, they do not fully realize the potential for maximum noise reduction [14]. The concept of achieving all three mechanisms simultaneously was advanced through the research conducted by Nilsson in the 1970s, focusing on the development of porous-elastic road surfaces (PERS). In PERS, both texture, compliance, and porosity are intended to work simultaneously to reduce noise. Subsequent research endeavors by Sandberg, Ejsmont, and Goubert [10, 11, 16, 17] further investigated the effectiveness of PERS. PERS is characterized by the composition of a road surface with a high level of voids (30 - 40 % by volume), the addition of rubber particles (up to 90 % by mass), and polyurethane binders. Its application has demonstrated a significant noise-reduction effect of up to 14 dB(A). However, a major drawback was the low durability of these structures, which sometimes failed after a very short period of use [10, 11, 16, 17]. Additional research projects such as VINNOVA, SILVIA, PERSUADE, and LIDAK [10,

11, 16, 17, 13] further investigated the issues of the earlier projects from 2000 to 2016 and achieved some improvements. However, the problem of low durability could not be resolved. The research project LIDAK, concluded in 2014 [13], stands out from the other mentioned projects due to its two-layered surface system consisting of a texture layer and an absorption layer. This system allows the texture layer to reduce noise through its defined surface at the source of generation, while the absorption layer ensures the significant effects of flexibility and porosity. Nevertheless, even in the case of LIDAK, the issue of low durability could not be resolved.

4.3 Approach and Methodology

In principle, traffic noise generation is attributed to the interaction between tires and the road surface being traversed.

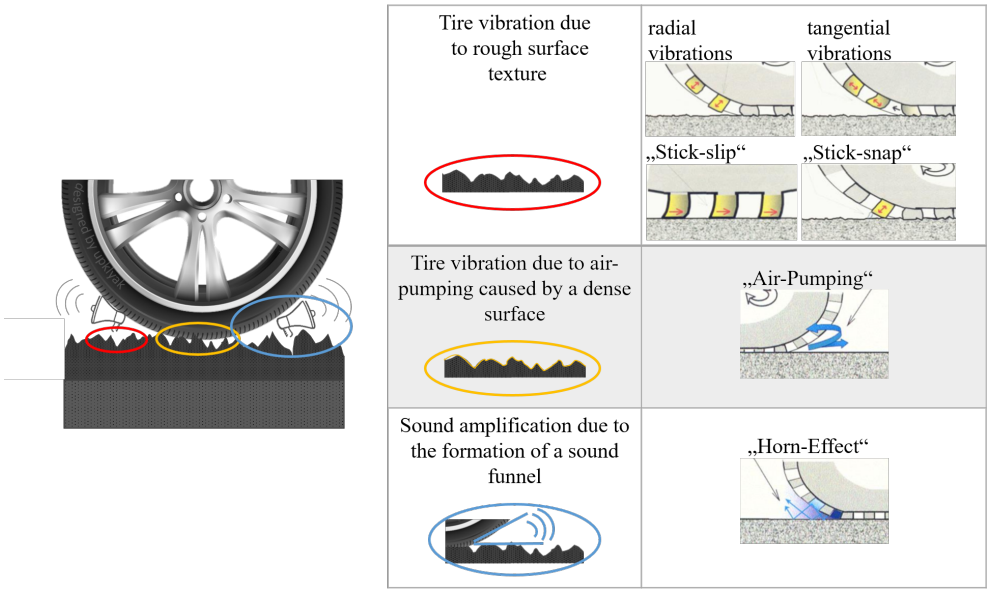

Figure 4.1: Origin of the tire-road noise [1, 2, 3]

Figure 1 summarizes the findings of Sandberg, Ejsmont, and Beckenbauer [1, 2, 3] and demonstrates that noise generation is caused by tire vibrations and sound amplification. To address this issue, the two-layered surface system LIDAK [13] was further developed as part of the INNO-PAVE research project [14]. The optimized surface concept in it comprises an absorption layer and a texture layer, each of which serves different functions in noise reduction (Figure 4.2). The absorption layer, composed of a polyurethane-bound aggregate and a rubber particle fraction, features an extensively porous pore structure and is more flexible than conventional asphalt surfaces due to the addition of rubber particles [14]. Applied on top of it is a texture layer consisting of a methyl-methacrylate binder, fillers, and a carrier textile, which reduces noise generation at its source through its texture [13, 18, 14, 4]. The development and construction of this texture layer are the focus of this study. Figure 4.2

illustrates the schematic structure of the two-layered surface system.

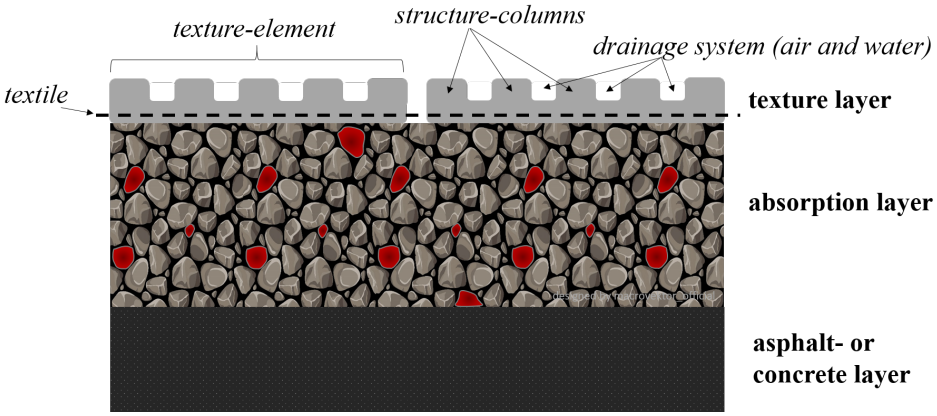

Figure 4.2: schematic representation of the surface layer concept

To address the issue of low durability of the system, the research simultaneously emphasized the shaping and material development of the texture layer. The focus of material development involved creating suitable binders, fillers, and textile yarns to obtain high-quality individual components for the implementation of the composite system. The shaping process was carried out concurrently to facilitate close alignment of the shape changes based on mechanical strength and noise generation. After determining the individual components and shaping, the composite material was implemented as a laboratory-scale prototype, where the validation of the composite system was conducted.

4.4 Texture Layer Development and Implementation

4.4.1 Shaping

The shaping of the texture layer serves two primary purposes in road traffic. Firstly, it achieves the desired noise reduction. Secondly, it creates a distinct texture that can be divided into macrotexture and microtexture, ensuring road grip. Macrotexture allows surface water to drain from the roadway and ensures direct contact between the tire and the road. Microtexture, which maintains the roughness of the surface material, influences the friction between the tire and the road, enhancing safety. Therefore, the shaping and stability of the texture layer traversed by traffic are crucial for the safety of road users. A failure of the layer, caused by issues such as material breakage or damage to the macro- and microtexture, could potentially lead to accidents.

The texture layer, consisting of structure-columns and a drainage system (Figure 4.3), was developed within the context of [13] and extensively examined for arrangement and geometry by Schacht [18], which was deemed suitable. Therefore, the results from these studies serve as a basis for further development in this study. However, during load tests according to

[13], the texture layer exhibited mechanical failures, manifested as damaged road structure elements.

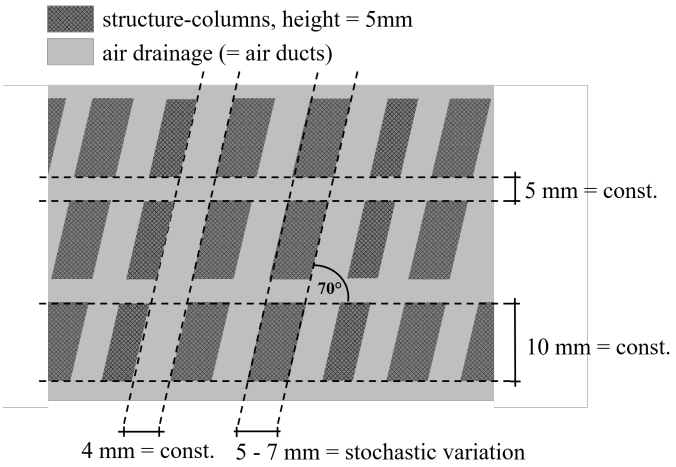

Figure 4.3: Preferred variant according to [13] and [18]

Due to the sharp edges and recessed corners of the structure examined in [13, 18], significant stress concentrations occurred, leading to failure. To counteract this, changes to the geometry concerning both mechanical and acoustic effectiveness were examined in several steps. Initially, the influence of varying fillet radii and heights of the road structure elements was investigated through 2D finite element simulations. Subsequently, a 3D shape optimization was conducted using the finite element program Abaqus.

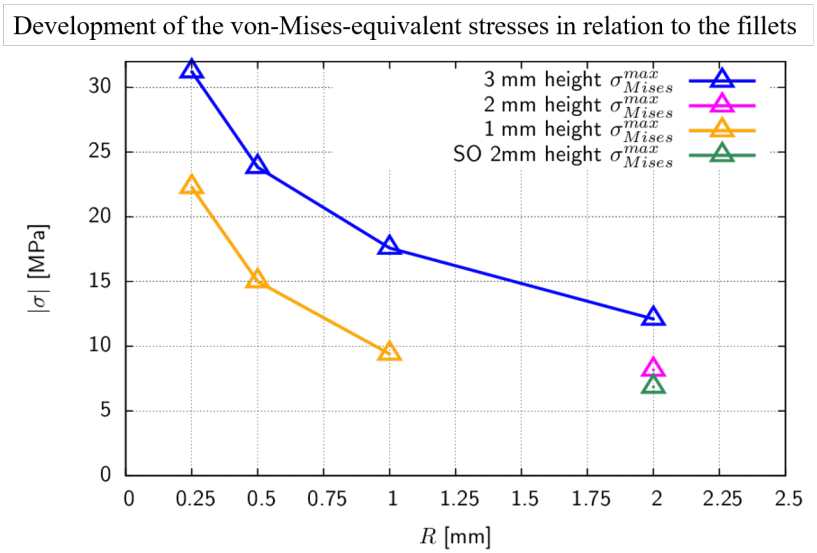

Figure 4.4: Evolution of the maximum von-Mises equivalent stresses as a function of the radius of the fillets and height or geometry of the structure

Selected results of this study are presented in Figure 4.4, which demonstrates that calculated maximum stresses can be significantly reduced with an increasing fillet radius. Tensile stresses could be reduced by 75 %, while compressive stresses were reduced by 57 %. The previously mentioned shape optimization further lowered the expected stresses by an ad-

ditional 16 %. Figure 4.5 displays the stress plot of an already optimized road structure element subjected to a compressive-shear load.

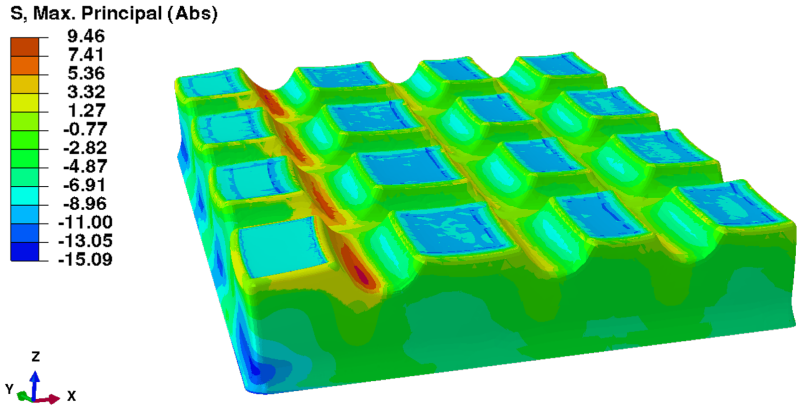

Figure 4.5: Stress contour diagram of a shape-optimized texture element

Subsequently, to design the underlying PERS layer, a simulation of the entire road system (as shown in Figure 4.6) was carried out to limit the maximum deflection of the pavement. To maintain numerical efficiency, only the most heavily loaded texture element was examined at a fine resolution, while the surrounding areas were approximated using homogenization.

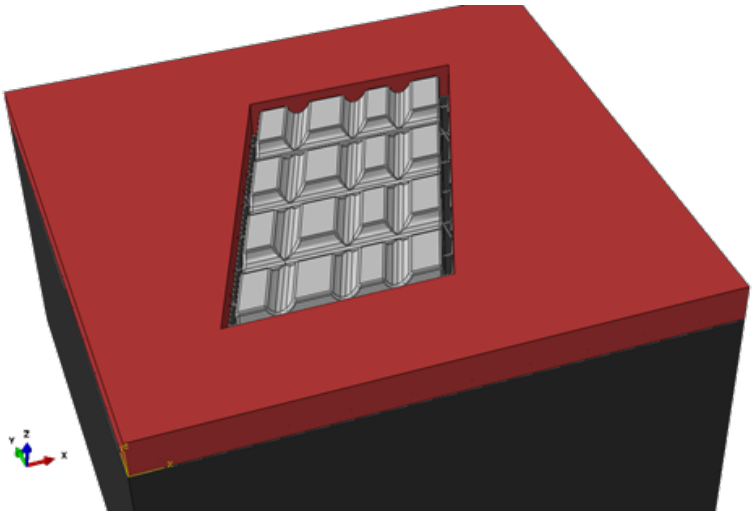

Figure 4.6: Section of the overall model of the INNO-PAVE pavement [14]. Gray: discrete texture layer; red: homogenized texture layer; white: textile; black: PERS.

Additionally, the effects of the texture layer on the deformation behavior of the system were also examined. This analysis revealed 10 % lower deformations in the shear direction in calculations involving a textile (as shown in Figure 4.7) with an absorption layer stiffness of 150 MPa [14].

To optimize the mechanical strength of the traversed texture layer, adjustments to the geometry were made, as seen in Figure 4.8. This involved varying the height of the structure-columns, which are the elements of the texture layer on which traffic rolls, and also adjusting

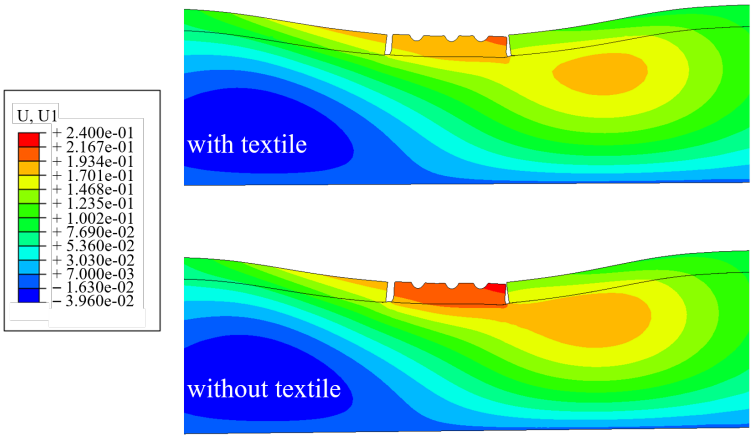

Figure 4.7: Comparison of the displacements in the direction of travel between results with and without consideration of the textile

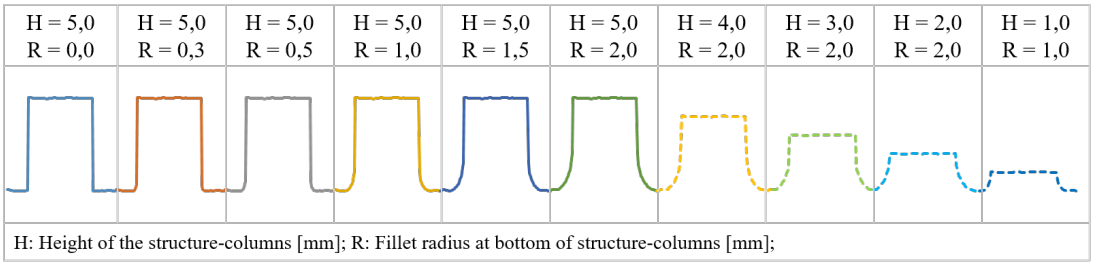

Figure 4.8: Process of geometric modification of the driving structure-columns to optimize mechanical strength. Radius (R) of the driving structure-column fillet on the shaft [mm], height (H) of the driving structure-column [mm] [14]

the fillet radius at the base of the structure-columns (shaft fillet). Besides its mechanical effectiveness, this shape modification also affects noise reduction. Changing the structure of the texture influences the volume of air drainage channels, leading to different effects on tire vibration, sound emission, and absorption.

The SPERoN® prediction model is used to determine tire-road noise based on a hybrid computational model. The model consists of a physical and a statistical sub-model, each providing predictions about tire force distribution on the texture, tire vibrations, flow noises, friction effects, torus noises (resulting from tire vibrations), and aerodynamic vehicle noises. Input parameters include factors like driving speed, road surface texture, and tire characteristics. The prediction model yields a sound pressure level of passing vehicle noise at a distance of 7.5 meters from the center of the road, at a height of 1.2 meters, for vehicles traveling at a speed of 120 km/h [6].

The SPERoN calculations in this study provided noise levels dependent on the height of the texture profile (the structure-columns) and the fillet radii at the base of the columns. Calculating various shape variants revealed a pattern of noise generation as depicted in Figure 4.9.

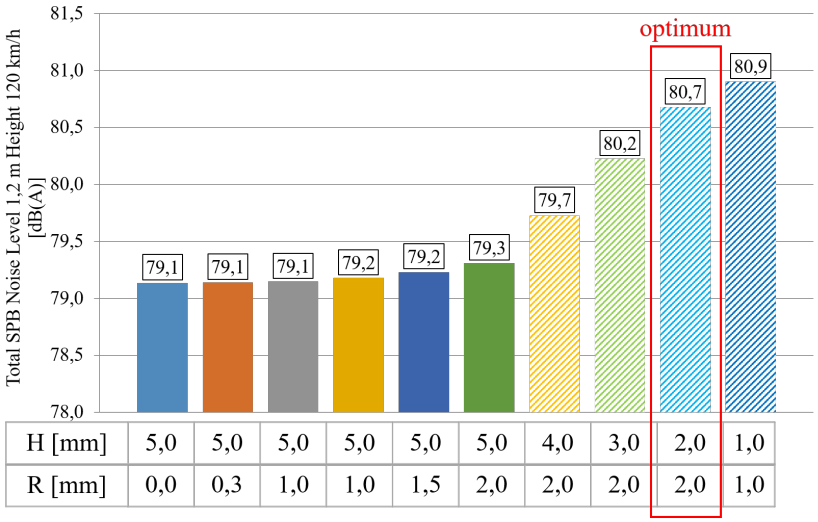

H [mm]	5,0	5,0	5,0	5,0	5,0	5,0	4,0	3,0	2,0	1,0
R [mm]	0,0	0,3	1,0	1,0	1,5	2,0	2,0	2,0	2,0	1,0

Figure 4.9: Influence of the heights (H) and the fillet radius (R) at the shaft of the structure-columns on the total noise level [dB(A)] simulated by the SPERoN-forecast model at 120 km/h pass-by speed [14]

Reducing the height of the structure-columns results in a reduction in noise reduction because sound-producing mechanisms are intensified due to a smaller drainage volume. Similarly, rounding the texture profile reduces the drainage area and promotes noise generation, even though to a lesser extent.

The small maximum grain size of the filler material MinMix AT 530, which forms the texture layer in conjunction with the methyl-methacrylate binder, reduces tire vibrations during traversal. MinMix AT 530 is a filler material from Quarzwerke GmbH, specifically optimized for use in methacrylate resins. It consists of a composition of quartz and feldspar with a maximum grain size of approximately 1 mm.

Furthermore, the drainage system of the texture layer reduces sound emission. The squeezing and suction of air through compression and decompression processes before and behind the tire during rolling are significantly reduced by the air drainage. This also greatly mitigates the horn effect, where sound emission is multiplied by the funnel-like space between the tire tread and the road surface. This is due to sound waves being directed through the openings in the texture layer into the substrate, where they are absorbed.

The compromise between mechanical optimization and simultaneous acoustic effectiveness is found to be optimal with structure-columns having a height of 2 mm and a shaft fillet of 2 mm. Further potential for reducing significant stresses was identified through shape optimization of the structural elements. The optimum total noise level calculated by SPERoN® shows a reduction of nearly 4.5 dB(A) compared to the SPB reference value of 85.2 dB(A) set by RLS-90 [5] for a non-grooved mastic asphalt.

4.5 Material Development

The development of the binder is significantly influenced by the requirements of mechanical properties to ensure that the texture layer can withstand the stresses imposed by accelerating, braking, and rolling traffic. Intensive research and parameter experiments led to the success of a binder based on methyl-methacrylate, which provides the necessary mechanical strength for the novel road surface layer over a temperature range of -20°C to +50°C. Methyl-methacrylate-based binders are characterized by their durability and excellent properties in industrial applications. To achieve the mechanical properties of the texture layer, a binder content of 20-30 % and a filler content of 70-80 %, using MinMix AT 530, are required. The polymer matrix is transitioned into a solid state through a radical polymerization process in suspension, using a initiator based on Di-Benzoyl peroxide.

In addition to the pure matrix material, the developed texture layer requires textile reinforcement for horizontal load transfer during the operational phase and to ensure rollability. The development of the textile reinforcement structure was built upon the results of the LIDAK project [13]. The biaxial fabric structure developed in [13] was based on glass fiber rovings and an epoxy resin coating. However, there were deficiencies, including the low shear strength of the glass fibers used and the high bending stiffness of the epoxy resin coating. The low shear strength of the glass fibers led to fiber breakage at the interface between the fiber and matrix. Additionally, the high bending stiffness of the epoxy resin coating prevented the textile-reinforced texture layer from rolling up in a consolidated state. Both of these deficiencies were addressed in the present study as part of the INNO-PAVE project [14]. Polymer fibers (PET and PVA) were tested as fiber materials, and three different flexible coating systems (dispersions) were compared during the investigations. Based on the previously determined maximum load case, which corresponds to a full braking of an overloaded truck, maximum forces in the longitudinal direction of $F_{longitudinal}$ = 89 kN/m and in the transverse direction of $F_{transverse}$ = 65 kN/m result [14]. To meet the specified requirements, the textile design was developed. In the first step, fibers and coating systems were preselected, and their properties were subsequently tested. The following Table 1 lists the preselected materials.

To withstand the maximum tensile forces (89 kN/m and 65 kN/m), the individual tensile strength of the rovings to be used must be relatively high to allow for an open-mesh structure of the reinforcement fabric. Therefore, a minimum tensile strength of 0.9 kN was set for the rovings to be used. This tensile strength can only be achieved with the high yarn counts of PET (16,500 dtex) and PVA rovings (13,860 dtex). To achieve the required FLängs = 89 kN/m, at least 99 rovings per meter in the warp direction (0°) of the fabric and 73 rovings in the weft direction (90°) of the fabric must be incorporated. This corresponds to a maximum warp thread spacing of 10.1 mm and a maximum weft thread spacing of 13.6 mm. Due to

Table 4.1: Investigated fibers and dispersions [14]

Type of fibre	**Coating-system**
PET, 1,100 dtex PET, 1,980 dtex	polymer-dispersion (B1)
PET, 7,700 dtex PVA, 7,920 dtex	polyvinylacetat-ethylen-copolymer-dispersion (B2)
PET, 16,500 dtex PVA, 13,860 dtex	polyurethane-dispersion (B3)

the alkaline resistance and excellent bond strength of PVA in concrete and in the Methyl Methacrylate-based binder to be used, further investigations focused on PVA rovings with a yarn count of 13,860 dtex. Tensile tests determined a tensile strength of 1.3 kN for the pure PVA rovings. Subsequently, an existing coating system was modified to impregnate the PVA rovings with the selected coating systems (see Figure 4.10).

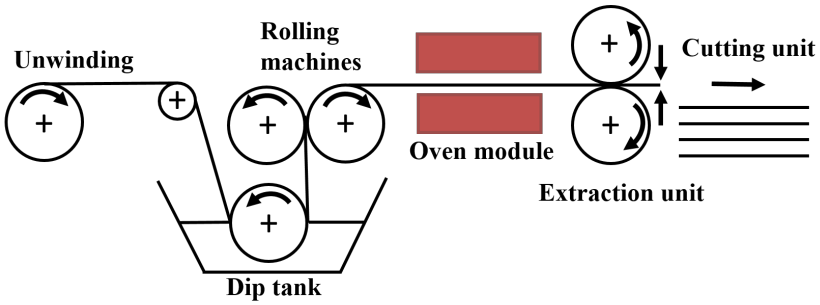

Figure 4.10: Process sketch of the coating plant at the Institute of Textile Technology (ITA) at RWTH Aachen University [14]

Subsequently, tensile tests on the impregnated PVA rovings were conducted again. The obtained results are presented in the following table 4.2.

Table 4.2: Results of the yarn tension tests with different coating compounds (mean values)

Sample	**tensile strength of yarn [kN]**
PVA 13,900 dtex, coating B1	0.76
PVA 13,900 dtex, coating B2	0.54
PVA 13,900 dtex, coating B3	0.57

The target value of 0.9 kN was not achieved by any of the samples. Based on microscopic images, it was observed that the coating systems could only penetrate the outer region of the rovings (10-15 % penetration depth, see Figure 4.11). Therefore, complete impregnation at the laboratory scale was not achieved.

This is partly due to the laboratory-scale coating machine at ITA. Subsequent investigations revealed that these issues do not occur in industrial-scale experiments. The examination of

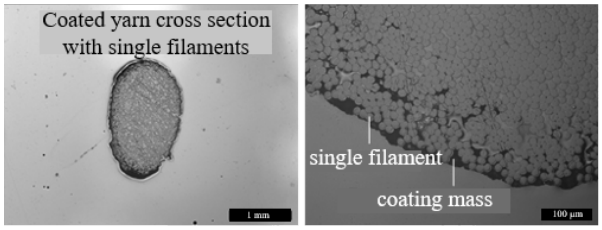

Figure 4.11: Microscopy images of the coated yarn cross-section

the texture layer was conducted in accordance with the testing standard DIN EN ISO 10319 - Tensile testing of composite materials [8] at the accredited testing laboratory of HUESKER Synthetic GmbH. The additional coating of the textile reinforcement allows the requirements for the composite system to be met.

4.5.1 Manufacturing and Testing of the Composite System

The texture layer elements with the optimized shaping consist of rhombus-shaped individual parts measuring 5.5 x 3.4 cm^2, which are interconnected by the textile reinforcement. To implement the composite system on a laboratory scale, the textile was integrated into the road texture layer elements by inserting it into the unreacted mass of the individual elements during the manufacturing process.

For the production of 32.0 x 26.0 cm^2 texture layer samples on a laboratory scale, an aluminum mold was created based on the available 3D data of the surface layer and subsequently molded with silicone. The resulting positive mold was then used to manufacture and test textile-reinforced texture layer samples. The flexibility of the silicone molds allowed for clean demolding of the cured binder matrix. To manufacture the test specimens, cutouts were provided in the edge area to accurately position the textile reinforcement in the mold. Subsequently, the mold was filled with the binder-filler mixture, which could be removed from the mold after curing (see Figure 4.12). The integrated textile provides flexibility to the road surface as it is exposed between the texture layer elements, allowing for the transmission of generated sound into the underlying layer. The textile reinforcement is also responsible for the durability of the composite system.

The texture layer samples produced using the process shown in Figure 4.12 serve as the basis for further laboratory tests to validate their effectiveness. Firstly, the previously mentioned strip tensile test was conducted to determine the tensile strength of the composite structure. Secondly, the samples were subjected to testing using the Aachen Ravelling Tester (ARTe).

The Aachen Ravelling Tester (ARTe) is used to assess the resistance to wear of asphalt surfaces. It applies shear stresses to the asphalt surfaces under test, which are typically encountered in real-world scenarios during cornering where the tire and road surface come

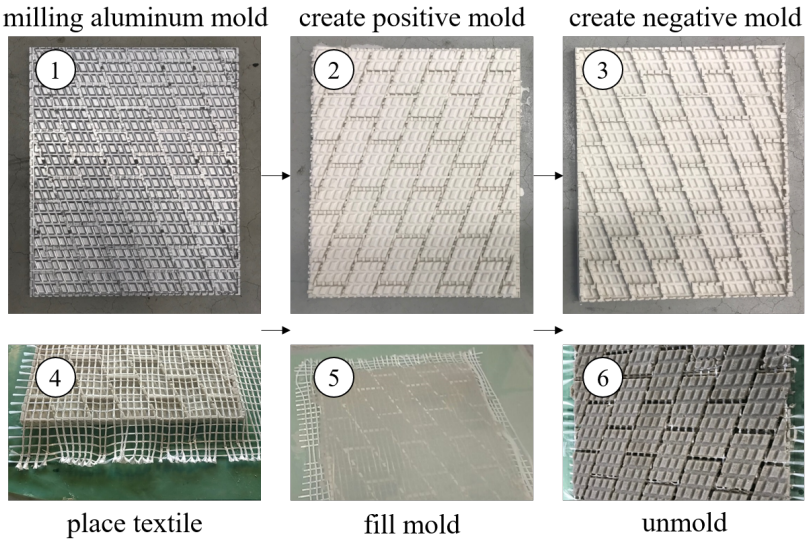

Figure 4.12: Production of the composite system on a laboratory scale (32.0 x 26.0 cm^2) [14]

into contact, often leading to material detachment from the road surface [7]. During ARTe testing, a dual-wheel setup with a defined axle load rotates around its own axis and exerts force on a sled. The sled holds two test specimens measuring 32 x 26 x 4 cm^3 and performs horizontal movement. The superimposed rotational and translational movements induce shear stresses that replicate realistic road conditions [7, 19].

The texture layer was tested using the ARTe. Various test specimens were prepared to assess the long-term durability of the texture layer. Texture layers with and without textile reinforcement were created and then bonded with a polyurethane-bound asphalt layer [14]. Polyurethane was used as the binder for the layer composite, serving to bond the rock and rubber particles in the absorption layer [14, 4].

The loading by the ARTe (with $F_{\text{Axle load,max}} = 450$ kg) demonstrated a significant influence of integrating textile reinforcement into the texture layer. No test specimen without textile reinforcement survived the testing without damage. It became evident that the inclusion of textile reinforcement is essential for the use of the texture layer. Under the loading conditions imposed by the dual wheels, shear stresses cause the textile to shear away from the substrate. With integrated textile, the texture layer is applied as a continuous surface on the substrate, whereas a texture layer without textile consists of individual texture layer elements adhered separately, providing no horizontal force transmission. Therefore, the textile enhances the overall system's resistance. Figure 4.13 and Figure 4.14 show the effects of ARTe testing with and without integrated textile.

No surface wear of the texture layer was observed due to the loading conditions. The material strength is sufficiently high, and no significant material loss was detected. Following testing with double the recommended number of passes, as outlined in the test procedure [7] (a

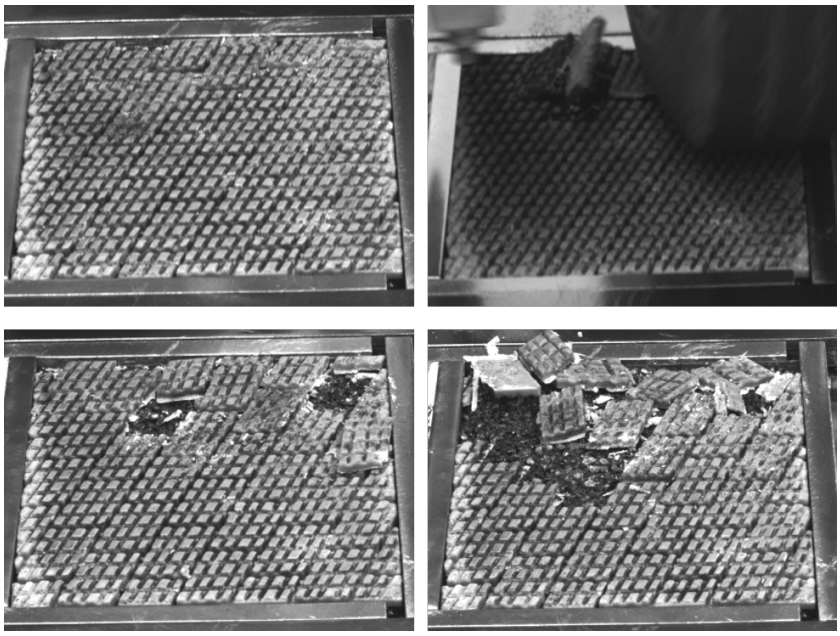

Figure 4.13: Texture layer in the course of loading by the ARTe without textile (video clips during loading - temporal order: top left, top right, bottom left and bottom right) [14]

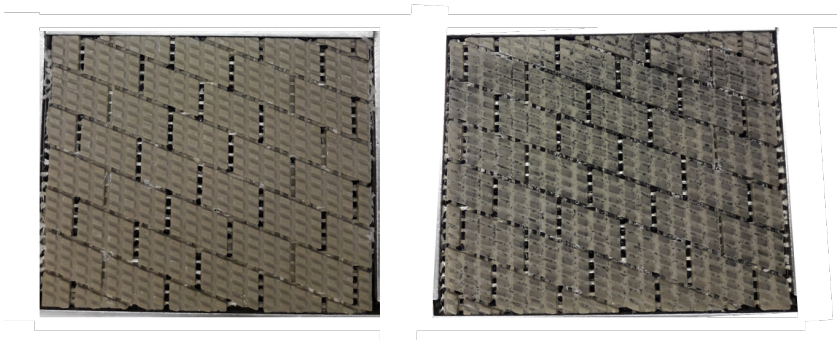

Figure 4.14: Record of the texture layer before (left) and after (right) loading by the ARTe with textile reinforcement [14]

total of 1,200 passes), only rubber abrasion from the tires was observed. Furthermore, the production of texture layer panels on a laboratory scale allowed for the determination of the achieved texture factor, which was determined through texture measurements using the ELA texture measuring device in accordance with DIN EN ISO 13473-1 [9]. The mean value from a total of five ELA texture measurements, with the ELA texture measuring device being repositioned before each measurement, serves to determine the mean texture factor, resulting in g = 86 %. The calculated texture factor indicates that, according to [12], a texture with high noise-reducing potential is present, a finding that is confirmed by the calculations of the SPERoN® prediction model.

4.6 Conclusion

The road surface system discussed in this study, consisting of the texture layer in combination with a polyurethane-bound absorption layer, has been optimized for resistance to surface-applied horizontal loads. Compared to the previous texture from [18, 13], the developed texture layer reduces the noise-reducing effect by approximately 2 dB(A). This reduction is attributed to the shape optimization that ensures the durability and stability of the system. However, the application of the SPERoN® computational model shows a noise reduction of 4.5 dB(A) compared to the reference pavement according to RLS 90 [5]. This noise reduction is solely attributed to the effect of the texture layer and does not consider additional noise reductions provided by the underlying absorption layer. For open-pore asphalts, which typically need replacement every seven to eight years, it is assumed that a noise reduction of 5 dB(A) is achieved in the new construction state, similar to the noise reduction achieved in this study. Since further noise reduction potential is expected through the use of the complete system, including both the texture and absorption layers, it is anticipated that implementing the entire system will result in additional noise reduction while maintaining long-term stability.

4.6.1 Integration into the Road Pavement

One possible application for the texture layer is mainly in urban highway areas or other heavily trafficked roads in built-up areas that allow speeds between 80 and 120 km/h. The texture layer can be used as an independent system with various substrates. However, it is recommended to use the texture layer in combination with the corresponding absorption layer, which consists of polyurethane-bonded rubber and stone particles and has a high porosity for a high absorption capacity. The composite system, consisting of the texture and absorption layers, should also be applicable to conventional asphalt pavement. Studies on the bonding behavior between conventional and new asphalt layers are currently being conducted. With pre-production of the texture layer under stationary conditions, prefabricated elements are always available as stock. In addition to manufacturing it as sheet material, which has been done so far [14], manufacturing it as roll material is also conceivable, allowing for more efficient application of the system. This installation method results in short installation times, which have a positive impact on reducing traffic congestion, as the duration of work zones can be significantly shortened.

References

[1] T. Beckenbauer. "Physik der Reifen-Fahrbahn-Geräusche – Geräuschentstehung, Wirkmechanismen und akustische Wirkung unter dem Einfluss von Bautechnik und Straßenbetrieb." In: *Geräuschmindernde Straßenbeläge in der Praxis – Lärmaktionsplanung* 4 (2008).

[2] Bundesministerium für Verkehrs- und digitale Infrastruktur, ed. *Einfluss der Fahrbahntextur auf das Reifen-Fahrbahn-Geräusch.* Forschung Straßenbau und Straßenverkehrstechnik. Bonn: Bundesministerium für Verkehr und digitale Infrastruktur, 2002.

[3] J. A. Ejsmont et al. "Tyre/road noise reduction by a poroelastic road surface." In: *Inter-noise 2014, 43rd International Congress on Noise Control Engineering, 16-19 Nov, 2014* (2014). URL: https://www.acoustics.asn.au/conference_proceedings/INTERNOISE2014/papers/p13.pdf (visited on 10/09/2023).

[4] S. Faßbender and M. Oeser. "Investigation on an Absorbing Layer Suitable for a Noise-Reducing Two-Layer Pavement." In: *Materials* 13.5 (2020).

[5] Forschungsgesellschaft für Straßen- und Verkehrswesen. *Richtlinien für den Lärmschutz an Straßen (RLS-90) (FGSV 334).* Köln, 1990.

[6] Forschungsgesellschaft für Straßen- und Verkehrswesen. *Textureinfluss auf die akustischen Eigenschaften von Fahrbahndecken (FGSV 442).* Köln, 2013.

[7] German Institute for Standardisation. *DIN EN 12697-50:2018: Bituminous mixtures - Test methods - Part 50: Resistance to scuffing.* Berlin, 2018.

[8] German Institute for Standardisation. *DIN EN ISO 10319:2015-09: Geosynthetics - Wide-width tensile test; German version EN ISO 10319:2015.* 2015.

[9] German Institute for Standardisation. *DIN EN ISO 13473-1:2021-11: Characterization of pavement texture by use of surface profiles - Part 1: Determination of mean profile depth, Corrected version 2021-06; German version EN ISO 13473-1:2019.* 2021.

[10] L. Goubert. *Above the development and use of the poro-elastic road surface.* Brussels, 2011.

[11] L. Goubert and U. Sandberg. "The PERSUADE project: Developing the concept of poroelastic road surface into a powerful tool for abating traffic noise." In: *Proceedings of the INTER-NOISE 2010 – 39th International Congress on Noise Control Engineering 2010, Lisbon, Portugal, 15-16 June 2010* (2010).

[12] B. Krieger and O. Ripke. "Einfluss der Fahrbahntextur auf das Reifen-Fahrbahn-Geräusch." In: *Straße und Autobahn* 52 (2001), pp. 456–458.

[13] M. Oeser and A. Schacht. *Abschlussbericht Leise innovative Deckschicht auf Kunststoffbasis (LIDAK), FE 88.0108/2011.* 2014.

[14] M. Oeser et al. *INNO-PAVE : Final report: "Grundlagen der konstruktiven Gestaltung, Struktur sowie neuer polymerer Werkstoffe für:Straßendeckschichtsysteme" im Verbundprojekt: "Grundlegende Erforschung polymerer Werkstoffe sowie innovativer Herstellungs- und Einbautechnologien für Straßendeckschichtsysteme" : Duration of research project: 09/2015-04/2019*. Aachen, 2019.

[15] U. Peschel et al. *Lärmmindernde Fahrbahnbeläge: Ein Überblick über den Stand der Technik*. Ed. by Umweltbundesamt, Wörlitzer Platz 1, 06844 Dessau-Roßlau. 2014. URL: http://www.umweltbundesamt.de/publikationen/laermmindernde-fahrbahnbelaege-0 (visited on 10/09/2023).

[16] U. Sandberg and J. A. Ejsmont. *Tyre/Road Noise Reference Book*. Harg, Kisa, Sweden: INFORMEX, 2002.

[17] U. Sandberg et al. "Tyre/road noise reduction of poroelastic road surface tested in a laboratory." In: *Proceedings of ACoustics 2013, 17-20 Nov 2013, Victor Harbor, Australia* (2013).

[18] A. Schacht. "Entwicklung künstlicher Straßendeckschichtsysteme auf Kunststoffbasis zur Geräuschreduzierung mit numerischen und empirischen Verfahren." PhD-Thesis. Aachen: RWTH Aachen University, 2015.

[19] D. Wang. "Schaffung des Bewertungshintergrunds zur Charakterisierung des Polierverhaltens der einzelnen, gesteinsbildenden Minerale und zur Untersuchung des Griffigkeitsverhaltens der Mineralaggregate in Abhängigkeit von den Polierbedingungen." PhD-Thesis. Aachen: RWTH Aachen University, 2011.

5 Assessing the Durability and Acoustic Performance of a Novel Two-Layer Pavement System

This paper was published under:

Tekampe, Sabine and Oeser, Markus: "Assessing the Durability and Acoustic Performance of a Novel Two-Layer Pavement System". In: Sustainability, 15(23), 16475, https://doi.org/10.3390/su152316475, 2023.

5.1 Abstract

In the quest for more sustainable pavement solutions, this study demonstrates the successful strengthening of a unique noise-reducing two-layer road surface. While existing noise-reducing pavements reveal high acoustic efficiency, but lack mechanical strength, earlier research efforts addressed the optimization of the individual components of this system, and a comprehensive perspective on its integrated performance remained elusive. Therefore, this research bridges this knowledge gap through an in-depth laboratory evaluation, in which the requirements for the realization of a full-scale demonstrator were defined, followed by a comprehensive performance assessment in terms of acoustic and mechanical strength. The post-construction assessment reveals the system's multifaceted strengths, considering noise reduction, resilience under heavy traffic, pavement deflections, and skid resistance, assessed by CPX measurements, accelerated pavement tests using the MLS 30, skid resistance tests employing the pendulum test as well as the slow-moving longitudinal friction test (Micro-Griptester), and Falling Weight Deflectometer (FWD) measurements. Although the optimized system implies lower noise-reduction potential, it exhibits great strength compared to previous noise-reducing pavements. In General, the system offers viable noise mitigation solutions for urban highways, particularly in settings where traditional noise abatement measures are constrained by space. The insights from this study serve as a valuable reference for the development and evaluation of innovative road engineering materials and technologies.

5.2 Introduction

Noise originating from road traffic has been a persistent companion for many residents for years, a phenomenon that continues to escalate due to the increasing volume of traffic [30]. It significantly affects the population residing in close proximity to roads in a predominantly adverse manner and can potentially lead to long-term health impairments [38]. To mitigate road traffic noise, noise-reducing road surfaces are currently being employed. These surfaces aim to diminish the noise generated by tire-road interaction during vehicle movement. This strategy enables a partial reduction of traffic noise, which encompasses propulsion, aerodynamic, and tire-road noise, through the design of the road surface. Among the existing noise-reducing road surfaces are noise-optimized bituminous asphalt [18], porous asphalt [23], poro-elastic road surfaces (PERS) [27, 19], polyurethane-asphalt (PU-asphalt) [25], and the two-layered noise-reducing surface system known as LIDAK [28].

Noise reduction functionalities of road surfaces can be categorized into three primary mechanisms. Open-pore surfaces with an extensively branched cavity system exhibit high absorption capacity, capable of capturing and absorbing aerodynamic noise. Additionally, they diminish compression and decompression noises (i.e., air-pumping) [3, 27]. Another

noise-reducing function involves a flat road texture ('plateau with grooves') that reduces tire vibration excitation [3, 23]. Furthermore, there exists the function of elasticity within a layer, causing the layer to yield upon tire impact, absorbing structure-borne noise from the tire and thereby reducing tire vibrations resulting from the impact. Furthermore, a frequency dependency of road-tire noises was observed. Airborne road noise, such as air pumping, pipe, and Helmholtz resonances, is perceptible in the higher frequency range above 1000 Hz. In contrast, structure-borne noise, like tire vibrations, stick-slip, and stick-snap sounds, tends to generate road noise in the lower frequency range below 1000 Hz.

Establishing a new pavement, in reality, requires the application of principles of pavement design, aiming to develop roads free from failures and with consistent functionality throughout their life cycle. Dimensioning focuses on avoiding structural and functional failures. Structural failures encompass damages leading to pavement collapse, rendering them incapable of withstanding traffic loads. On the other hand, functional failures result in significantly compromised comfort or safety for road users. These damages occur when traffic loads or environmental influences were inadequately considered during road design or have significantly changed over time. They may also stem from the failure of the materials used (surface fatigue, consolidation, or shear). Many damages can be attributed to the quality of the bound and unbound subgrade. However, some relate to failures within the wear layer. For instance, in flexible pavements, failure of the top layers might emanate from underdesigning regarding layer thickness, inadequate compaction, or poor internal friction, causing structural damages like cracking, rutting, or shear failure. Functional damage, for instance, can arise from an excessive use of bitumen leading to the phenomenon of bleeding, significantly diminishing skid resistance [39].

Merely possessing maximum acoustic noise-reducing effects does not suffice for the practical implementation of noise-reducing road surfaces. They must also adhere to the mentioned design principles and withstand the loads from traffic and the environment.

In the literature, it is evident that noise-reducing road systems, despite exhibiting high noise reduction efficacy, tend to experience structural failures under real loads. Porous asphalts carry a high risk of ravelling over their service life [23]. Poro-elastic road surfaces (PERS) have been observed to detach from the base layer or suffer aggregate breakage [19]. LIDAK demonstrates significantly low mechanical strength in the texture layer, since assessments using the Aachen Ravelling Tester (ARTe) revealed considerable surface wear after just 30 minutes of shear stress [28].

In previous studies by [5] and [6], the LIDAK system underwent optimization in its individual components. The concept of the optimized LIDAK system is depicted in Figure 5.1. This illustration portrays a texture layer comprising numerous texture elements. A textile mesh ensures interconnection among the texture layer elements, facilitating airflow through

the apertures into the underlying absorption layer. The dual-layered system significantly diminishes the generation of tire-road noise owing to the unique texture of the texture layer. Simultaneously, any resulting aerodynamic noise (including environmental sources) can be absorbed by the absorption layer beneath.

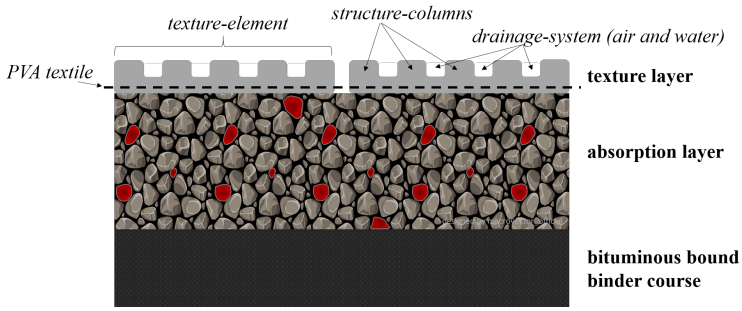

Figure 5.1: Concept of the optimized noise-reducing two-layer system by [5, 6].

The individual layers of LIDAK (texture layer and absorption layer) have been further developed in terms of their stability. The composition of the absorption layer from LIDAK, consisting of a high proportion of crump rubber, aggregates and polyurethane binder, was modified to enhance its mechanical stability. This was achieved through a substantial reduction in the rubber content, which decreases the elasticity of the layer and the use of a high strength polyurethane (Elastan® 6568/103, BASF Polyurethanes GmbH, Lemförde, Germany). Through the remaining proportion of crump rubber, it still enables a certain elasticity, which should lead to low mechanical tire vibrations. In the study by [5] the absorption layer was comprehensively examined and enhanced in terms of its performance characteristics: deformation behavior, low-temperature behavior, and fatigue behavior, showing high resistance to deformation and fatigue, and reasonable resistance to low-temperature. The absorption behavior reached an absorption coefficient (α) of nearly 1.0. The textured top layer, consisting of cold plastic, was mechanically optimized as well to enhance its resistance to ravelling. This involved a new material definition, geometric adjustment and the integration of a textile, resulting in increased resistance to ravelling and no visible wear of the texture layer during shear stress tests in the ARTe. With this optimization, the texture layer could withstand forces from heavy truck loads (such as an overloaded full-breaking truck) [6].

Based on insights from the literature, there is a necessity to optimize noise-reducing systems concerning their structural integrity. This study aims to leverage the optimizations conducted by [5] and [6] regarding the LIDAK system to integrate its individual components into a comprehensive system. A holistic examination of distress prevention cannot be conducted due to insufficient knowledge about the subgrade of the demonstration area. However, there is an opportunity to determine the strength of the evolved surface layer system. In this case, overall strength comprises the individual strengths of the layers (previously investigated in [5, 6]) and the bond between these layers. This can be further examined through bond

strength and accelerated pavement tests that will be evaluated by visual assessment as well as skid resistance and load-bearing tests. Additionally, it is possible to assess the functional condition of the surface layer system, characterized by its skid resistance and noise-reducing effectiveness, which can be achieved through skid resistance and acoustic measurements.

5.3 Materials and Methods

A polymethyl methacrylate*[1] (PMMA) binder is the binding agent of the texture layer. PMMA is the basic component of road markings, that are already used in road infrastructure and it is characterized as a brittle material with high strength, high modulus of elasticity, and high surface hardness (scratch-resistant). It can be polished, is weather-resistant without stabilization, and resistant to weak acids, alkalis, non-polar solvents, greases, oils, and water [2]. Due to its mentioned durable properties it is suitable for use as a texture layer. The specific methyl methacrylate used in this study retains its mechanical properties in the temperature range from -20°C up to + 50°C. A fine-grained ($\leqslant$ 1 mm max. grain size) mineral filler*[2] is added to the polymer binder, to receive a rough and strong surface. The final mixture consists of 75 wt.-% mineral filler and 25 wt.-% PMMA binder. 1% of hardener powder*[3] (as a proportion of total formulation) is finally added to initiate the reaction [6]. The texture layer is applied to an absorption layer composed of 7.5 vol.-% crump rubber*[4] and 92.5 vol.-% mineral aggregates*[5, *6], and 13 vol.-% polyurethane binder*[7] (PU) is added to the aggregate mix. More information about the material composition and the origin of the materials are available in the Appendix 5.7, Tables 5.2 and 5.3.

5.3.1 Production of the Absorption and Texture Layer

According to [5] the absorption layer will be mixed batch-wise. For this purpose, crumb rubber, mineral aggregates, and mineral filler are pre-mixed in a mixer. After short pre-mixing, the homogenized polyurethane binder is added and the mixing continues until all components are completely wetted with polyurethane. After that, the mix is filled and spread into molds with the size of 32 x 26 x 4 cm^3 (W x L x H) and compacted with a static hand compaction roller to receive plates with an even surface. The polyurethane in the mixture forms a thin layer around the rubber and aggregate particles and bonds the contact points, leading to a high tensile strength. The production method delivers a strong grain structure and a target void content of 35 vol.-% (Figure 5.2).

5.3.2 Preparation of the Texture Layer Plates

To produce the texture layer with the special geometry, a silicone mold was used with the designed geometry from [6]. It was found, that the strength of the cured layer was best

Figure 5.2: Production process of the absorption layer: (a) aggregates, (b) mixing tool, and (c) compacted mixture in mold.

when the mold was filled with the compound first and the PVA-textile placed into the fresh compound afterwards. This process allowed a processing time of around 10 minutes, which required fast and careful handling. To receive an even surface layer, during curing a heavy plate and a foil as an intermediate were placed on the fresh-filled silicone mold. After a full chemical reaction time of 20 - 25 minutes, the finished layer could be released from the mold (Figure 5.3).

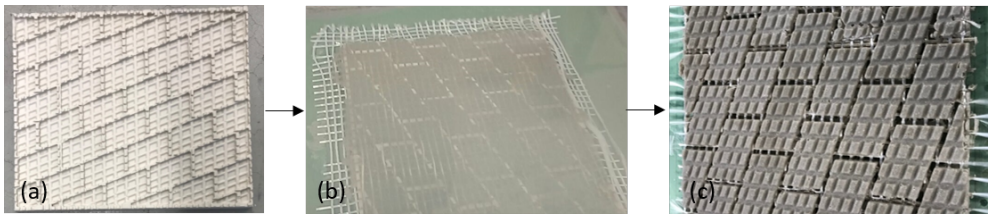

Figure 5.3: Production process of the texture layer: (a) silicone mold, (b) filling the mold and placing textile, and (c) releasing texture layer from mold.

After the completion of both layers, the texture layer is applied to the absorption layer, which is shown in Figure 5.4.

Figure 5.4: Combination of texture and absorption layer.

5.3.3 Methodology

The objective of this study is to first develop the strength of the entire system through experimental tests on a laboratory scale. After the successful implementation of a real-scale demonstrator, the actual effectiveness will be verified through a full-scale analysis.

The investigation of the system on a laboratory scale is necessary to obtain insights into

the functionality of the system, which can be recognized at a small scale, such as the skid resistance and the interaction between the individual layers. Therefore, fundamental laboratory tests are initially employed to generate information for the upscaling process and the effectiveness of the system. In detail, the first part of this study examines the skid resistance, the bonding between the texture and absorption layers, and rutting behavior using the SRT pendulum [16], the shear bond strength test [14], and the rutting test [13]. From these tests, the bonding requirements between the texture and absorption layers are derived to prevent delamination of the layers. After this, an investigation is carried out to determine to what extent and under which conditions a strong bond can be established between the permeable open-porous absorption layer and conventional bitumen-bound binder layers. This involves not only preventing delamination between the absorption and binder layers but also ensures the sealing of the bituminous binder layer to prevent water ingress into the asphalt layers and potential damage from water ingress. In the second part of the study, the system is investigated on a large scale in terms of acoustical and mechanical performance. For this purpose, acoustic measurements such as the CPX procedure [17] are employed to generate an overall noise level of the system. Additionally, mechanical durability is a focus of this study, which is why a heavy load test is conducted using the MLS 30 [34] to demonstrate that the system can withstand high stresses. To further evaluate the system's performance, a visual failure assessment combined with Falling Weight Deflectometer (FWD) measurements as well as skid resistance tests with the micro GripTester, were conducted, which are intended to show the impact of the heavy load on these properties.

5.3.4 Laboratory Study

Skid Resistance Test

According to [16], the pendulum test (skid resistance test - SRT), which is a stationary measuring instrument, is used for localized determination of the surface grip. The pendulum device consists of a spring-loaded sliding body made from standardized rubber, which is attached at the end of a pendulum arm. Upon releasing the pendulum arm from a horizontal position, the sliding body swings over the test surface, causing a decrease in its rise height and the energy loss is measured using a calibrated scale. The results are output under a "Skid-Resistance Test Value" (SRT value).

Aachen Ravelling Test

The Aachen ravelling test (ARTe) is used to assess the resistance to wear on asphalt surfaces. The ARTe applies shear stresses to the asphalt surfaces, which are encountered in real-world scenarios during cornering when the tire contacts the road, often leading to material loss on

the road surface. During the ARTe test, a dual-wheel setup with a defined axle load rotates around its own axis, exerting force on a sled. The sled accommodates two test specimens with dimensions of 32 x 26 x 4 cm^3 and performs horizontal motion. The superimposed rotational and translational movements induce shear stresses that replicate realistic road conditions [15, 36]. In the testing device, the weight of the axle load is adjustable to a wheel load from 250 kg (basic load) up to 450 kg and the number of tire loads is adjustable as well. The test is merely used as a load-bearing device.

Wheel Tracking Test

The rutting test with the Wheel Tracking Test (WTT) according to [13] is employed to assess the susceptibility to deformation of asphalt materials. The criterion for evaluation is the rut depth formed during the test, which is generated by repeated passes of a loaded wheel at a constant temperature. In this study, a solid rubber-tired wheel applies a load to a test specimen plate for 20,000 wheel passes in an air bath at 60°C. The derived parameters from this are the rutting depth and the proportional rutting depth.

Shear Bond Strength Test

The shear bond strength test (SBST) according to [14] is conducted to assess the resistance to horizontal shear stresses in the interlayer of two pavement layers. In this test, cylindrical test specimens are subjected to controlled temperature and constant shear loading. In detail, the sample core with a diameter of 150 mm is placed within four clamps. The clamps encompass the two layers of the core sample while leaving the layer boundary free. Then a static load is applied on the upper layer until the interlayer bond fails. During the test, the evolution of shear deformation and shear force is recorded, and the shear strength (in MPa) at the interface between the layers is determined as the highest recorded shear stress.

Tensile Bond Strength Test

The tensile adhesion test (TAT) by [14] is used to assess the tensile bond strength between two pavement layers. The test method is generally applicable to thin surface layers and can be used to evaluate the interlayer adhesion quality of adhesive or binder films and the internal cohesion between two pavement layers. Within the test, the upper layer from a cylindrical asphalt test specimen consisting of two asphalt layers is pulled apart with a test stamp attached vertically to its surface with a constant speed of 200 N/s until it fractures. Consequently, the adhesion strength is determined, which represents the maximum force applied relative to the cross-sectional area of the specimen.

Permeability Test

According to [12], the method for determining the vertical permeability of cylindrical asphalt specimens with interconnected voids involves applying a water column of constant height to a cylindrical test specimen, allowing the water to flow through the specimen in the vertical direction for a specified duration. The resulting water flow rate, denoted as Q_v, is a calculated measure of the permeability value k_v. The test is conducted at ambient temperature.

5.3.5 Large Scale Study

Sound Absorption Measurements

To determine tire-road noise, the near-field method, as outlined in the European standard [17], is employed. This method, also known as the Closed Proximity Method (CPX), allows for the measurement of sound pressure levels in close proximity to the tires within a sound-insulated trailer towed by a vehicle. This measurement allows most noises to be eliminated outside the tire-road noise since the microphones are oriented to record the tire-road noise. The sound pressure level coming from the tire road noise is continuously recorded and averaged over the traveled distance. The measurement can be conducted at speeds of 50, 80, or 110 km/h and is applicable to both truck and passenger car tires. In this case, Uniroyal Tigerpaw (SRTT) Car tires were used.

Accelerated Pavement Testing

To investigate the long-term effects of traffic volume on road construction, accelerated pavement testing (APT) is employed. In this context, the Mobile Load Simulator (MLS 30), available in Germany, was utilized to assess the functionality and durability of the noise-reducing road pavement. This simulator is capable of applying uniaxial loading to a 3.5-meter road section with a constant wheel load (super-single tires). The road section was subjected to loading at the maximum tire speed of 21 km/h, equivalent to 6,000 tire passes per hour, with a wheel load of 45 kN (approx. 5 tons of wheel load) [35].

The analysis of the results from the accelerated pavement testing using the MLS 30 is conducted through the examination of surface images. These surface images provide the opportunity to depict the test section before and after loading, allowing for the detection of differences caused by the loading. As per Wacker [34], a cross-sectional area of 0.5 m^2 (1.0 m x 0.5 m) is always considered. A high-resolution camera is positioned with a defined camera angle above the area of interest, ensuring directly comparable and analyzable images. Within this study, images were captured both before (0 passes) and after loading (after 160,000 passes).

Deflection Measurements

To provide insight into the load-bearing capacity of the two-layer surface system, Falling Weight Deflectometer (FWD) measurements according to [8] were conducted. The resulting load-bearing capacity obtained from these measurements offers insights into the deformation resistance of road construction under short-term loading conditions, yielding a deformation basin. The deformation basin consists of deformations within the substrate induced by an impulse load (50 kN) at a load application point, which has a diameter of 300 mm. This impulse load simulates the rolling over of a heavy truck at the measurement point. As the distance from the load application point increases, the localized deformation, detected using nine geophones, decreases.

To evaluate the results, this study employs the calculation of the radius of curvature R_0 and the bearing capacity number T_Z, determined directly from the normalized deflection curve ("Jendia method" [20]). The radius of curvature at the load center can be determined based on a regression equation from the deformations w_0 [mm] (directly at the load center) and w_{210} [mm] (at a distance of 210 mm from the load center). The curvature radius is thus obtained according to Equation 5.1 [8].

$$R_0 = 24.494 \cdot (w_0 - w_{210})^{(-0.899)} \tag{5.1}$$

And from this, the bearing capacity number T_Z [-] is determined according to Equation 5.2 [8].

$$Tz = (\frac{R_0 \cdot 1,000}{w_0})^{0.5} \tag{5.2}$$

As per [37], the deflection w_0 indicates the load-bearing behavior of the unbound layers in the asphalt structure at the load application point. The curvature radius R_0, on the other hand, describes the deformation behavior of all bound layers in the asphalt structure at the load center. Since both parameters contribute to the determination of the bearing capacity number T_Z, it is a measure of the comprehensive load-bearing behavior of the asphalt pavement structure at the load center. This means, the higher the bearing capacity number, the higher the load-bearing capacity of the road pavement.

In use is an FWD measurement instrument provided by the Federal Highway Research Institute. The FWD measures the load-bearing capacity before and after the MLS 30 loading.

Skid Resistance Measurements

To measure the skid resistance of the overall surface, a Portable Friction Tester (PFT), the microGriptester by the company Mastrad Ltd. was used. In contrast to the measurement with the SRT pendulum, the GripTester uses the method based on the slow-moving longitudinal friction coefficient (LFC) [24] recorded in walking pace [21].

According to the British standard BS 7941-2:2000 [31] the GripTester measures the LFC under wet conditions with a small test wheel operating at a fixed slip ratio of 15%. The testing wheel is attached to a stub axle and is mechanically braked through a fixed gear and chain system connected to the drive wheel axle. As the wheel is pulled along the wet pavement surface at a consistent speed, it experiences slippage, and both the slipping force and the vertical load are measured. During the measurement, the data is collected and the resulting friction coefficient across the measured distance, called Grip Number (GN), is recorded.

5.4 Results and Discussion

5.4.1 Results of the Experimental Study on a Laboratory Scale

The test results from the explained experiments will be presented, analyzed, and discussed in the following. This will be done in a sequence where fundamental manufacturing processes and laboratory tests are considered first, as they provide essential insights necessary for the implementation at full scale. Following this, an explanation of how the full-scale demonstrator is constructed will be provided. After this, the presentation, analysis, and evaluation of the full-scale experiments will be addressed.

Skid Resistance of the Texture Layer

To ensure that the adapted geometry by [6] provides sufficient skid resistance, the skid resistance was examined using the SRT pendulum [16] in combination with the ARTe test [15]. The study investigated the initial skid resistance and how it changes over a short loading period of 600 cycles at two different axle loads. This is meant to determine whether the layer has high or low resistance to wear.

A total of five SRT values, following the loading cycles of 0, 200, 400, and 600 cycles, were determined in accordance with [16], and their mean value was calculated. Since two plates were tested for each loading weight, the values from both plates were also averaged. Figure 5.5 presents the results in a bar chart, depicting the mean SRT values as a function of the number of load cycles.

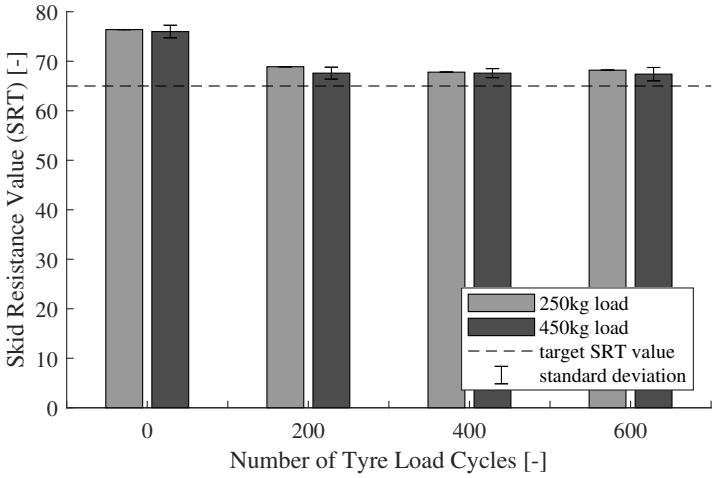

Figure 5.5: Development of the skid resistance of the texture layer.

Figure 5.5 shows the mean initial skid resistance of the texture layer, which is at a value of 76 SRT units. After loading 200, 400, and 600 tire passes, the SRT units reduce to a mean value of around 68 SRT units. We can observe that the magnitude of the wheel load (250 kg (light grey) or 450 kg (dark grey)) has little influence on the SRT value and that the loading shows no significant signs of wear and tear. Since the SRT measurement results on the 250 kg plates have emerged exactly the same, no standard deviation exists. A comparison to [28] reveals that the SRT values of the texture layer in this study are superior. [28] obtained SRT values for his material, ranging between 50 and 65 SRT values. Also, [19] tested the friction indexes using the SRT pendulum on their developed PERS layers, which yielded values ranging between 48 and 64 SRT values and one deviating value of 78 SRT values. The German standard [9] suggests a method to categorize the SRT values into friction classes. Within this method, the SRT values will be associated with values that describe the condition of the surface with regard to friction. In reference to the method, the initial SRT value of 76 describes a very well condition of the surface, because it is classified as higher than an SRT value of 65, which is a target SRT value when installing a new asphalt top layer in Germany. The following SRT-values loaded by 200, 400, and 600 load cycles still achieve a mean SRT value of 68, which is still higher than an SRT value of 65 and therefore is classified as a good condition as well. The number of chosen load cycles only represents a short usage of the texture layer, which might not deliver a long-term declaration of the surface condition yet. However, it shows that the surface structure is able to fulfill the required road administration conditions, which ensure traffic security in terms of friction. Nevertheless, the SRT Pendulum is a tool, which merely conducts a stationary measurement of the friction. It can certainly indicate the road's level of grip, but cannot continuously assess skid resistance across a whole road section area. This is why a large-scale demonstrator skid resistance test with the micro GripTester will follow.

Analysis of the Interlayer Bond of the Texture Layer and the Absorption Layer

The texture layer is applied to the absorption layer, using the binding agent polyure-thane which is used as a binder in the absorption course. To assess an adequate bond between the layers, the shear bond strength test (SBST) [14] in conjunction with the load from the Aachen Ravelling Test (ARTe) [15] were applied.

Within this experiment, three variants were tested to determine the best option. In order to produce the composite test specimens, the texture layer material was prefabricated as cylinders (∅=150 mm) for all variants. In the production of variant 1 (Var 1), the absorption layer was freshly prepared with a binder content of 6.3 wt.-%, poured into the mold and compacted. Immediately after that, the texture layer, which was roughened on the bottom side by sandblasting, was applied to the absorption layer. The aim was for the fresh binder to simultaneously act as a binder and adhesive. For the second variant (Var 2), the production process was similar, but the binder content was increased to 8.3 wt.-%. In contrast, for the production of variant 3 (Var 3), the texture layer and the absorption layer were prefabricated and cured independently. Later, the absorption layer was flatly ground to ensure the largest possible net contact area with the layer above it, because the grinding of the absorption layer ensures the removal of stone peaks, thus providing a larger bonding area between the two layers. The contact areas of both layers (0,0177 m^2) were then thinly coated with polyurethane (15 g each = 30 g in total) using a coating roller, followed by the application of the sandblasted underside of the texture layer.

It turned out that variant 3 (Var 3) exhibits the best layer bond. Therefore, the amount of polyurethane adhesive in between the layers was varied again, in order to detect whether even higher maximum shear forces can be achieved. Table 5.1 gives an overview of the composition of the tested variants.

Table 5.1: Overview of tested variants for the layer bond of the texture and absorption layer.

Variant	**Var 1**	**Var 2**	**Var 3**	**Var 3.1**	**Var 3.2**
absorption layer	fresh	fresh	prefab.	prefab.	prefab.
binder content [wt.-%]	6.3	8.3	6.3	6.3	6.3
top layer	prefab.	prefab.	prefab.	prefab.	prefab.
adhesive [g]	0	0	30	20	10
adhesive [g/m^2]	0	0	1695	1130	565

In Germany, the bonding strength between an asphalt surface layer and an asphalt binder layer is considered sufficient when the maximum shear force is at least 15 kN [11]. However, this method cannot be used as a condition for the bonding system investigated in this study, as it involves entirely different materials. Nevertheless, this minimum threshold can serve as a reference point and is thus included in the analysis. Furthermore, there are currently

no comparable systems for direct comparison of shear forces related to bonding between existing layers, as [28] did not investigate the bonding effectiveness of his development.

Figure 5.6 depicts the maximum shear forces of the different variants in a bar chart. It can be observed that the variants, that exhibit meager shear forces, are those where the texture layer is applied on the fresh absorption layer (Var 1 and Var 2). The fresh binder in the absorption layer should ideally act as an adhesive, but it is presumed that the contact points between the texture and binder layers are not sufficiently coated. Additionally, in these variants, the peaks of the stones were not eliminated, resulting in a reduced net contact area between the layers. Using the approach where both layers are manufactured separately and then bonded, all variants (Var 3, Var 3.1, Var 3.2) can achieve high shear stiffness values. It can be observed that the more binder is applied as an adhesive between the layers, the higher the maximum shear stiffness becomes. Taking into account the minimum shear strength proposed in Germany, these variants would meet the requirements. Variant 3 (Var 3), which had a mean maximum shear force of 23.2 kN is defined as the best and safest option.

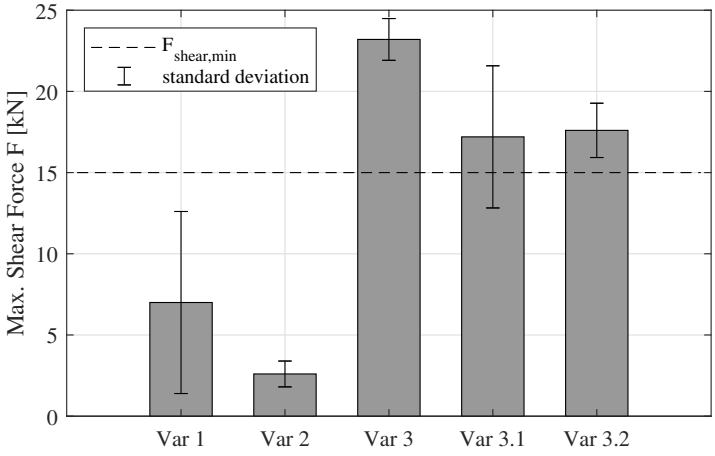

Figure 5.6: Maximum shear forces yielded from the shear bond strength test (SBST).

Since the best option variant from the shear bond strength experiment was selected, a test to ensure that the variant withstands real-scale conditions was carried out. For this purpose, it was subjected to load in the Aachen Ravelling Tester (ARTe) to determine the influence of shear forces on the layer bond. Two samples were loaded with rotating tires 1200 times with a wheel load of 450 kg without using water and a polishing agent. In contrast to the experiments in the shear bond strength test device, the bottom of the texture surface could not easily be ground for the ARTe test and was therefore applied on the prefabricated absorption layer without treatment. We found, that the tested samples of Var 3 withstand the shear loads, indicating that the interlayer bond is at a high level.

Rutting Behavior of the Noise-Reducing Two-Layer System

After conducting the wheel tracking test (WTT), it was found, that the rutting depth of the two-layer system is very low, almost negligible. The final absolute rut depth after 20,000 wheel passes was found to be 0.3 mm and the proportional rut depth, which includes the proportion to the specimen height, is 0.6%. Figure 5.7 shows the course of the rutting depth across the number of wheel passes. The rutting phenomenon of the two-layer system is much lower compared to a conventional Hot Mix Asphalt (HMA), such as the German asphalt surface mix (AC 11 DS). The high resistance to rutting can be attributed to the high strengths of the two polymer-based layers. After the curing process, these layers maintain consistent strength even at elevated temperatures, in contrast to asphalt, which exhibits temperature-dependent viscosity and, therefore, deforms at higher temperatures under constant load. Accordingly, it can be concluded that the two-layer system exhibits high resistance to rutting.

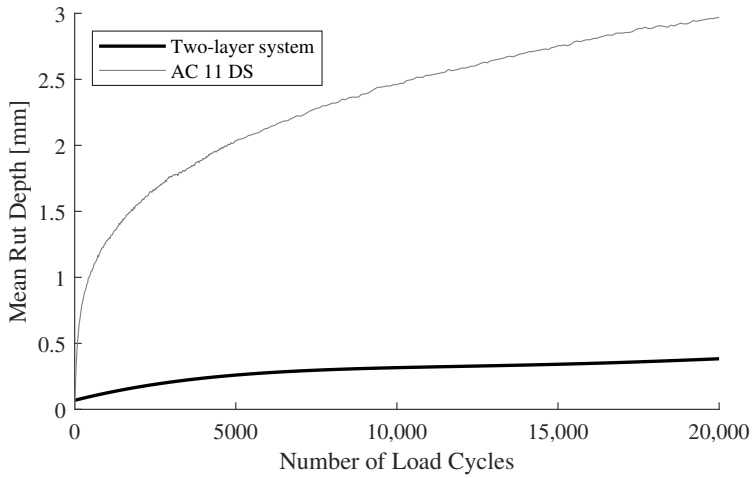

Figure 5.7: Rut depths of the two-layer system compared to an HMA AC 11 DS.

[28] did not cover the performance of the entire two-layer system in terms of the rutting phenomenon, so no direct comparison can be made to his experiments. However, in general, in [32] researchers defined, that a maximum permissible permanent deformation of 6 mm after 20,000 tire passes considers an asphalt sample to be resistant against rutting. The research focused on the evaluation of the American standard AASHTO T324 [1], which differs from the German standard [13] in terms of a 10°C lower air temperature during testing (50°C). Both in Figure 5.7 compared layers meet the specified requirements from [32], with it being evident that the two-layer system exhibits minimal rutting.

Testing the Application of the Two-Layer System on Conventional Bituminous Bottom Layers

To promote the sustainability of the noise-reducing system, it should be integrated into the existing infrastructure. This means that new road structures based on polymer materials should not be constructed from scratch; instead, the polymer system should be applied to existing bituminous layers, such as replacing worn-out asphalt surface layers. In this context, it is necessary to verify whether an adequate bond can be achieved between the polyurethane-bound absorption layer and conventional bitumen-bound binder layers. Additionally, it is essential to protect the dense layers in the asphalt structure from water ingress to prevent damage, since the noise-reducing surface layer system is characterized by a highly porous and permeable structure, which on the one hand enables noise absorption, but on the other hand, leads to effective water drainage. Therefore, this study examines how sealing of the bituminous substrate can be achieved.

To find out more about a sealing medium, that meets the requirements of an adequate interlayer bond, a study with three different sealing mediums was carried out. In detail, three tests, such as the shear bond strength test [14], the tensile bond test [14] and the permeability test [12], were conducted. The aim of this experiment was to determine which sealing medium successfully passed all three tests with good results, thus making it a suitable interlayer between the two-layer system and a bituminous binder course. The following layers were investigated: a thin polyurethane layer (Elastan 6568/120) (PU), a thin bitumen emulsion layer (C60BP4-S) (BE), and a 20 mm mastic asphalt layer (MA 11 N) (MA). During the preparation of three test samples for each variant, the polyurethane layer and the bitumen emulsion layer were applied with a painting roller. With this method, thin layers of polyurethane of 10 g and thin layers of bitumen emulsion of 20 g could be realized. The selection of the adhesive quantities and the layer thickness was made in accordance with the recommendations from German regulations. The 20 mm mastic asphalt layer was applied by hand, coated with scattering material (aggregates 2-5 mm), and compacted with a roller compactor.

Figure 5.8 (a) shows the results of the maximum shear force test according to [14]. It can be observed that the bond between the absorption layer with the PU and the BE medium is noticeably weaker compared to the bond between the absorption layer and the MA medium. With regard to the suggested minimum shear force from the German regulations, both mediums, PU and BE, would not meet the requirements [11]. The 20 mm thick mastic asphalt medium MA 11 N achieves a mean maximum shear force of $F_{shear,max}$ = 19.6 kN, which passes the 15 kN minimum shear force from the standard. The reason for the significantly higher shear strength between the absorption layer and MA is likely due to the scattering of the mastic layer with basalt aggregate, which forms a strong bond with the bitumen on

the bottom and the polyurethane on the top. In contrast, in the PU and BE variants, there is a polyurethane or bitumen layer as an intermediate layer. It appears that the bonding behavior between bitumen and polyurethane, which accumulates at the layer boundary, is very low. The illustrated standard deviation of the variant MA in Figure 5.8 (a) is caused by a high deviation of one of three measured values, which was very low. It may influence the interpretation of the behavior of this variant. The other two values of MA exceed the minimum suggested requirement, though. [19] tested the bond between their developed PERS layer with various adhesive quantities and a conventional sub-layer as well. They obtained significantly lower maximum shear forces ranging from 2.3 to 6.6 kN, which could be a reason for the reduced durability and stability of their system compared to the implemented noise-reducing two-layer system of this study.

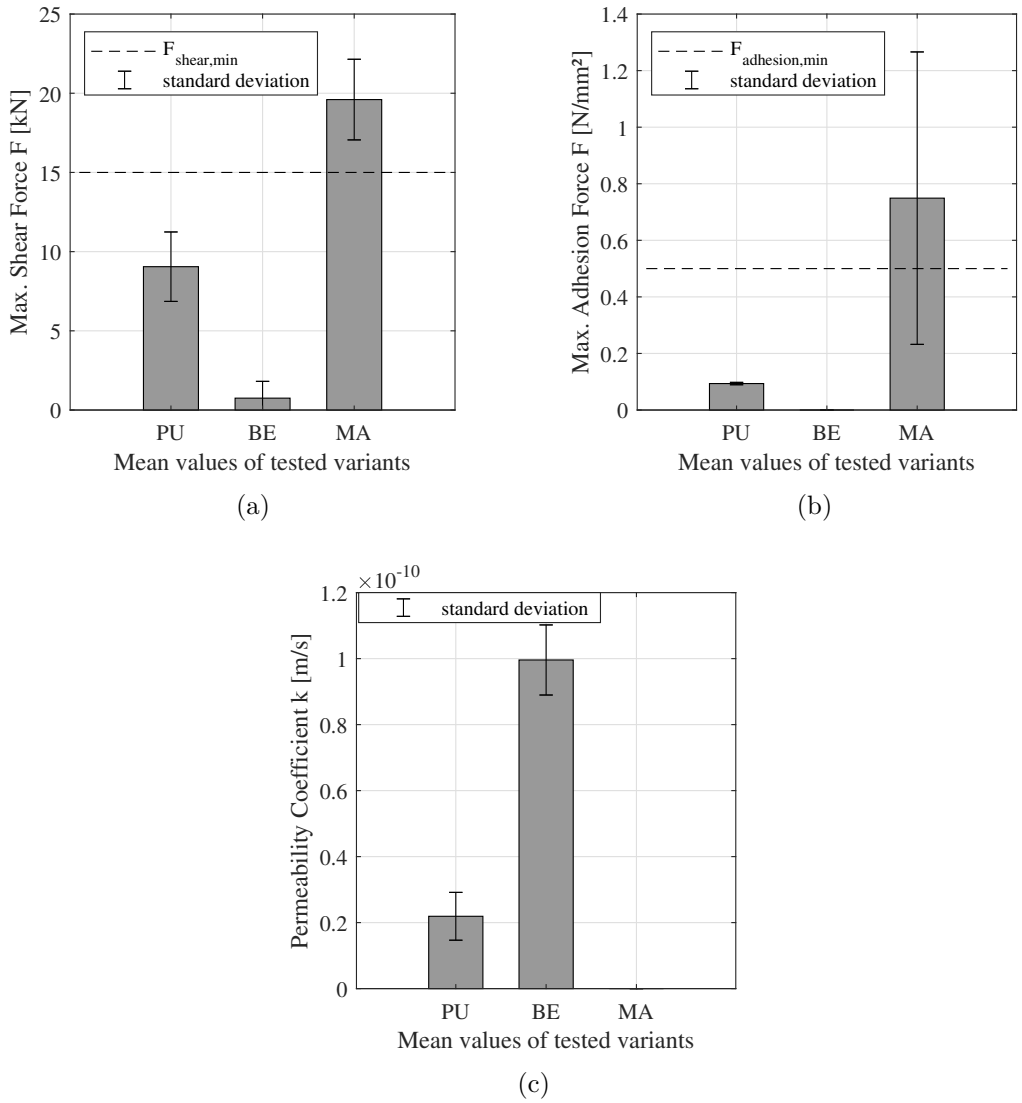

Figure 5.8: Results of interlayer (a) and adhesion (b) bond and permeability (c) tests

Beyond that, Figure 5.8 (b) shows the maximum adhesion forces between the absorption

layer and the asphalt binder course yielded by the tensile bond strength test (TAT). All tested samples with the bitumen emulsion medium (BE) collapsed during the drilling of the test cores, which is why only PU and MA test samples are illustrated in the figure. Due to the collapse during preparation, it is assumed, that the bond of the BE samples is fragile and therefore can be represented with 0 N/mm². Compared to this, the mean maximum adhesion force value of PU is at 0.0936 N/mm², and of MA is at 0.7491 N/mm², which is, in comparison, much higher. In general, the bond strength between MA and the absorption layer is the highest and can therefore be considered as the decisive factor. However, the large standard deviation suggests that the mean adhesion force may not necessarily be representative. Since the German regulations suggest that an adhesion value of 0.5 N/mm² would be a minimum qualification to yield adequate adhesion resistance [14] between asphalt layers, only the MA medium would meet the requirement.

At the end of the laboratory study, the permeability values of the sealing mediums are examined, which were determined using the permeability test according to [12], and are shown in Figure 5.8 (c). Considering the figure, a clear imbalance among the tested variants is evident. The PU and MA variants seem to exhibit minimal to no permeability ($k_{PU} = 2.1915e^{-11}$ m/s and $k_{MA} = 0$ m/s), whereas, in contrast, the BE variant appears to be more permeable ($k_{BE} = 9.9589e^{-11}$ m/s). In general, it can be stated that all variants provide effective sealing, since a permeability coefficient of around $1.0e^{-10}$ m/s is still almost waterproof. This phenomenon is likely influenced by the density of the bituminous binder layer beneath, which is inherently hardly permeable to water. Nevertheless, the goal is to achieve maximum sealing to the bituminous asphalt layers beneath the permeable layer to mitigate potential risks of water ingress and allow water to drain above the binder layer into the subsequent drainage systems, which can be achieved with the construction of a non-permeable MA sealing.

In summary, considering all tested tests and variants, it can be concluded, that the use of a 20 mm mastic asphalt layer (MA 11 N) in between the two-layer system and a bituminous bound binder course is the optimum solution to yield interlayer bond, adhesion, and a full sealing at the same time. The PU and BE variants are not suitable for use in this construction due to their respective deficiencies.

5.4.2 Implementation of the Large Scale Demonstrator

In order to carry out the implementation of the full-scale demonstrator, the findings from the laboratory study must be taken into account. Accordingly, the absorption layer should be mixed and installed on-site to prevent premature hardening of the layer. On the other hand, the texture layer is pre-produced in a binder-to-filler ratio of 25/75 % and then applied to the absorption layer as panels. The bonding is done using the polyurethane binder from the

absorption layer at a rate of approximately 1700 g/m² on a previously abraded absorption layer surface.

Location and Conditions of the Test Section

The Federal Highway Research Institute provides a test area for research projects involving large-scale research conducted under real-world conditions. This test area, known as duraBASt, is a non-publicly accessible site located within the Cologne-East motorway interchange in Germany. This means that the test site is not subject to actual traffic but provides the opportunity to implement demonstrators on road sections measuring 100 x 3 m², exposing them to real environmental conditions such as weather. The loading is performed through the accelerated pavement testing facility MLS 30.

On this test site, the two-layer noise-reducing system was implemented in full-scale. The substructure consisted of a 300 m² area with an asphalt structure composed of a rigid gravel subbase layer on the bottom and a combined base-surface-layer (AC 16 TD) above, on which, the two-layer surface system consisting of the texture and the absorption layer could be applied on an area of 50 x 3 m² (length x width). The sealing medium evaluated in the laboratory study, which was based on mastic asphalt, was not implemented in full-scale for cost reasons.

Paving of the Absorption Layer

Using a dosing system specifically designed for rock-polymer mixtures according to [22], the mix for the absorption layer was prepared on-site and placed in front of the paver. The dosing system combines the individual components in proportions according to the mix composition, illustrated in 5.3. To distribute and compact the absorption layer material, a concrete paver suitable for PU asphalt installation was used. Within this compactor, the modified compaction unit consists of panels that smooth the laid mix to a preset height on the layer. The material is compacted with the panels into a denser arrangement, as the compaction panels press the absorption layer material at a constant force, causing it to interlock and form a solid particle structure. Consequently, an even surface of the absorption layer can be achieved in-situ. The polyurethane binder reacts after the layer's completion, allowing the contact areas of the aggregates to form a strong bond, ultimately creating a quasi-monolithic body, which was found by [25] as well.

Grinding of the Absorption Layer

After the chemical reaction of the absorption layer, its surface was ground, using concrete grinding machines, and cleaned to create a maximum net contact area between the grains and the texture layer plates.

Prefabrication of the Texture Layer Plates

The large-scale texture layer was produced in a technical center. For practical reasons, it was previously found to manufacture texture layer panels with dimensions of 0.75 x 1.0 m^2 [22]. To ensure a pourable compound an extruder machine was used for the mixing of the compound, consisting of 75 % filler and 25 % binder. This offers the possibility to produce an ideally composed homogeneous compound from all individual ingredients, which could be poured directly into the prepared molds through a hose. Then, a silicone mold was filled with the extrudate and the PVA-textile was applied to the compound. For the chemical reaction, the silicone mold was completely closed by a steel mold in order to exclude possible deformations, prevent floating of the textile, and smoothen the bottom of the texture layer [22]. After a reaction time of approximately 25 minutes, the texture layer panel could be removed from the mold for post-processing. Unfortunately, it was not possible to create the texture layer plates as fully permeable, as proven to be a very time-consuming process and, therefore, could not be carried out within the intended time frame. Consequently, there were no open gaps between the texture layer elements; instead, only parts of the texture layer plates were cut in transverse direction to enable the partial transfer of the resulting noise from tire-road noise to the absorption layer.

Application of the Texture Layer on the Absorption Layer

The application of the texture layer on the absorption layer was adopted from the laboratory study. For this purpose, the prefabricated texture layer plates and the absorption layer were spread with the polyurethane binder and then applied to each other (Figure 5.9).

Figure 5.9: Full-scale two-layer pavement system after construction.

5.4.3 Results of the Full-Scale Experiments

After the completion of the full-scale two-layer noise-reducing system, the second study was conducted to determine the acoustic and mechanical performance of the system. In this context, the experiments presented in the methodology were carried out. These experiments involve the determination of road-tire noise using the CPX method and the assessment of mechanical resistance against heavy traffic using the MLS 30. Subsequently, the system's load-bearing capacity and skid resistance are tested and evaluated, with changes induced by the influence of the MLS 30 load.

Analysis of the Acoustic Performance

To determine tire-road noise, the Closed Proximity Method (CPX) is applied in this experiment. On the duraBast site, the maximum driving speed is limited to 50 km/h, which limited the maximum speed within the test. By performing three measurements with passenger car tires (SRTT), the averaged sound pressure level over a total of six 20-meter sections was determined to be 90.7 dB(A), taking into account the temperature correction. Ref. [28] tested his development in a full-scale demonstrator as well and evaluated the sound pressure level with the CPX method. In his study, he was able to test higher car speeds of 60, 80, 100, and 120 km/h with an SRTT tire. However, at a speed of 60 km/h, he observed a sound level of 90 dB(A) [28], which rises in dependence on the speed. In comparison to the result of this study, the value by [28] of 90 dB(A) is roughly at the same level. However, it can be assumed that the CPX value from [28] at 50 km/h would be approximately 2-3 dB(A) lower. A linear interpolation of his noise level at 50 km/h yields a noise level of 87.8 dB(A), which is 2.9 dB(A) lower compared to the noise level from this study (Figure 5.10 (a)). Further comparison with PERS pavements developed by [19] indicate that the PERS pavements have a higher noise-reducing effect ($L_{CPX,50,\,PERS}$= 82-87 dB(A)) compared to the two-layer pavement evaluated here (Figure 5.10 (a)). But taking into account conventional asphalt reference values from [19] (SMA 0/16 and SMA 0/11), they indicate noise levels up to 3.1 dB(A) higher compared to the two-layer system from this study, which leads to the statement, that the developed two-layer system causes a noise reduction compared to conventional asphalt pavements.

In addition to providing the CPX level, the third-octave spectrum of the measurement results is presented (see Figure 5.10 (b)). The CPX value (50 km/h) as a function of frequency starts at a level of approximately 80 dB(A) in the low-frequency range, then decreases in the frequency range between 500 and 630 Hz. Subsequently, it rises to 82.5 dB(A) (at 1000 Hz) before remaining there up to a frequency of 2000 Hz, after which it decreases to 70 dB(A). The sound level depicted in Figure 5.10 (b) is on the same level of sound pressure coming from loud music within the auditory range of the human ear [33]. Upon closer inspection

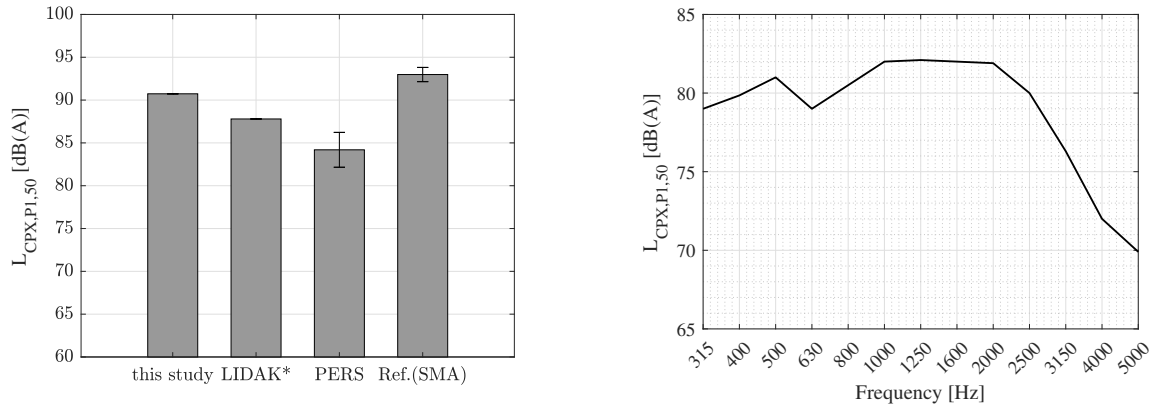

(a) (b)

Figure 5.10: Comparison of the maximum sound pressure levels of LIDAK (*linear interpolated) [28] and [19] (a) and result of third-octave spectrum of the two-layer system (b).

of the sound level curve, a discontinuity can be observed in the range between 500 Hz and 1000 Hz, evident as a downward inflection. From the literature, it is known that specifically, tire-road noises arising from structural factors constitute the noise in the frequency range < 1000 Hz [3]. By combining this assertion with the present sound pressure level curve, it can be inferred that the distinctive texture layer of the system being tested here is the reason for this inflection. Therefore, it can be concluded that the texture layer induces lower structurally related noise (e.g., tire vibrations).

A comparison to the Literature is shown in Figure 5.11. Ref. [4] conducted assessments of two noise-reducing asphalt pavements (P and PCR) and a reference asphalt (E1) using the CPX method at 50 km/h. The corrected sound pressure levels obtained were 88.5 dB(A) (P) and 87.8 dB(A) (PCR) with an SRTT P225/60 R16 tire. Considering the third-octave-curves, it is observed that the sound levels of [4] (grey lines) are at a similar level compared to this study (black line). However, the two-layer surface system from this study exhibits lower sound pressure levels in the frequency range between 500 and 800 Hz. Given that the pavements discussed by [4] are modified asphalt pavements with a typical asphalt surface texture, the deviation in the curves here can also be attributed to the unique geometry of the texture layer within the two-layer system. Additionally, the figure includes the third-octave band from [28] (represented by the black dashed line), recorded at a speed of 60 km/h. Direct comparison with data from [28] is not feasible due to the difference in measurement speeds. The band would register at a lower level for a measurement speed of 50 km/h. However, it can be observed that the data from [28] also exhibits an inflection in the third-octave band in the frequency range of 400 to 800 Hz, which can also be attributed to the defined geometry of the texture layer.

Considering the entire frequency range, the third-octave band of the two-layer system in

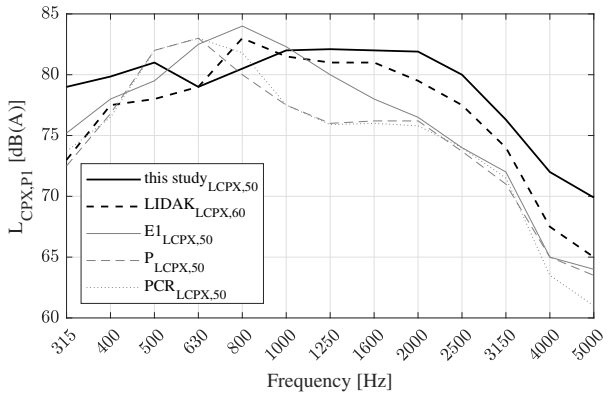

Figure 5.11: Comparison of third-octave-band to LIDAK [28] and literature from [4].

the range > 1000 Hz is above the comparison values from the literature, indicating that the current construction of the system does not mitigate aerodynamic noises through vehicular passage. As mentioned earlier, due to resource constraints, the texture layer could not be created as maximally permeable for the experiments. This might be the cause for higher noise levels occurring in the frequency range > 1000 Hz. Consequently, the generated noise couldn't be directed into the underlying absorption layer for absorption, resulting in the absence of detectable aerodynamically induced noise reduction in the measurement results.

Analysis of Accelerated Pavement Testing

To assess the damage to the surface layer system due to heavy load stress with the accelerated loading facility MLS 30, a visual examination of the degree of damage and potential ravelling is conducted. This is complemented by an analysis of skid resistance, directly associated with surface wear of the texture layer. To determine the level of damage occurring at the material level within the surface layer system, the deflections obtained from the Falling Weight Deflectometer (FWD) measurements are also subjected to closer inspection.

The literature analysis provided information about pavement distress, which can be categorized into functional and structural failures often occurring in pavements due to inadequate design. To verify if the design and implementation of the two-layer system were compliant with requirements, a visual inspection is conducted to identify the occurrence of these failures. Expected indications would include cracks or material breakage, texture column collapse, or the breaking out of individual texture layer elements, which are both types of ravelling. Delamination of the texture layer from the absorption layer, rutting deformation, and material abrasion could appear as well.

Figure 5.12 presents a comparison of a detailed section of the texture layer in the unloaded state (Figure 5.12 (a)) and under load (Figure 5.12 (b)). This section was selected as representative of the entire loaded area to illustrate structural changes. A direct comparison

reveals marking abrasion from the pavement and rubber abrasion from the tire. The wear of the marking paint is attributed to repeated wheel loading and the limited bonding of the ordinary marking paint to the texture layer material. However, this paint was solely used for positioning the MLS 30 and is irrelevant for assessing the strength of the surface. Rubber abrasion, akin to conventional road surfaces such as asphalt or concrete, results from the frictional interaction between the tire and the pavement. When the tire rolls, there is both slippage at the tire interface causing mechanical abrasion of the tire material and the generation of thermal energy. At a certain tire temperature, this thermal energy softens the tire material, leading to material transfer onto the road surface [29]. However, the phenomenon of tire abrasion is not further explored in this study.

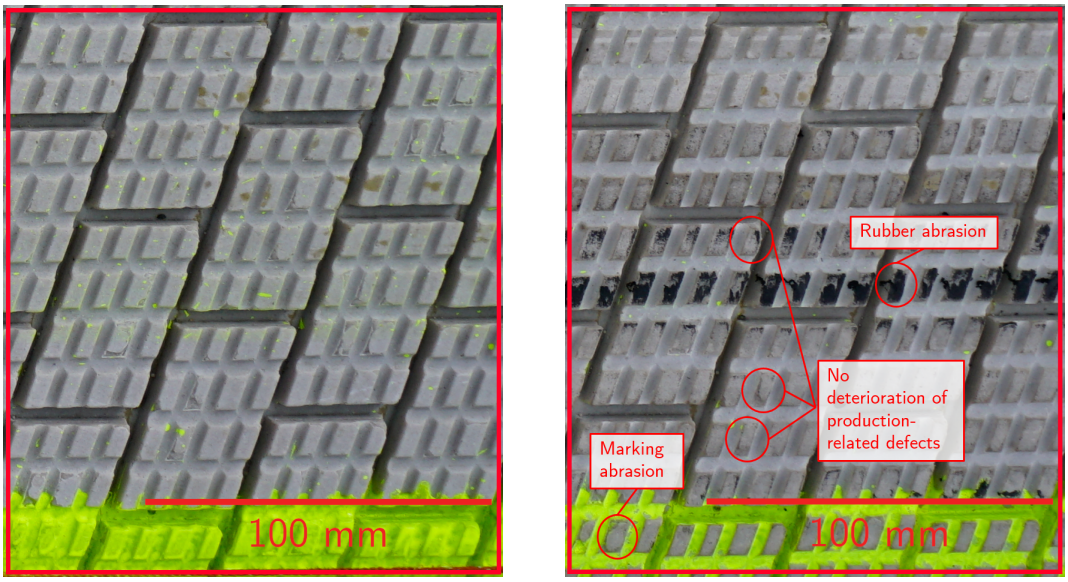

(a) (b)

Figure 5.12: Comparison of unloaded (a) and loaded (b) section.

Figure 5.12 (a) exhibits production-related imperfections in certain areas, such as the rounded edges of the texture columns. These arose during the texture layer production, where the material inadequately filled the silicone mold corners. Upon reevaluation of these defects after loading (Figure 5.12 (b)), it is evident that there is no continuation of damage; the flaws remain unaltered and stable. This indicates that the texture layer material exhibits high resistance against horizontal and vertical forces from the heavy truck load. The other potential damages mentioned (i.e., cracking, rutting deformation, inadequate layer bonding) cannot be visually induced by the MLS 30 load. Material abrasion resulting from the MLS 30 load also remains visually unnoticeable. However, the assessment of skid resistance tests indirectly provides insight into any potential degradation of the surface's skid resistance due to loading. Thus, the micro-Griptester was utilized to determine the skid resistance changes.

The entire skid resistance assessment covered a section of the texture layer surface of a

length of around 40 meters. The mean walking pace was 0.76 m/s. To account for the influence of the MLS 30's passage, the measurement area was selected in such a way that both an unloaded section and the section loaded by the MLS 30 could be included in the grip measurement analysis. Figure 5.13 (a) shows a measurement record of one run from the distance of 15 m to 41 m, which illustrates the influence of the MLS 30 loading in the height of the Grip Number.

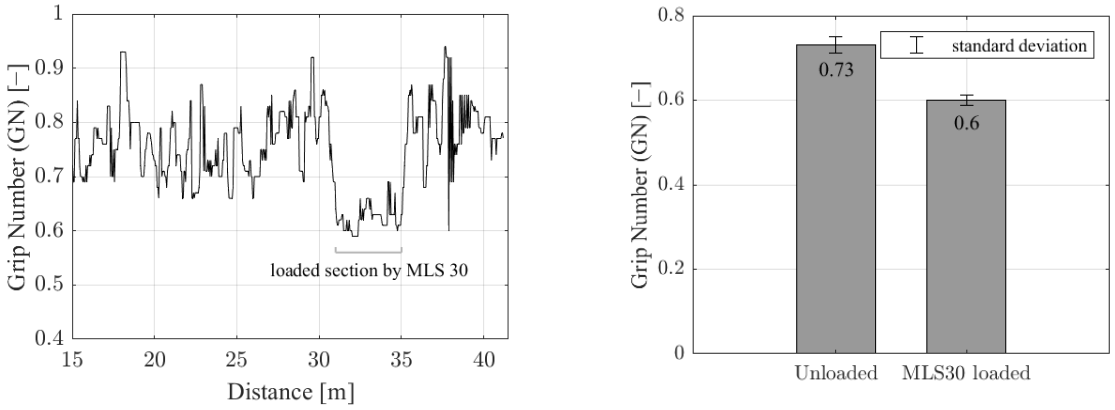

(a) (b)

Figure 5.13: Grip Number (GN) across the measurement distance (a) and Grip Numbers of loaded and unloaded sections of the top layer system (b).

In general, it could be observed that on the new texture layer surface, an average texture value GN of approximately 0.73 exists. This value is derived from the mean of all micro GripTester passes over the unloaded surface. After the heavy load stress, it is reduced on average to GN = 0.6 (Figure 5.13 (b)).

Through the accurate tracking load of the 5-ton wheel load, there is a presumed removal of texture layer material on the surface, which explains the decreasing frictional coefficient. This phenomenon becomes evident only under the heavy load, which was not predicted in the laboratory study. It could be attributed, for instance, to the use of different tires and the number of wheel loads in this setting or due to the texture layer being affected by environmental factors for the weeks between installation and testing. A comparison with the laboratory study is somewhat limited here since the results are obtained from different measurement methods. However, the decrease in grip values over the load cycles can be determined proportionally. During the laboratory study, there is a 10 % decrease in skid resistance concerning the SRT value after 600 passes, while in-situ, concerning the GN values, there is an 18 % decrease after 160,000 passes. To determine the long-term skid resistance behavior, a targeted study should be conducted in the ARTe, where the material removal is determined, the duration of loading is significantly increased, and environmental influences

are tested.

Ref. [19] provided measurements for the use of a Portable Friction Tester (PFT) for PERS as well. The measurements yielded friction indexes (PFT) that are comparable to the Grip Number ranging from 0.62 to 0.78, some of which could only be achieved through additional grinding of the surface. A comparison to the values determined here (0.73 in the initial state and 0.6 after loading) indicates that the skid resistance values are at a similar level, meeting the administrative requirements.

The heavy load stress leads to a reduction in skid resistance values, indicating material abrasion and alterations in the texture's surface. These changes represent a functional failure, which could potentially reduce skid resistance and consequently affect road safety in the long term. However, the current tests do not reveal a drastic decline in skid resistance values, suggesting that a functional failure of the surface layer system in this regard is not anticipated.

To ascertain the strength and stability of a pavement, the deflections generated from Falling Weight Deflectometer (FWD) measurements are analyzed. FWD measurement is a non-destructive testing method that provides an impression of the structural capacity of a multilayer pavement. In the development of the absorption layer's performance, a maximum deflection of the absorption layer of 0.5 mm was defined in [5] to mitigate the generation of high mechanical stress peaks. When the two-layer system is subjected to loading, the texture layer deforms and pushes the corners of its texture layer elements, which are connected by the textile, into the absorption layer. The reduction of these stress peaks can be achieved by reducing the deflection of the absorption layer (lower elastic modulus), which therefore was defined as a maximum of 0.5 mm (equivalent to 500 micrometers). This led to the target elastic modulus of 300 MPa for the absorption layer composition [5].

By conducting FWD measurements, the surface deflections from the full-scale implemented two-layer system were determined and are shown in Figures 5.14 and 5.15. Figure 5.14 shows a comparison between the maximum assumed deflection from [5] and the maximum deflections that are yielded from this study and it demonstrates that the measured deflections at the load application point ($\pm$ 450 µm) within the real-scale two-layer demonstrator confirm the previously assumed deflections. This allows the statement, that the full-scale implementation of the two-layer system achieves the target layer elasticity. Additionally, Figure 5.14 reveals a change in the mean maximum deflections in dependence of the heavy truck load. Because after MLS 30 loading, the maximum deflection in the load center increases. According to [26], the deflections at the loading point serve as an indicator for pavement stiffness, rather than providing an assessment of the pavement's condition or its projected lifespan. A comparison to the deflections investigated by [26] on various asphalt structures, reveals that

the present two-layer system can be classified under a flexible pavement category, as it exhibits similar high deflections (ranging between 400 to 1000 µm) as the flexible pavement in their study. This is further corroborated by a direct comparison to the deflections of asphalt pavements from [26], where the use of stiffer base courses resulted in maximum deflections of only up to 180 µm, indicating a significantly stiffer pavement.

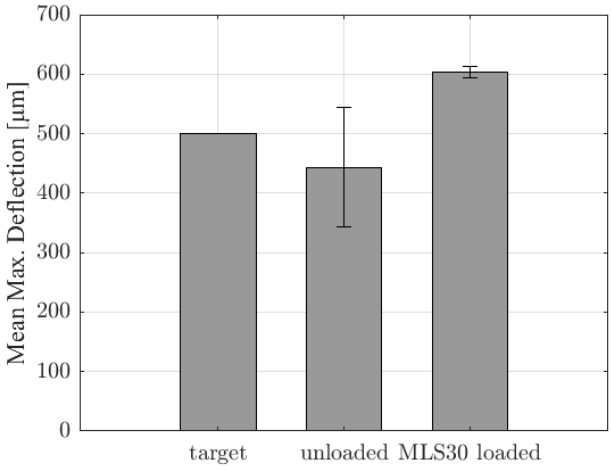

Figure 5.14: Comparison of the target deflections from [5] to the deflection results from this study before and after MLS 30 loading.

The utilization of the MLS 30 allowed for the consideration of changes in the load-bearing capacity of the examined system in the analysis. The deformation curves, which result from the localized load applied by the FWD before and after the MLS 30 loading, are illustrated in Figure 5.15. In detail, the average deformations of the measurements are depicted as a function of the distance from the load application point. More precisely, two average deformation basins are illustrated for measurements before (black) and after (gray) MLS 30 loading. It is evident that the deformation basin before loading is not as pronounced as the one after loading, indicating that the MLS 30 loading with 160,000 wheel passes has an impact on the load-bearing capacity of the layer system. In particular, the deformations in the immediate vicinity of the load application point up to approximately 500 mm distance reveal the influence of the heavy load, since the curves in this region vary significantly. For example, compared to before loading, the deformation basin after loading exhibits approximately 1.7 times higher deformation at the load center and nearly 2 times higher deformation at a distance of 200 mm from the load center. All measurement points located further away converge and are therefore negligible for the assessment.

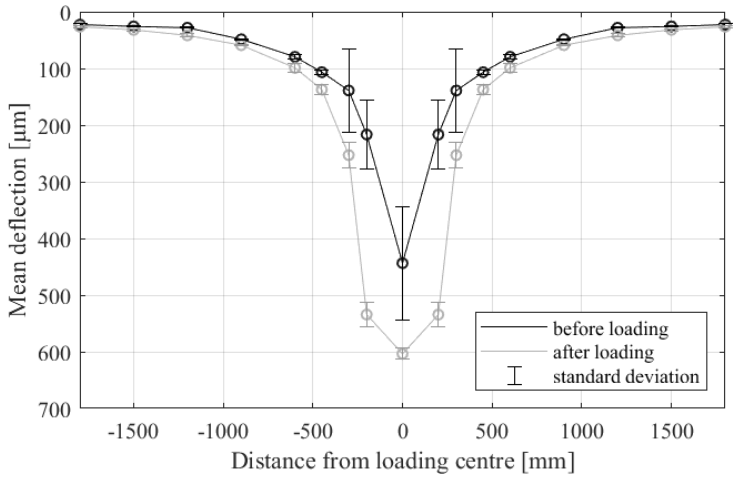

Figure 5.15: Deformation basins before and after loading with the MLS 30.

To facilitate a comparison with conventional asphalt road construction, key performance indicators for assessing load-bearing capacity, as per [7], will be employed in Germany. This allows for the determination of a load-bearing capacity index, denoted as T_Z, based on the deformation basins. Before the MLS 30 loading, an average T_Z value of 0.6 (according to Equations 5.1 and 5.2) is obtained, which reduces to 0.4 after heavy wheel loading. Considering the reference values from [7], the two-layer system can be classified into a load class Bk0.3 (according to [10]) which represents the lowest pavement class in Germany. Taking this classification into account, it is evident that the existing surface layer system can be categorized as flexible, being assigned to a lower construction class. When calculating R_0 and T_Z according to the German guideline, the maximum deflection at the load point and its immediate vicinity are significantly considered, implying that, as per the assertion by [26], the focus primarily involves an assessment of the surface stiffness rather than a comprehensive evaluation of the pavement as a whole.

Although the MLS 30 load seems not to visibly affect the resilience of the two-layer system, its impact can be observed through FWD measurements, revealing higher deflections and thus reduced bearing capacity values. The heavy load could potentially cause damage within the elastic absorption layer. Considering the assumption by [25] that the tensile and compressive strengths of PU-asphalt are very high, the amount of rubber particles integrated within this layer could potentially lead to the behavior that results in the decrease of the bearing capacity parameters. The use of these rubber particles induces an elastic behavior in the material due to the rubber's elastic properties. However, this phenomenon provides an initial glimpse into the load-bearing capacity potential of this two-layer surface system, which warrants further in-depth investigation.

In summary, a comparison with traditional asphalt road construction led to the statement, that this surface layer system acts more flexibly than conventional bituminous bound pave-

ments, to ensure a higher noise reduction, which was the aim of this study. However, whether this measurement method provides informative data in this context remains unclear, as it does not allow for an assessment of the overall pavement structure, and stiffness can also be calculated through laboratory experiments.

5.5 Conclusions

The aim of this study was the realization and examination of a two-layer noise-reducing polymer-based road surface in terms of its performance characteristics. The challenge arising from the findings from the literature was to address the conflict of targets between acoustic and mechanical effectiveness because many studies have shown that noise-reducing road surfaces could be highly effective acoustically but lacked mechanical strength.

Through a comprehensive laboratory study, it was possible to implement a real-scale demonstrator, which could be evaluated in terms of acoustic efficacy and durability. Therefore, the laboratory study concluded skid resistance tests, ravelling tests, wheel tracking tests, layer bond tests, and permeability tests, to define the required steps for the realization of the full-scale demonstrator. After completion of the real-scale two-layer pavement, an assessment of the noise reduction potential through CPX measurements and the evaluation of the strength and durability of the system using accelerated pavement testing in combination with skid resistance and falling weight deflectometer tests were conducted.

In the context of this study, it has been demonstrated that the two-layer system can be implemented stably. However, the stabilization of the system results in a lesser noise reduction compared to the noise-reducing pavements from the literature. Although the changes in the geometry and composition of the layers indicate minimal tire vibrations, which reduces structure-based noise emission, aerodynamically generated noise cannot be significantly reduced. Sufficient strength of the two-layer system was evidenced through the execution of accelerated pavement tests, because no visual damages to the system, such as ravelling, material breakage, or layer delamination, occurred following the MLS 30 loading. The system appears to be more stable compared to other noise-reducing systems where these failures have been observed. Additionally, Falling Weight Deflectometer (FWD) measurements allow the determination of deflections, categorizing the system as flexible. The heavy wheel loading results in increased deflections, which could indicate material damage and should therefore be further investigated in the future.

This study provides an outline of the analysis of the short-term impact of the system, highlighting the need for further research. Specifically, long-term monitoring would be a valuable addition to assess, for instance, the influence of the environment and increased load numbers, as well as to evaluate the driving experience of road users. As polymeric materials are being

used as an alternative to conventional pavements, it is recommended to conduct a Life Cycle Analysis (cradle-to-cradle) of the system to verify its suitability in terms of functionality and sustainability.

On the whole, stabilization compromises the acoustic effectiveness of the two-layer system, although there is still a noise reduction of 3.1 dB(A) compared to conventional bitumen-bound pavements. The current research stage of the stabilized system allows the system to be utilized as a prototype in road traffic, aiming to mitigate the noise disturbance caused by road traffic for the population.

5.6 Acknowledgements

Thank you to our master and bachelor students Martin, Lea, Jule, and Jonas, who helped us generating the research results. We also thank the team of the Federal Highway Institute (BASt), who gave us the possibility to use the demonstration area duraBASt and the testing facilities.

5.7 Appendix

Table 5.2: Composition of texture layer

	Component	**Proportion**	**Company, Location, Country**
*1	methyl-methacrylate (PMMA)	25 wt.-%	Röhm GmbH, Darmstadt, Germany
*2	silica sand filler (< 1 mm) (MinMix AT530)	75 wt.-%	Quarzwerke GmbH, Frechen, Germany
*3	⋆1% dibenzoyl peroxide (Swarco Limburger Lackfabrik GmbH, Diez, Germany)		

⋆ as a proportion of total formulation

Table 5.3: Composition of absorption layer

	Component	**Proportion**	**Company, Location, Country**
*4	crump rubber super grob (2-6 mm)	7.5 vol.-%	Genan GmbH, Dorsten, Germany
*5	basalt aggregates (2-5 mm)	85.5 vol.-%	Basalt Quarry Hühnerberg, Königswinter, Germany
*5	basalt sand (0-2 mm)	3 vol.%	Basalt Quarry Hühnerberg, Königswinter, Germany
*6	limestone filler	4 vol-%	Kalkwerk-Natursteinwerke GmbH und Co. KG, Üxheim-Ahütte, Germany
*7	⋆13 vol.-% of polyurethane binder (Elastan 3538/103)		

⋆ as a proportion of total formulation

References

[1] American Association of State Highway and Transportation Officials. *AASHTO T 324-2023: Standard Method of Test for Hamburg Wheel-Track Testing of Compacted Hot-Mix Asphalt (HMA)*. Washington, D.C., 2023.

[2] Erwin Baur et al. *Saechtling Kunststoff Taschenbuch*. 31. Auflage. München: Carl Hanser Verlag, 2013.

[3] T. Beckenbauer. "Physik der Reifen-Fahrbahn-Geräusche – Geräuschentstehung, Wirkmechanismen und akustische Wirkung unter dem Einfluss von Bautechnik und Straßenbetrieb." In: *Geräuschmindernde Straßenbeläge in der Praxis – Lärmaktionsplanung* 4 (2008).

[4] J. Cesbron et al. "Acoustical characterization of low-noise prototype asphalt concretes for electric vehicles." In: *Euronoise 2021 (e-Congress), Octobre 2021, Madere, Portugal* (2021).

[5] S. Faßbender and M. Oeser. "Investigation on an Absorbing Layer Suitable for a Noise-Reducing Two-Layer Pavement." In: *Materials* 13.5 (2020).

[6] S. Faßbender et al. "Entwicklung einer neuartigen polymerbasierten Straßendeckschicht mit Fokus auf Lärmreduzierung und Dauerhaftigkeit (Engl. Development of a novel polymer-based road surface layer with focus on noise reduction and durability)." In: *Bauingenieur* 10 (2022), pp. 323–330.

[7] Forschungsgesellschaft für Straßen- und Verkehrswesen. *Arbeitspapier - Tragfähigkeit für Verkehrsflächenbefestigungen - Teil C 2.1 Falling Weight Deflectometer (FWD): Auswertung und Bewertung - Asphaltbauweise (AP Trag Teil C 2.1)*. Köln, 2014.

[8] Forschungsgesellschaft für Straßen- und Verkehrswesen. *Arbeitspapier Tragfähigkeit von Verkehrsflächenbefestigungen - Teil A: Messsysteme (AP Trag Teil A) (FGSV 433 A)*. Köln, 2020.

[9] Forschungsgesellschaft für Straßen- und Verkehrswesen. *Merkblatt zur Bewertung der Straßengriffigkeit bei Nässe (M BGriff) (FGSV 401)*. Köln, 2012.

[10] Forschungsgesellschaft für Straßen- und Verkehrswesen. *Richtlinien für die Standardisierung des Oberbaus von Verkehrsflächen (RStO) (FGSV 499)*. Köln, 2012.

[11] Forschungsgesellschaft für Straßen- und Verkehrswesen. *Technische Prüfvorschriften für Asphalt (TP Asphalt-StB) - Teil 80: Abscherversuch (FGSV 756/80)*. Köln, 2012.

[12] German Institute for Standardisation. *DIN EN 12697-19:2020: Bituminous mixtures -Test methods - Part 19: Permeability of specimen*. Berlin, 2020.

[13] German Institute for Standardisation. *DIN EN 12697-22:2020: Bituminous mixtures - Test methods - Part 22: Wheel tracking*. Berlin, 2020.

[14] German Institute for Standardisation. *DIN EN 12697-48:2021: Bituminous mixtures - Test methods - Part 48: Interlayer Bonding*. Berlin, 2021.

[15] German Institute for Standardisation. *DIN EN 12697-50:2018: Bituminous mixtures - Test methods - Part 50: Resistance to scuffing*. Berlin, 2018.

[16] German Institute for Standardisation. *DIN EN 13036-4:2011: Road and airfield surface characteristics - Test methods -Part 4: Method for measurement of slip/skid resistance of a surface - The pendulum test.* Berlin, 2011.

[17] German Institute for Standardisation. *DIN EN ISO 11819-2:2017-10: Acoustics - Measurement of the influence of road surfaces on traffic noise - Part 2: The close-proximity method*. Berlin, 2017.

[18] D. Gogolin. "Rheologische Kennwerte bitumenhaltiger Bindemittel zur Charakterisierung akustischer Eigenschaften von Asphaltdeckschichten." PhD-Thesis. Bochum: Ruhr University Bochum, 2012.

[19] L. Goubert and U. Sandberg. *Construction and Performance of Poroelastic Road Surfaces Offering 10 dB of Noise Reduction: PERSUADE Final Technical Report*. 2016.

[20] S. Jendia. "Bewertung der Tragfähigkeit von bituminösen Straßenbefestigungen." PhD-Thesis. Karlsruhe: University of Karlsruhe, 1995.

[21] Mastrad Limited. *Managing your network for skid resistance micro GripTester (μGT) - data sheet*. Ed. by Mastrad Limited. URL: https://www.mastrad.com/microgt.pdf (visited on 10/04/2023).

[22] M. Oeser et al. *INNO-PAVE : Final report: "Grundlagen der konstruktiven Gestaltung, Struktur sowie neuer polymerer Werkstoffe für:Straßendeckschichtsysteme" im Verbundprojekt: "Grundlegende Erforschung polymerer Werkstoffe sowie innovativer Herstellungs- und Einbautechnologien für Straßendeckschichtsysteme" : Duration of research project: 09/2015-04/2019*. Aachen, 2019.

[23] U. Peschel et al. *Lärmmindernde Fahrbahnbeläge: Ein Überblick über den Stand der Technik*. Ed. by Umweltbundesamt, Wörlitzer Platz 1, 06844 Dessau-Roßlau. 2014. URL: http://www.umweltbundesamt.de/publikationen/laermmindernde-fahrbahnbelaege-0 (visited on 10/09/2023).

[24] M. Rasol et al. "Progess and Monitoring Opportunities of Skied Resistance on Road Transport: A Critical Review and Road Sensors." In: *Remote Sensing* 13 (2021).

[25] L. Renken. "Development of PU-Asphalt - from the concept to the practical implementation." PhD-Thesis. Aachen: RWTH Aachen University, 2019.

[26] L. Rodrigues de Andrade et al. "Structural Performance Using Deflection Basin Parameters of Asphalt Pavements with Different Base Materials Under Heavy Traffic." In: *International Journal of Pavement Research and Technology* (2023).

[27] U. Sandberg and J. A. Ejsmont. *Tyre/Road Noise Reference Book*. Harg, Kisa, Sweden: INFORMEX, 2002.

[28] A. Schacht. "Entwicklung künstlicher Straßendeckschichtsysteme auf Kunststoffbasis zur Geräuschreduzierung mit numerischen und empirischen Verfahren." PhD-Thesis. Aachen: RWTH Aachen University, 2015.

[29] G. Seipel. "Analyse der Einflussgrößen auf die Entstehung und Intensität von Reifenspuren." Doctoral Thesis. Darmstadt: Technical University of Darmstadt, 2013.

[30] Statista. *Straßen in Deutschland*. 2023. URL: https://de.statista.com/statistik/studie/id/12547/dokument/strassen-in-deutschland-statista-dossier/ (visited on 10/31/2023).

[31] The British Standards Institution. *BS 7941-2:2000: Methods for measuring the skid resistance of pavement surfaces - Test method for measurement of surface skid resistance using the GripTester braked wheel fixed slip device*. London, 2000.

[32] B.-W. Tsai et al. "Evaluation of AASHTO T 324 Hamburg-Wheel Track Device test." In: *Construction and Building Materials* 114 (2016), pp. 248–260. URL: https://www.sciencedirect.com/science/article/pii/S095006181630472X.

[33] G. Várallyay, S.V. Legarth, and T. Ramirez. *Music lovers and hearing aids.* 2016. URL: https://www.audiologyonline.com (visited on 11/21/2023).

[34] B. Wacker. "Zeitraffende Belastungsversuche mit integriertem Einsatz zerstörungsfreier Messverfahren." PhD-Thesis. Bochum: Ruhr-Universität Bochum, Universitätsbibliothek, 2020.

[35] B. Wacker et al. *Belastungseinrichtung Mobile Load Simulator MLS30: Sensorik zur Beanspruchungsdetektion im ersten gemeinsamen Versuchsbetrieb*. Ed. by Bundesanstalt für Straßenwesen, Brüderstr. 53, 51427 Bergisch Gladbach, Germany. Bergisch Gladbach, 2016.

[36] D. Wang. "Schaffung des Bewertungshintergrunds zur Charakterisierung des Polierverhaltens der einzelnen, gesteinsbildenden Minerale und zur Untersuchung des Griffigkeitsverhaltens der Mineralaggregate in Abhängigkeit von den Polierbedingungen." PhD-Thesis. Aachen: RWTH Aachen University, 2011.

[37] A. Wolf and W. Schickl. *Restnutzungsdauer von Asphaltschichten: Prüfung der Grundlagen zu ihrer Berechnung*. Ed. by Federal Highway Institute. Bergisch Gladbach, 1998.

[38] J. Wothge. "Die körperlichen und psychischen Wirkungen von Lärm." In: *UMID 01/2016 Umwelt und Mensch - Informationsdienst* (2016), pp. 38–43. URL: https://www.umweltbundesamt.de/sites/default/files/medien/2218/publikationen/umid_1_2016_uba_laerm.pdf (visited on 11/04/2023).

[39] E. J. Yoder and M. W. Witczak. *Principles of Pavement Design*. 2nd ed., 1975.

6 Overall Conclusion

The aim of this work was the advancement of a noise-reducing pavement system constructed from polymeric materials. The starting point was the two-layer LIDAK system developed by Schacht [2], which laid the foundation for a functionalized noise-reducing system that mitigates the noise generated by tire-road interactions. The development also addressed the use of polymeric components, thus delving into the use of alternative construction materials for roadways. However, LIDAK bears the significant disadvantage of having very low mechanical strength and resistance against stresses from road traffic, primarily due to its focus on maximum noise reduction. Under the condition that the LIDAK system is optimized with significantly enhanced stability, the system could be a milestone in achieving the UN sustainability goals and, in turn, the German sustainability strategy. This is because the system would exhibit noise reduction efficacy and be so robust that it could endure the stresses of road traffic without incurring excessive damage. This advancement would contribute to realizing the sustainability strategy's sub-goals, ensuring a healthy life for all, making infrastructure and cities resilient and sustainable, implementing active measures to combat climate change, and promoting sustainable consumption and management of our ecosystem.

The research question that emerged was the extent to which the LIDAK system could be further developed to achieve greater stability while maintaining its acoustic effectiveness.

To address the research question, the fundamental methodology in this study aimed to conduct a multiscale examination of the optimization of the two-layered pavement system. This method, focused on breaking down the study into sub-goals, has proven effective in the realization of the demonstrator. Consequently, it was possible to respond to and resolve issues at a small scale (e.g., at the material level). Moreover, the quantitative research approach adopted in this study allowed for comparisons with other research projects using similar testing methods, enabling ongoing evaluation of the pavement system's development.

In retrospect, there is criticism regarding the chosen approach. Essentially, this study is purely experimental, allowing for an answer to the research question. The criticism revolves around the limitation of experimental studies in representing a variety of different use cases due to resource and time constraints. Therefore, an alternative approach could have involved integrating simulations into the research project to portray various scenarios (e.g., load

scenarios, integration into infrastructure, environmental impacts, etc.), aiming to address a greater number of research inquiries within the study.

Based on the health aspects that arose during the study, there was a swift transition to an alternative polyurethane, which limited the direct comparison of results between the third and second chapters. However, this fact revealed that the use of similar binders can lead to significant deviations from the expected outcomes, thus opening up new research aspects (i.e., the influence of the polyurethane binder type on the performance properties of mixtures). Nevertheless, this decision was necessary from an ethical perspective.

Additionally, it must be criticized that the study was based on a time-limited research project, which consequently had its own time constraints. Specifically, the opportunity to test the demonstrator on a large scale was limited to two weeks, and a monitoring phase could not be implemented. It would have been beneficial to monitor the demonstrator over an extended period and subject it to a variety of loads to gather further information on the long-term durability of the system. Furthermore, the elaborate production of the texture layer panels was affected, as it could not achieve the desired permeability at a large scale due to the workload surpassing the available resources, thereby necessitating a reduction in the qualitative standards.

In summary, the work demonstrates that the two-layered pavement system can be significantly enhanced in terms of its stability and resilience to the traffic load. However, the acoustic efficacy of the system is compromised, as its aerodynamic mechanisms are reduced due to geometric modifications. This leads to an inability to achieve a consistent level of noise reduction compared to LIDAK.

The study aimed to investigate how the constituents, the absorption layer and the texture layer of the pavement system, can be individually optimized while balancing the conflicting objectives of mechanical and acoustic efficacy. Subsequently, the components were integrated to form a complete system on a real-world scale, and the actual impact was evaluated at the meso and macroscale levels.

To further enhance the stability of the absorption layer, a novel composition of the mix constituents was introduced, comprising aggregates, rubber particles, and polyurethane binders. The rubber content was drastically reduced to ensure a stable aggregate structure while preserving a certain proportion of rubber content to maintain the layer's mechanical impedance. An iterative combination of the mixed constituents into various formulations was conducted through a parameter study, aiming to achieve the defined elasticity modulus and simultaneously high sound absorption characteristics. Therefore, a series of performance tests were employed to determine the material behavior of these variants concerning deformation,

fatigue, and low-temperature properties. Eventually, an optimal mix composition was identified, suitable for implementation in the two-layer pavement system as an absorption layer, delivering both stability and noise reduction features.

Due to a strong focus on sustainability, an exploration was conducted to investigate whether the absorption layer, in the form of reclaimed asphalt (PU-RAP), could be employed in manufacturing a new absorption layer. In this investigation, PU-RAP was incorporated in different proportions during the creation of the new absorption layer to ascertain the potential impact on performance characteristics (deformation, fatigue, low-temperature behavior, and absorption). The findings revealed that the addition of PU-RAP did not influence the maximum absorption level but caused a shift of the absorption curve towards the lower frequency range defined as pivotal in Chapter Two, thereby positively affecting noise reduction. This shift is possibly attributed to alterations in the pore structure, leading to higher tortuosity of the pore system due to the inclusion of PU-RAP. However, negative effects were observed in terms of deformation, fatigue, and low-temperature properties. This is likely due to the utilization of a different polyurethane binder in this study, which inherently presents differing performance characteristics compared to the base absorption layer described in Chapter Two.

The next step involved optimizing the texture layer. This entailed a change in geometry, adjustments to the integrated textile, coating adaptations, and finalizing the mixture for the PMMA-bound surface. Through the geometry modification of the texture layer and the utilization of plastic-coated PVA yarn, the layer became capable of withstanding significantly higher loads from traffic loads, resulting in noticeably enhanced strength. However, the geometry adjustment also led to a reduction in the large-scale air drainage system of the texture layer, causing a decrease of 1.6 dB(A) in its noise-reducing effectiveness. With the defined material composition and the new geometry, the texture layer was subjected to various stressors to assess its resistance to wear and incoming shear forces. As a result, it was demonstrated that the system withstood these pressures without sustaining damage, thus exhibiting high durability.

The final phase of the study involved examining the combination of the absorption and texture layers and their interactive capabilities, initially in the laboratory scale and subsequently in the real-scale scenario. Various composite layer variants between the two primary components (absorption and texture layers) as well as between the absorption layer and a bitumen-bound subbase were examined, and the optimal variants were determined. Through these studies, the prerequisites required for the realization of the two-layer system on a large scale were established. The large-scale implementation of the system followed by its evaluation revealed that the evolved surface layer system can withstand traffic loads without failure and also contributes to a minimum noise reduction of three dB(A).

Compared to the LIDAK system, a noticeable increase in strength and resistance against traffic loads was achieved. However, regarding the acoustic effectiveness, the increased strength of the system leads to a reduced noise reduction potential, attributed to the structural alterations influencing aerodynamic noise generation.

Outlook on Future Research

Alternative sustainable binders in this work are deemed sustainable as they can be developed from renewable resources or consist of a high proportion of recycled materials, thereby counteracting raw material depletion. However, the CO_2 emissions arising from the manufacturing and use of these alternatives have not been considered thus far. This subject should be thoroughly investigated by experts through life-cycle analyses to determine whether these alternatives diverge in terms of their pollutant emissions from asphalt production or similar construction material productions used in the road sector. Furthermore, the health aspect in the processing of polyurethane binders must be reconsidered. Processing has shown that some users experienced allergies, despite adhering to safety measures. Therefore, the compatibility of the binders should be re-examined to ensure no adverse effects on the health of individuals working with them.

In addition to the use of alternative binders, the development of innovative and functionalized road surfaces should also consider the finite resource of stone. Stones are highly durable and can be recycled multiple times. Even when used in asphalt mixtures and concrete, these construction materials, upon reaching the end of their life cycle, can be processed and reused to a significant extent. In the asphalt industry, the addition of recycled asphalt is already a standard practice, contributing to a high level of sustainability. However, for a comprehensive evaluation, it would be necessary to identify sustainable alternatives for the stone resource in the construction sector and determine if they exhibit comparable or even superior properties compared to conventional types of stone. This study should also take into account the level of resulting CO_2 emissions.

For the integration of the further developed surface layer system into the transportation infrastructure, its functionality and durability are not the only relevant factors. Equally important is the connection of this system to the existing transportation routes. We have demonstrated the system's compatibility with bitumen-bound bases. However, linking it to potential drainage systems or ensuring the adequate infiltration of surface water into groundwater must also be considered. Particularly concerning the water infiltration, the issue arises that precipitation water from traffic surfaces is materially contaminated (i.e., Tyre Road Wear Particles (TRWP), Polycyclic Aromatic Hydrocarbons (PAH), oil losses [5]) and requires purification before being allowed to infiltrate into the groundwater. In relation to this matter, the research project "Urban Drain Road" has been proposed to the

German Federal Environmental Foundation (DBU), aiming to develop a surfacing system that further addresses this issue (the project has not yet been approved).

Furthermore, the current focus of research lies in the digitalization of future roads, which aims to render our entire transportation infrastructure management transparent and contemporary, incorporating digital aspects. The digitalization strategy unites five key areas: the development of Digital Twins, the advancement of automation processes and robotics (such as autonomous driving and automated routine maintenance), the utilization of digital and transparent data for all stakeholders (planning, construction, administration, maintenance), and the development of smart materials, all of which should be driven forward considering sustainability. The development of smart materials is particularly relevant in the context of this work, as it aims to promote decarbonization (reduction of CO_2 emissions) and the creation of materials that can provide insights into their own condition, enabling early maintenance actions. These smart materials should also deliver functions for environmental protection, such as pollution reduction or noise mitigation, which were the focal points of this work. Moreover, the newly developed smart materials are intended to advance digitization, signifying that the materials will become self-sensing and allow the integration of smart sensors to generate data from the road network that can be processed by transportation infrastructure management. Research is being conducted globally, with notable initiatives such as the "Digital Twin Road" project by the collaboration between RWTH Aachen University and Dresden University in Germany [1, 3] and the "Digital Roads for the Future" program by the University of Cambridge, England [4].

Given this future perspective, the noise-reducing pavement system presented here provides a foundation for further development. The functionalities regarding noise reduction and decarbonization have been explored in this study. For instance, the texture layer could be advanced into a self-sensing material by incorporating conductive nanoparticles to detect loads and their localization. These fundamentals are also considered in the "Digital Twin Road" research project [1], contributing to transparent, interdisciplinary, and digital transportation infrastructure management throughout its entire life cycle.

Finally, it can be summarized that the study comprehensively addressed the research question and demonstrates that, albeit with a reduction in acoustic effectiveness, the LIDAK system introduced by [2] can be further developed to achieve mechanical stability and resilience.

References

[1] M. Kaliske and M. Oeser. *Digitaler Zwilling Strasse: Physikalisch-Informatorische Abbildung des Systems "Straße der Zukunft" (Einrichtungsantrag/ Transregio)*. Dresden, Aachen, 2021.

[2] A. Schacht. “Entwicklung künstlicher Straßendeckschichtsysteme auf Kunststoffbasis zur Geräuschreduzierung mit numerischen und empirischen Verfahren.” PhD-Thesis. Aachen: RWTH Aachen University, 2015.

[3] Sonderforschungsbereich SFB/TRR 339. *Digitaler Zwilling Straße*. URL: https://www.sfbtrr339.de/de/ (visited on 11/07/2023).

[4] University of Cambridge. *Research Programme: Digital Roads for the Future (DRF)*. URL: https://drf.eng.cam.ac.uk/research (visited on 11/07/2023).

[5] A. Welker. “Schadstoffströme im urbanen Wasserkreislauf: Aufkommen und Verteilung, insbesondere in den Abwasserentsorgungssystemen.” habilitation thesis. Kaiserslautern: Technical University of Kaiserslautern, 2004.